5-4-2018

Toward Fault Adaptive Power Systems in Electric Ships

Maziar Babaei Laktarashani

Toward fault adaptive power systems in electric ships

By

Maziar Babaei Laktarashani

A Dissertation
Submitted to the Faculty of
Mississippi State University
in Partial Fulfillment of the Requirements
for the Degree of Doctor of Philosophy
in Electrical Engineering
in the Department of Electrical and Computer Engineering

Mississippi State, Mississippi

May 2018

Toward fault adaptive power systems in electric ships

By

Maziar Babaei Laktarashani

Approved:

Joni Kluss
(Major Professor)

Sherif Abdelwahed
(Co-major Professor)

Masoud Karimi Ghartemani
(Committee Member)

Yong Fu
(Committee Member)

James E. Fowler
(Graduate Coordinator)

Jason Keith
Dean
Bagley College of Engineering

Name: Maziar Babaei Laktarashani

Date of Degree: May 4, 2018

Institution: Mississippi State University

Major Field: Electrical Engineering

Major Professor: Joni Kluss

Title of Study: Toward fault adaptive power systems in electric ships

Pages of Study: 120

Candidate for Degree of Doctor of Philosophy

Shipboard Power Systems (SPS) play a significant role in next-generation Navy fleets. With the increasing power demand from propulsion loads, ship service loads, weaponry systems and mission systems, a stable and reliable SPS is critical to support different aspects of ship operation. It also becomes the technology-enabler to improve ship economy, efficiency, reliability, and survivability. Moreover, it is important to improve the reliability and robustness of the SPS while working under different operating conditions to ensure safe and satisfactory operation of the system. This dissertation aims to introduce novel and effective approaches to respond to different types of possible faults in the SPS. According to the type and duration, the possible faults in the Medium Voltage DC (MVDC) SPS have been divided into two main categories: *transient* and *permanent* faults.

First, in order to manage permanent faults in MVDC SPS, a novel real-time reconfiguration strategy has been proposed. Onboard post-fault reconfiguration aims to ensure the maximum power/service delivery to the system loads following a fault. This study aims to

implement an intelligent real-time reconfiguration algorithm in the RTDS platform through an optimization technique implemented inside the Real-Time Digital Simulator (RTDS). The simulation results demonstrate the effectiveness of the proposed real-time approach to reconfigure the system under different fault situations.

Second, a novel approach to mitigate the effect of the unsymmetrical transient AC faults in the MVDC SPS has been proposed. In this dissertation, the application of combined Static Synchronous Compensator (STATCOM)-Super Conducting Fault Current Limiter (SFCL) to improve the stability of the MVDC SPS during transient faults has been investigated. A Fluid Genetic Algorithm (FGA) optimization algorithm is introduced to design the STATCOM's controller. Moreover, a multi-objective optimization problem has been formulated to find the optimal size of SFCL's impedance. In the proposed scheme, STATCOM can assist the SFCL to keep the vital load terminal voltage close to the normal state in an economic sense. The proposed technique provides an acceptable post-disturbance and post-fault performance to recover the system to its normal situation over the other alternatives.

DEDICATION

To my mom Marziyeh, dad Abbas, my beloved wife Nazanin, brothers Mehdi and Mohammadreza, and sisters Sara and Negar,

ACKNOWLEDGEMENTS

Here, I would like to express my deepest gratitude to my former advisor and current co-advisor, Dr. Sherif Abdelwahed, for giving me this opportunity to work under his supervision during my Ph.D. His patience, courage, dignity always inspired me through the professional work. I am thankful to my current advisor, Dr. Joni Kluss for his support, especially in the last year of my Ph.D. I am sincerely grateful for all the knowledge and support that I received from Dr. Masoud Karimi during my study at MSU. I would also like to thank Dr. Yong Fu for serving as my committee member. I am also grateful to my friend Roy Jafari for his guidance and help during my PhD.

I would like to thank my brother Mehdi for his endless support throughout my whole life. Without him, I could not imagine myself where I am today. I am highly indebted to my supportive and understanding wife Nazanin for her courage and love. I am also greatly thankful to my mom and dad for their self-devotion, courage, support, and infinite love.

I also would like to acknowledge my friends in Simrall, especially Thaer Qunais for his valuable discussions. I am thankful to all my friends, Ashkan, Hyla, Shahriar, Ali, Hadi, Kamran, Pedram, Mojtaba, Aref who made my life in Starkville more colorful.

I would also like to thank the Office of Naval Research (ONR) for the financial support.

TABLE OF CONTENTS

LIST OF TABLES

LIST OF FIGURES

CHAPTER I

INTRODUCTION

1.1 Background

Shipboard Power System (SPS) plays a significant role in next-generation Navy fleets. With the increasing power demand from propulsion loads, ship service loads, weaponry systems and mission systems, a stable and reliable SPS is critical to support different aspects of ship operation. It also becomes the technology-enabler to improve ship economy, efficiency, reliability, and survivability. Minor faults in SPS can result in destructive consequences, making fault-tolerance an important consideration during the early design stages of the SPS. A robust fault management framework for the analysis and design of the SPS is necessary and becomes an urgent requirement for the design of future onboard power systems. One of the key priorities in this undertaking is the survivability of the SPS when experiencing fault conditions. More specifically, this entails stopping the system from further deterioration and restoring it to its normal working condition. Intelligent control architecture is vital in this regard, as it allows for the withstanding of faulty conditions. Furthermore, this strategy allows the system to work as efficiently as possible and meet reliability requirements by utilizing the ship's own resources. A properly-designed fault management framework is crucial for overcoming faults and improving survivability for the SPS. In summary, a well-designed fault management system is able to preserve the integrity of the SPS.

1.2 Challenges and motivations

A fault management system is necessary for the SPS to take corrective actions to mitigate the consequences of the faults. Instead of solely isolating the faulty parts from the system, the system is expected to minimize the impact of the fault by some control actions. The unique characteristics of SPS have made the fault management techniques dramatically different than other terrestrial power systems. Implementing these methods require specific considerations. Coordination between different stages of fault management need to be carefully addressed during the designing process.

The different types of possible faults in the MVDC SPS are summarized as follows.

1. **Transient faults including:**
   - Single line to ground fault on the AC load (including load and generator side)
   - Double line to ground fault on the AC load (including load and generator side)
   - Three phase to ground fault on the AC load (including load and generator side)
2. **Permanent faults including:**
   - Lose of Main generator due to fault
   - Lose of Auxiliary generator due to fault
   - DC faults on DC side of the system

In operation of the SPS, before and after fault occurrence, it is desirable to maximize the delivery power to the systems' loads. However, in post-fault condition, the system operator may not be able to fully meet all the demand, thus need to prioritize the loads and/or perform load shedding. Furthermore, the system operator may need to change the topology of the SPSs in order to facilitate the delivery of the power to the loads which have higher priority to be served. This corrective action mainly being performed by changing the status of the branch/loads switches and commonly being referred as optimal reconfiguration of the SPS. Several papers have considered the reconfiguration problem to deal with permanent faults. The reconfiguration objectives include power loss reduction [89], preserving the stability margins [120], minimization of the number of switch operations [12], and maximizing the number of the served loads [91]. However, in SPS, due to the tightly-coupled distribution network, the active power loss in an electric ship is considered negligible compared to the other power networks and thus does not constitute a critical objective for the SPS reconfiguration problem.

Real-time power system simulations can be done through Real Time Digital Simulator (RTDS) and its Graphical User Interface (GUI)-based design platform (RSCAD). A reconfiguration problem is essentially an optimization problem in which commercial simulation programs such as MATLAB and RTDS-MATLAB interface platforms are used to simulate and implement the problem [74, 107]. In [74], an intelligent reconfiguration strategy for a Medium Voltage AC (MVAC) is implemented in the RTDS, where the reconfiguration algorithm is executed on the Digital Signal Processor (DSP). A Real-Time Automation Controller (RTAC) is used in [107] to perform the reconfiguration. However, those approaches require intensive computation overhead and need extensive simulations due to the complexity of SPS models. Therefore, there would be an inconsistency between the time required for actual hardware operation and that for software computation.

Another critical issue concerning fault management in SPS is dealing with unsymmetrical transient faults. These types of faults can affect the system for a short period of time. When a transient fault occurs in the SPS, a voltage dip will appear on the AC load side of the system, where certain vital loads, such as propulsion loads, are connected to. Therefore, riding through the short-term disturbances, especially under unbalanced system AC faults, and maintaining the voltage stability during different faults in SPS is one of the most challenging issues. One of the suggestions is to employ Flexible AC Transmission System (FACTS) devices that help the system by controlling the injected reactive current to keep the voltage at the desired value in post-fault situations.

In the SPS, viewed as a low impedance power distribution system, high fault currents are a major concern. In some cases, large fault current levels may exceed the rating of the power system's components. Therefore, the problem of designing the system's components to withstand the fault currents are becoming more serious in marine applications. Many devices such as split bus bars, transformers with higher impedance, and fuses have been widely used in industry to reduce the level of fault currents. Utilizing these devices can reduce the availability of the power system or increase the power loss. In order to overcome the drawbacks of the traditional methods for fault current limiting methods, Superconducting Fault Current Limiters (SFCLs) are adopted by utilities and often used in the situations where insufficient fault current interrupting capability exists. Previous research works in optimal sizing of the SFCL are studied only for a three-phase short circuit fault. There is no research work that considers all types of possible fault, including single line to ground fault and double line to ground fault, in order to design the SFCL. To compute the optimal impedance of the SFCL in case of the fault, various types of short circuit faults must be considered.

1.3 Contribution of the dissertation

This dissertation addresses the problem of fault management in MVDC SPS. The contributions of this dissertation in terms of proposing the new methods and approaches are expressed as follows.

- **Real-time implementation of MVDC SPS**

  An important issue regarding the real-time implementation of the SPS reconfiguration problem is the communication delay between the RTDS and other optimization platforms. One approach to deal with this issue is to utilize the script environment inside the Runtime environment of RSCAD software in the RTDS to reduce the communication delays. With the proposed approach, the implementation of the optimization technique is executed inside the RTDS and it will remove the extra communication between RTDS and other computational platforms such as MATLAB. To the best knowledge of the author, there has been no systematic approach to address the MVDC SPS reconfiguration problem, particularly with a full RTDS implementation. This study aims to implement an intelligent real-time reconfiguration algorithm in the RTDS platform through an optimization implemented inside the RTDS.

- **Application of Static Synchronous Compensator (STATCOM) in MVDC SPS**

  This dissertation proposes a solution to deal with the unsymmetrical transient faults in the MVDC SPS, which is employing STATCOM on the AC side of the SPS. An improved Genetic Algorithm (GA) approach is also introduced for optimal design of the STATCOM. The underlying optimization problem is to identify the STATCOM controller parameters using the Fluid Genetic Algorithm (FGA) optimization technique. The performance of the proposed FGA-based controller design has been tested under different fault scenarios.

- **An improved Genetic Algorithm (FGA) for optimal STATCOM design**

  FGA is a novel heuristic optimization algorithm that takes inspiration from the area of genetic algorithms. This algorithm is, in fact, a GA with some fundamental differences. The pivotal idea of FGA is that an FGA's chromosome is not another representation of an answer, but the predisposition of an individual before an answer is produced. Because of this, the crossover operation has to change and the need for mutation is eliminated. Furthermore, diversity rate and generation blue print are other gifts of the proposed fluidity in FGA, making it more adjustable for different needs and problems. In this dissertation, FGA is utilized to find optimal STATCOMs controller parameters in MVDC SPS to minimize the effects of the faults.

- **Simulated Annealing (SA) approach for MVDC SPS reconfiguration**

  In this dissertation, a powerful optimization technique has been utilized to solve the reconfiguration optimization problem. For the real-time implementation of the MVDC SPS, Simulated Annealing (SA) optimization technique, which enjoys some advantages over other meta-heuristic methods, is employed to solve the reconfiguration problem in RTDS. The main advantage of SA optimization technique is the simplicity of the algorithm, even for complex problems. In addition, this algorithm is not a population-based algorithm, which makes the algorithm less computationally expensive.

- **Multi-objective multi-criteria approach for optimal design of Super Conducting Fault Current Limiter**

  This dissertation proposes a novel approach to select the optimal size of the Super Conducting Fault Current Limiter (SFCL) in power systems to improve the system's stability during unsymmetrical transient faults. To determine the optimal size of the SFCL, a multi-objective multi-criteria approach is introduced. Various types of short circuit faults are considered in order to obtain the optimal impedance of the SFCL in case of the fault. The performance of the proposed scheme to minimize the faults is confirmed through the time-domain simulations. Simulation results show that the proposed method achieves a favorable solution in order to minimize the effects of the transient faults.

1.4 Dissertation organization

This dissertation is organized as follows: Chapter 2 provides an overview of the SPS architecture followed by a review of current fault management techniques in electric ships and different existing approaches to minimize the effects of the faults. In Chapter 3, a novel Simulated Annealing (SA)-based approach for implementing intelligent real-time reconfiguration in MVDC SPS has been proposed. In this chapter, an overview of the MVDC SPS model is discussed in details. The reconfiguration problem formulation, the SA-based optimization, and the detailed hardware implementation of the reconfiguration problem is also discussed in this chapter. In Chapter 4, an optimal design of combined STATCOM-SFCL in MVDC SPS application is provided. This section describes the STATCOM operation principle, model, and its control structure. The STATCOM and SFCL designing problem formulations are also presented in this chapter. Lastly, in Chapter 4, the conclusion and future work of this research work have been drawn.

CHAPTER II

BACKGROUND AND LITERATURE REVIEW

2.1 Overview of the SPS structure

SPS is an autonomous microgrid and is powered by distributed generation systems. The structure of the traditional SPS is based on radial power distribution. The need for higher survivability, efficiency, and reliability motivated navy fleets to employ Zonal Electrical Distribution (ZED) architecture as an alternative for the SPS to achieve these goals [20]. Currently, there are three different structures that have been studied for the electric ship power systems: *Medium Voltage AC (MVAC)*, *Medium Voltage DC (MVDC)*, and *High frequency AC (HFAC)*.

The general topology of MVAC SPS is depicted in Figure 2.1. The main AC bus is set to 4.16 kV and 60 Hz frequency. Two main generators and two auxiliary generators provide power to the load centers in MVAC SPS. The system is divided into a number of electric zones, and each zone has load centers that can be connected to both Port bus or Starboard bus [109].

The MVDC SPS is identified as a new system integration and power distribution architecture as an alternative for AC system for the naval warships. The model that represents an MVDC architecture is shown in Figure 2.2. The MVDC architecture utilizes a 5 kV MVDC ring bus and fed from the main and auxiliary generators through transformers and rectifiers. Similar to the MVAC SPS, loads are distributed as zonal loads. Electric power is converted into mechanical power through propulsion induction motors and propellers [134]. The advantages of MVDC power system in comparison to AC-based architecture are summarized as follows [10].

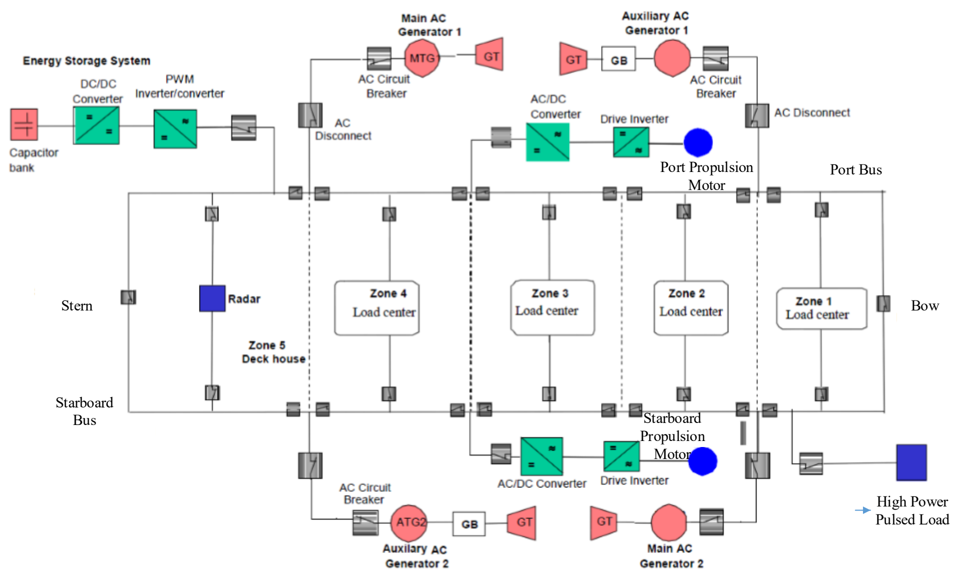

Figure 2.1: Baseline System Model for MVAC shipboard distribution system [38]

- Higher power transfer capability for a given (DC) current level
- Easy connections and disconnections for both power sources and loads through the use of power converters as connection interfaces.
- Better management of faults and disturbances by utilizing the controlled power electronics devices.

Designing a protection system for SPS is a challenging task due to the limited power sources in a limited space. The protection system design needs more consideration for the MVDC SPS architecture. In this system, it is important to properly coordinate the power electronics and protection devices to design a robust protection system [98]. For example, DC arcs are hard to be extinguished in the absence of a voltage or current zero crossing. Therefore, the traditional fault management techniques employed by the conventional power networks are not desirable for the MVDC SPS application. On the contrary, the MVDC SPS can take advantages of power electronic converters to identify and isolate the faults.

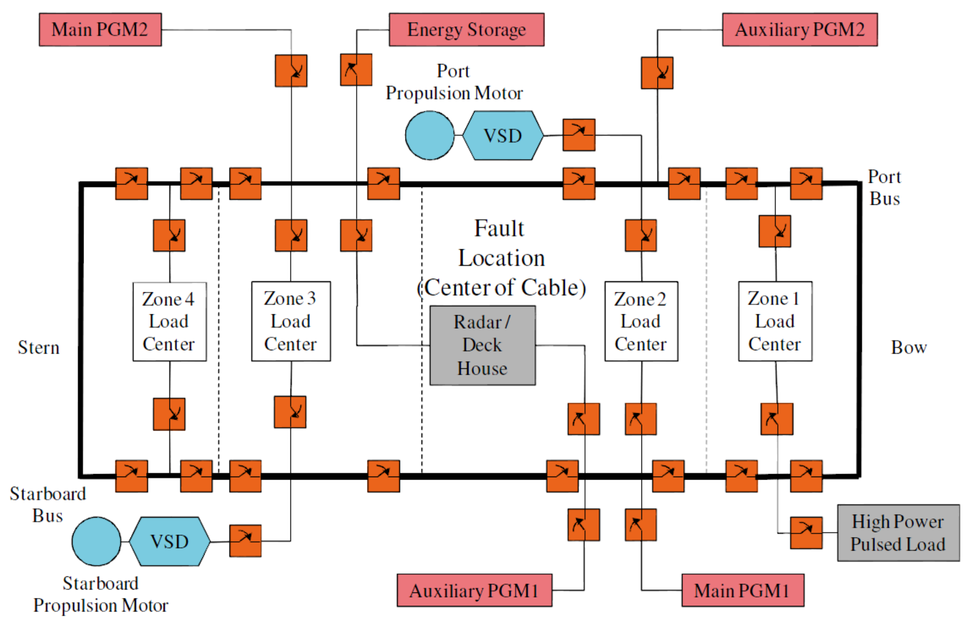

Figure 2.2: Baseline System Model for MVDC shipboard distribution system [38]

2.2 Faults in SPS

In [24], the authors define a *fault* as a deviation of a component operating from the expected status. A common expression that has been used to describe similar effects is *failure*. Although by definition, failure indicates a complete breakdown of a component, whereas fault suggests tolerable phenomena. In this dissertation, we refer to any abnormal operations in the system's components as faults. By this definition, we consider a broad range of disruptive events that prevent the system from functioning properly.

Faults in the SPS can be categorized as follows.

- **Physical system faults:** Short circuit faults are included in this type of fault [62]. In MVDC SPS, this fault includes short circuits on the MVDC bus among any two or three line or short circuits fault on the MVDC bus between any line and ground [85]. High impedance, arcing faults [83], and short circuit faults such as single line to ground and three phase faults on the AC load side are also included in this type of fault [64]. Rail to rail and rail to ground short circuits caused by component or control failure and any of the converters or sub-systems attached to the MVDC bus are some other examples of this type of fault.

- **Measurement faults:** These faults are caused by malfunctions, failure, or error of the measurement devices such as the relevant control system, associated communication systems, and sensors [62, 111]. These faults are caused by bad calibration, abnormal environmental situations, and aging of the measurement devices.

Both physical and measurement faults need to be responded to in a way that their impact on the SPSs performance is minimized.

2.3 Need for fault management in SPS

A robust fault management framework is crucial to increase a system's ability to accomplish the desired operation in the presence of faults. In SPS, a minor fault can result in destructive consequences such as endangering the survivability of the SPS, damage to components and equipment, and threatening the continuity of electric service for the vessel. Therefore, fault-tolerance becomes an imperative consideration during the early-design steps of the SPS [43]. In [3], authors conduct a comprehensive review of four widely used concepts: *fault-tolerance*, *reliability*, *security*, and *survivability*. Figure 2.3 shows that by combining fault-tolerance, survivability, and security together, the overall reliability of the SPS is improved by:

- **Enhancing Fault-Tolerance:** fault management is used to increase the capability of the SPS to continue the proper service in the presence of faults.
- **Improving Survivability:** by employing fault management techniques, the SPS can have the ability to identify faults, adapt to them, and restore to minimize the effects of the faults.
- **Ensuring Security:** SPS can preserve the integrity of the system by an appropriately-designed fault management system.

Recently, researchers have developed various techniques to deal with faults in SPS. These techniques include [43, 3]:

- **Fault Detection and Localization:** to identify the fault existence and the location of the fault.

- **Fault Isolation:** to isolate a fault and impeding its propagation.
- **System Reconfiguration:** to remain in operation status using a reconfiguration strategy under the presence of faults.

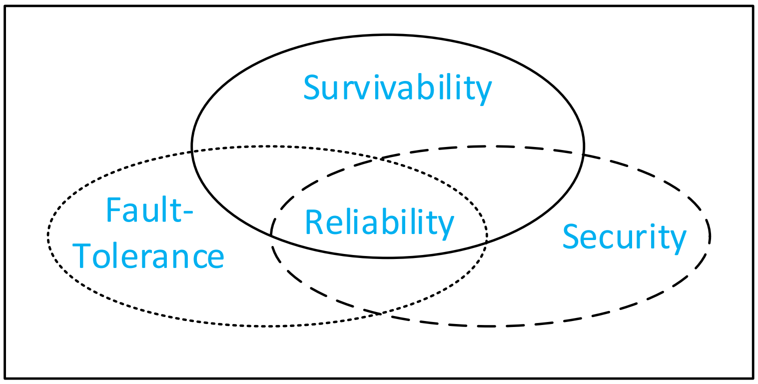

Figure 2.3: Relationship with different concepts from [3]

As a fault propagates through the SPS, it will result in malfunctions in the ship's operation. It is possible for a single fault to cause multiple consequences. Once a fault manifests itself, detection of fault occurrence depends upon the presence of the fault detection system. The integrity of the service will be compromised if a fault remains undetected. The ability to detect the fault is a prerequisite to fault management. Therefore, the role of the first step is to discover the existence of faults in the system and obtain information about the faults as well as the faulty parts of the system. When a fault is detected, the isolation of the faulty component must be performed to disconnect the affected part from the rest of the system. It is most desirable to remove the effects of the fault in a way that guarantees a ship's survivability and effectively maintains a particular level of performance. It is the responsibility of the system reconfiguration system to restore the system to an acceptable safe operation level. Remedy actions are taken by the fault management system to maintain appropriate operating conditions for the post-fault system. All of the system reconfiguration methods are based on the assumption that the faulty part is disconnected from the rest of the system using the information provided by a Fault Detection and Identification (FDI) system through the protection devices. Under this assumption, the goal of the system reconfiguration is to return the system to a stable working condition with minimum service interruption.

The post-fault system reconfiguration process needs to handle faulty situations after the fault type is revealed and the faulty parts are disconnected from the rest of the system. Therefore, the process and design issue of the reconfiguration controller and its integration with FDI scheme should be investigated.

2.4 Fault detection and localization

The detection and localization of different types of faults within the SPS is a challenging topic in the design process due to the close proximity of electrical and physical components within the ship and the rigorous performance and safety regulations. The first step in dealing with a fault is to determine the fault location. Fault location indicates the physical position of a fault in the system. This information is very useful for isolating the fault and impeding the fault's propagation in the system. When a fault occurs in a part of the system in an SPS, it is crucial to identify the fault location as precisely and quickly as possible for assuring the service reliability.

Existing fault detection schemes for SPS are summarized as follows.

2.4.1 Distance protection scheme

The basic principle of the distance protection scheme is based on the estimation of distance to a fault by calculating the impedance between the relay location and selected reach point. The impedance of the cables in SPS are in the order of 0.04 ohm/1000 feet due to shorter length of the cables compared to the other power system networks. The difference between measured impedance and calculated impedance is relatively large with respect to the cable's impedance. This issue makes the application of distance protection scheme impractical in SPS [118].

2.4.2 Overcurrent protection scheme

The overcurrent protection scheme is another conventional fault detection and localization method in the power system. The overcurrent relays operate once the current flowing into a protected part of the system exceeds a predefined threshold. In SPS, the generators' breakers are equipped with overcurrent relays. The power is supplied by multiple generators, and this makes the coordination of the overcurrent relays a tedious task to meet the selectivity requirement of the protection system. Therefore, due to the underlying tightly-coupled distribution network, the overcurrent protection is not a suitable protection scheme as a primary fault detection scheme in SPS [44]. Conventional backup schemes including distance and overcurrent approaches were initially implemented to protect the SPS, but they both failed due to problems introduced by the short cables' length in SPS.

2.4.3 Current Differential scheme

This method is based on Kirchhoff's current law which states that the sum of the currents flowing into a node is equal to the currents flowing out of the same node [127]. In this method, the currents entering a system's component are observed, and if their sum is not equal to zero, the presence of the fault is revealed. The main advantages of this method are its acceptable accuracy and speed with a relatively excellent sensitivity. The main disadvantages of this method [64] are the need for a connection between all the terminals in the system, and only sections between the measurement points are protected. Moreover, backup protection for other parts of the system is not guaranteed, and current transformer malfunction can affect its functionality.

This method of protection works properly in systems with short cables. In power networks with relatively short cable length, the performance of the current differential scheme will not be affected. The main features of this scheme are its accuracy, speed, and high sensitivity to locate the faults even in the systems with short cables. This allows to precisely discriminate between faults even under the effect of disturbances such as power swings. Moreover, although the length of the cables is short in SPS, differential protection is highly dependent on the communication between the differential relays. This issue reduces the reliability of the SPS. Each SPS component needs a differential relay to locate the fault effectively. The SPS includes a multitude of loads and devices, thus making the implementation of this method impractical.

2.4.4 Active Impedance Estimation (AIE) scheme

In this method, a power converter connected to the bus injects short-duration currents within spread frequency spectrum to calculate the bus impedance [34]. The system's impedance seen from the Point Of Measurement (POM) is evaluated using the measured voltage and current as represented in (2.1),

$$Z = \frac{F(V_{measured})}{F(I_{measured})} \tag{2.1}$$

where F is the Fourier transform operator. If an abnormal condition is detected, the power converter injects current. In this method, the harmonic of the voltage and current signals are obtained by Fast Fourier Transform (FFT). The information on both the fault location and the fault severity are evaluated by the system's impedance calculated at POM. The main challenge regarding this method is to select the proper frequency during which the calculated impedance can yield a high resolution and precise system's value within a short period of time. In [34], AIE method has been utilized to accurately find the location of DC faults on the main DC bus in an MVDC SPS model.

2.4.5 Wavelet analysis technique

In this method, wide-band and non-stationary signals are decomposed into specific time-frequency resolutions [64]. Wavelet Transform (WT) can then be employed to obtain the sudden-changing feature of the voltage and current signals (for example, raise in current during short circuit fault). In the power system, wavelet analysis techniques have been widely exploited for fault detection, localization and classification [30, 31]. This method can be used for detection of various faults occurring in SPS such as short circuit fault, and ground faults in Voltage Source Converters (VSC). This method of fault detection has also been used to detect different possible faults in MVDC SPS including short circuit faults on the primary DC bus and short circuit faults on the AC side such as phase to phase faults in [64, 63]. To obtain the features of different types of faults, an MVDC SPS model has been modeled in the Real-time Digital Simulator (RTDS), and WT-based method has been employed to analyze the simulation data in MATLAB.

In terms of accuracy, the WT-based fault detection technique has the best performance among the fault detection schemes [64]. In this method, the use of WT as a feature extractor significantly enhance the performance of the detection scheme.

2.4.6 Traveling wave fault location scheme

This fault localization method has been widely-used for precisely locating the faults in transmission and distribution lines in power systems [11]. In a transmission line, the voltage at the fault location drops instantly when a fault occurs. In this case, from the location of the fault, high frequency traveling waves propagate in both directions. Traveling wave fault location method is performed by making time-synchronized measurements at both ends of the transmission line (double-ended) and time-tagging the arrival of the initial traveling waves usually using a Global Positioning System (GPS) timing signal [49]. This type of protection scheme can be used to locate the faults on the main DC bus of the MVDC SPS, but the main obstacle to using this method is that for a small scale physical system in the SPS, it is difficult to measure the time difference with enough accuracy.

2.4.7 Artificial Neural Network (ANN)-based method

In ANN-based fault detection method, the fault location is determined by using the transient information contained in the fault voltage and current waveforms [28]. This method is effective in detecting the type and location of the faults, especially in DC power systems. The main drawback of this method is that using the sampled data as inputs of ANN has lead to long training procedures and significant calculation burden; at the same time, due to the sophisticated structure of ANN, it cannot be used for online fault localization. In SPS, it is essential to precisely identify the faulty component and discover the fault type to minimize the negative impacts of a fault. This is fulfilled by monitoring the system states including voltage, current, and frequency of the system in fault situations. This type of fault localization method has been used in [28] to locate three possible faults including positive rail to ground fault, rail to rail fault, and negative rail to ground fault in an MVDC SPS.

2.5 Fault isolation

Based on the fault identification and localization, the protection system needs to prevent or limit the fault's destructive effects by disconnecting the SPS's faulted part [65, 33, 119, 55]. Fault Isolation (FI) in a system is enabled to isolate the faulted sections with switches. The success of a FI system depends on analyzing the information extracted from the monitored signals and the communications between components.

SPS is a tightly-coupled system due to the short length of the connection cables and heavy dependency between the various system's components. This issue cause fast propagation of the fault currents throughout the system, so the problem of fault isolating is more critical to SPS compared with other power systems. The SPS fault isolation system must be fast, secure, sensitive and highly-adaptive to the system's configuration. The onboard fault isolation system is categorized into the two main following types.

2.5.1 Breaker-based methods

In breaker-based methods, which are the most common forms of the protection in power systems, mechanical circuit breakers are used to protect the distribution system. In MVDC SPS, the currents need to be extinguished by extra devices due to the lack of natural zero crossing. Because of the limited voltage and current ranges, DC circuit breakers can extinguish the arc caused by the faults. These breakers use different structures to dissipate and cool the arc adequately such that the arc voltage finally surpasses the system's voltage and forces the current to zero [27].

An interesting technological trend in SPS protection device design is the use of Solid State-based Circuit Breakers (SSCB) and Z-source breakers. These methods of fault isolation belong to the breaker-based methods. SSCBs are composed of solid state switches such as IGBT or IGCT thyristors and a snubber circuit. These breakers are a combination of resistances, capacitors, and Metal Oxide Varistors (MOVs) to dissipate energy during the interruption process [40]. This type of switch is capable of interrupting the fault currents in a very short duration compared with the existing methods. Figure 2.4 shows a typical SSCB that is used for fault interruption. To increase the functionality of the SS-

CBs, additional devices such as mechanical switches or capacitor can be incorporated with the switch.

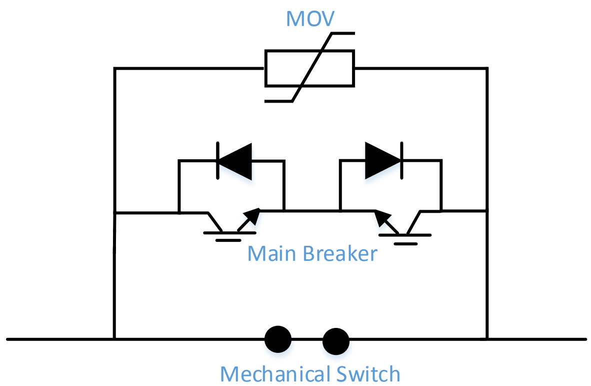

Figure 2.4: Schematic of typical SSCB

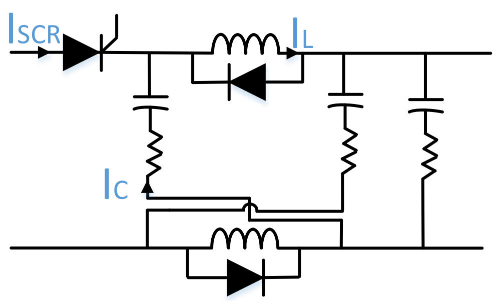

Figure 2.5: Schematic of conventional Z-source breaker

The detailed architecture of SSCB is discussed in [60]. It is shown in that fast fault interruption, low peak current, flexible and programmable coordination, and mechanical isolation are the key features of these type of fault isolation in MVDC SPSs. In [87], the design of system protection for MVDC SPS using SSCBs is provided to interrupt the DC fault. This method of protection offers higher reliability and faster speed to the DC shipboard distribution. The major challenges of employing this type of breakers are their higher loss compared with conventional methods.

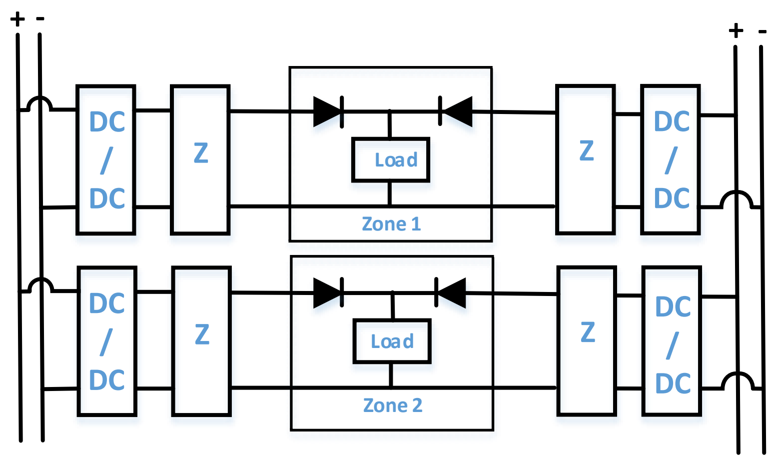

Figure 2.6: MVDC SPS with Z-source breakers

The application of Z-source breakers in MVDC SPS is also investigated in [69, 68, 35, 29]. The configuration of this type of breaker is shown in Figure 2.5. Z-source breakers consist of a Silicon Controlled Rectifier (SCR), a crossed L-C connection, diodes, and resistors. During steady state operation, the current takes the path from the source to the load through the SCR and inductors. When a fault occurs, its transient-state current flows through a path involving the capacitors which are in opposition to the SCR current. Therefore, this fault current will quickly drive the SCR current to zero, causing the SCR to switch off. Rapidly and automatically, the faulty load is removed from the system. Figure 2.6 shows one possible way to integrate Z-source breakers into the zonal SPS. In the MVDC SPS, these types of breakers could be an effective method to handle the DC faults on the main DC buses. In [69], a modified Z-source circuit breaker has been proposed to overcome the limitation of the conventional Z-source circuit breakers in the SPS application. The proposed breaker can improve the performance of the protection device to deal with large transient faults. In [68, 35, 29], the application of the Z-source breaker with some improvements to its topology has been explored in the MVDC SPS.

2.5.2 Breaker-less methods

Fast fault protection is required to impede damage to system equipment due to quickly increasing DC fault currents caused by low inductance in MVDC SPS. However, fast DC protection is hard to achieve with conventional circuit breakers. In breaker-less fault isolation methods, the VSC that uses self-turn-off power electronic devices employs converters for fault current interruption [18]. The breaker-less approaches have the fault detection scheme inside the power converters itself. In the event of a fault, the VSC may be switched to a block mode to prevent the fault propagation in the system. In [27], a fault protection strategy for DC shipboard distribution based on the coordination of bus switches and power supply converters has been proposed. An active fault current foldback via firing-angle control is implemented in the thyristor rectifier in an MVDC SPS to protect the system from short-circuit fault [39].

As it is shown in these studies, the DC-DC or AC-DC converters must be fully controllable, and they cannot be of topologies such as diode rectifiers or simple DC-DC boost converters. The advantages of using this approach are higher fault interruption speed, performance improvement, and lower cost. The drawbacks of using this type of fault isolation in MVDC SPS are summarized as follows.

- All types of DC faults cannot be controlled by this method since some parasitic paths could be present in converters and systems.

- Additional series switches are required to interrupt the fault current.

- In case of faults, the converters may not tolerant the fault currents which leads to cascading failures.

- This method of fault protection may affect all sections fed by the DC bus, not only the faulted section of the system.

One of the main issues regarding this type of fault isolation is high loss due to use of power electronic devices. These losses could result from Switching and Conduction losses. The switching losses are due to transition from the blocking state to the conducting state and vice-versa. Conducting losses occur when a power electronic device is in the conduction states.

Table 2.1: Comparison between different methods for fault isolation in SPS

Method	Type	Mechanism	Advantage(s)	Disadvantage(s)
Breaker-based methods	a) Mechanical circuit breakers	Provide protection to the system components by interrupting the fault currents with simple open and close mechanism	a) Easy to install b) Lower cost; c) Low power loss (less than (0.001% of the breaker less methods)	a) Ineffective at higher voltages, b) Larger component. c) Loss of power to un-faulted sections. d) Effects at the fault Location. e) Longer switching response (up to 60 ms)
	b) Additional devices integrated with mechanical circuit breakers	External device to generate an artificial current zero, or arc-less extinguishing way for the fault current.	a) Faster switching response than electromechanical breaker; b) Reasonable power loss (0.1% of the breaker less methods)	More components need to be protected and monitored.
Breaker-less methods	Use VSC as a fault interruption	In overload or a faulty condition protection by minimizing the current flow by gate control of the power electronic devices	a) Ultra-fast (less than a ms) b) Reliable; c) Don't need to install additional circuit breakers	High on-state losses, high capital costs.

Table 2.1 summarizes the common methods that are used to isolate the faults in SPS and their advantages and disadvantages.

2.6 Post-fault reconfiguration

After the faulty components are separated from the rest of the system, it is important to quickly restore the power supply to the affected parts of SPS by adjusting the system configuration to improve the system reliability and ensure safe and satisfactory operation of the system. This process is named reconfiguration. Similar to terrestrial power systems, onboard post-fault reconfiguration aims to ensure the maximum delivery power/service to the system loads following a fault [13].

To deal with the reconfiguration problem in power systems, some research works are conducted in [102, 93, 5, 90, 61, 16, 46]. A review on publications related to power distribution system reconfiguration has been performed in [102]. In [93], a new reconfiguration method has been presented to minimize the real power loss and improving the voltage profile in the presence of distributed generations. In [5], a probabilistic reliability evaluation method has been incorporated to the reconfiguration problem in power distribution system to maximize the reliability of power supplied to the loads. A modified plant growth simulation algorithm has been used in [90] to minimize power loss in a radial distribution network. In [61], a Lagrange relaxation approach has been applied to the reconfiguration problem to minimize the power losses, total cost of energy losses, switching operation and network reliability. A comprehensive review on different methodologies for reconfiguration in power distribution systems embedded with distributed generation is presented in

[16]. A Tabu search optimization algorithm has been utilized to solve the reconfiguration problem in [46] for improving the stability of the power distributions.

The reconfiguration objectives considered in the literature include:

- Power loss reduction [90].
- Preserving the stability margins [46].
- Minimization of the switch operations [102].
- Maximizing the number of the served loads [75].

However, the active power loss is considered negligible compared to other types of power systems due to the tightly-coupled distribution network in SPS and thus does not constitute a critical objective for SPS reconfiguration problem [75]. Another unique feature of SPS is that the priorities of the loads in different missions are different. The loads tend to change priorities according to the current operating conditions or the mission requirements. Therefore, the loads' priorities needs to be taken into account during the process of reconfiguration. These features have motivated researchers to investigate reconfiguration methodologies exclusively for the SPS [126, 57, 26, 25, 21, 22].

The optimization formulation for the electric SPS reconfiguration problem is represented generally in the form,

$$\max \sum_{i=1}^{N} X_i.W_i.P_i \tag{2.2}$$

subject to:

$$\sum_{i=1}^{M} X_{Gi} P_{gen} \geq \sum_{i=1}^{N} X_i P_i \tag{2.3}$$

In Equations (2.2)-(2.3), N and M are the number of the loads and generating units, respectively. W_i is the priority level associated with i^{th} load based on the operating ship's mission, P_i is the power consumption for i^{th} load; P_{gen} is the generated power for i^{th} generation unit; X_i is a breaker status corresponding to the i^{th} load; X_{Gi} is a breaker status corresponding to the i^{th} generator. The status of the breaker can take binary values: 0 and 1, representing the breaker `open` status and `closed` status, respectively.

A key point regarding this objective function is that the amount of the generation must be optimized. It means that the difference between the total generation and load consumption needs to be minimized. The inequality constraint in (2.3) implies that the total generation from the generation units must be greater than the available loads during the reconfiguration process. Power flow constraints for the power balancing requirements, voltage limits, and lines capacity must also be considered in this problem. If a solution does not satisfy these constraints, the optimizer tool must search for a new solution. In the reconfiguration problem, the decision variables are a set of binary variables representing the status of the loads' breakers. The reconfiguration objective is to find the optimal set of the loads' breakers statuses according to the objective function defined in (2.2).

Reconfiguration techniques in SPSs are classified into two categories according to the implementation strategy as discussed next.

2.6.1 Centralized Approach

Traditionally, centralized reconfiguration for service restoration of SPS has been recognized as an optimization problem where the objective function is to maximize the delivery power/current to the loads [126, 19]. To do so, one or more central controller(s) are required to deal with the reconfiguration problem of the distribution network(s). Currently-used techniques to solve the SPS reconfiguration problem include: heuristic search techniques [25], graph theory [113], network flow approach [26], expert system [100], etc. For instance, as a heuristic optimization approach, Genetic Algorithm (GA) is widely-utilized as one of the most powerful methods where the binary GA's variables are integrated into the problem formulation to search the optimal network configuration [131, 82, 7]. In [108], authors have proposed combined GA and graph theory algorithms to solve the reconfiguration problem for real-time configuration of the SPS. Particle Swarm Optimization (PSO) with Ant Colony Optimization (ACO) is used in [121] to find the optimal topology of the SPS's network while meeting the security constraints. In [123], a quantum differential evolution algorithm is proposed to solve the reconfiguration problem in SPS. In [105], GA and PSO optimization techniques are used for the real time implementation of reconfiguration problem in the SPS. However, as the number of feasible solutions increases during the reconfiguration process, the size of the optimization problem becomes critical, and the convergence properties may be affected as well. Therefore, existing approaches may not be appropriate for real-time operation of the SPSs. Dynamic Neighborhood Small Population Particle Swarm Optimization (DNSPPSO) is proposed in [126] to solve the reconfiguration problem in SPS. Compared to the conventional PSO, this optimization technique is much faster to find the optimal solutions.

Table 2.2: Comparison of different reconfiguration approaches

Reconfiguration Approach	Type	Remarks
Heuristic search techniques [7],[25],[121],[131]	Centralized	• These methods usually reach the optimum solution much faster than other techniques due to lesser computations • Due to their speed to find the final solution, they are suitable for online implementations
Graph theory [113]	Centralized	• SPS is modeled as a set of nodes and edges. • The faulted component is removed from the system. • Enables an extremely fast searching technique for nodes and branches of the tree • Enables an algorithmic arrangement of the list after a change in radial network structure
Network flow approach [26]	Centralized	The power and current flows are determined from the load flow analysis in the SPS.
Expert system [100]	Centralized	• Use of rule-based expert system by utilizing historical operating data such as system topology, load priorities. • This system may consist of several subsystems such as Failure Assessment System and Expert System based Restoration System
Multi-agent systems [114],[129]	Decentralized	• Instead of relying on centralized solution, distributed agents depend on component level solutions and cooperative performance of the agents

2.6.2 Decentralized Approach

Decentralized reconfiguration in an SPS can be achieved through a Multi-Agent System (MAS) approach. In this technique, the power supply is locally allocated to the loads after the faults take place to return the system to normal operation temporarily after an interruption in service [22]. In an MAS, several agents work jointly to achieve the target. Multi-agent models are adjusted to have cooperation and collaboration as well as autonomy [80, 70, 50]. In [114], the feeder automation system based on MAS is proposed for SPS restoration after contingencies. In the proposed operation scenario, since the capacity of the reserve generation is not sufficient to support all the loads, a load shedding strategy is used to restore service based on the loads and feeders priority. A novel fully-distributed MAS-based load restoration strategy is proposed in [129], where each agent makes synchronized load restoration decisions based on the local information, and each of the agents is assigned a direct communication channel with their direct neighbors.

2.6.3 Remarks on current approaches for system reconfiguration in SPS

Table 2.2 provides an overview of the different approaches to address the reconfiguring problem in the SPS. One of the main advantages of the centralized approaches for reconfiguration is that the central controller has access to all the required information. Therefore, in the case of a contingency, the central controller updates the system states to deal with the reconfiguration problem. The drawbacks of the centralized approach are their operation cost [79] and the fact that it may result in a single point of failure in the system if the system lacks redundancy [51, 112]. Meanwhile, the centralized problem formulation only considers global optimality of power delivery for the whole SPS which may not be ideal when only certain onboard sections are of interest [22]. In the decentralized approach, there is no central controller, and this prevents the system from a single point of failures. Moreover, the decentralized approach is more robust and has more flexibility compared to the centralized approach. The main disadvantage of the decentralized approach is that their capability to find the global optimal solution is limited compared to the centralized approach due to the limited access to the global system state.

2.7 Application of STATCOM situations in power systems

STATCOM is a Voltage Source Converter (VSC)-based regulating device which has the capability of absorbing and generating reactive power in AC transmission and distribution systems. STATCOM is a member of the Flexible Alternating Current Transmission System

(FACTS) devices family, which operates in shunt with the power system and has the ability to regulate voltage, damp oscillation, and improve the system stability in various transients, voltage flicker, and sag-swells [104]. It is also used to control the active and reactive power in the power system [133]. In order to maintain power system stability, many technical challenges need to be addressed; one of the most important issues is to minimize the effect of the short-term disturbances, particularly under unbalanced faults. In the case of faults in power systems, STATCOM will help the system by injecting reactive current to keep the bus voltage at the desired value, and it can also improve transient stability for the post-fault voltage recovery.

Several papers in the literature have addressed the application of the STATCOM in power systems to help the system to preserve the stability during the fault situations. A step-by-step approach has been presented in [99, 124] for the design of a nonlinear controller based on feedback linearization for STATCOM connected to the load bus of a single-machine infinite-bus power system. The results presented in these papers show an acceptable damping to the electromechanical oscillation of the synchronous generator under transient disturbances. In [78], the authors propose a proportional-integrator type adaptive critic design-based neuro-controller for a STATCOM design problem in a small and large multimachine power system during large-scale faults, as well as small disturbances.

2.8 Application of FACTS devices in SPS

There are only a few research works that have been done in the area of application of FACTS devices in electric ship power systems. In [128], an active filter is proposed for high-power adjustable-speed motor drives in electric ship propulsion systems in MVDC SPS as a viable solution to mitigating harmonic related issues caused by diode or thyristor rectifier front-ends. The application of a STATCOM to improve the power quality in a ship power system during and after pulse loads is investigated in [73]. It also proposes a novel adaptive control strategy for the STATCOM design problem based on Artificial Immune System (AIS). In [71], a series DC active filter is proposed in MVDC SPS to smooth out DC link ripples and improves overall system damping. The series active filter is providing a highly stabilized low-ripple DC-bus, which is crucial for the reliable operation of entire system. A Power Electronics Building Block (PEBB)-based shunt active power filter with digita1 control for future naval electric distribution systems has been proposed in [52] to maintain some minimum acceptable level of power quality.

2.9 Application of Superconducting Fault Current Limiters (SFCL) in power systems

There are many solutions proposed in the literature to minimize the effect of the fault current in the power systems [130]. These methods include reconfiguring the power system topology [74], installing a Current-Limiting Reactor (CLR), increasing Circuit Breaker (CB) capacity, and utilizing Superconducting Fault Current Limiters (SFCL) [36, 76]. Recently, application of SFCLs to minimize the fault current in power systems have been attracted many research works. In the normal operation, the SFCL has a negligible impedance. If a current flown through the SFCL passes a certain threshold, the impedance of the SFCL will be increased to impede the fault current [47]. The SFCLs can improve the stability of the power system by mitigating the fault current level in a fast and effective way. There are two major categories for the SFCL including resistive and inductive SFCLs. Resistive-type SFCL (R-SFCL) is the simplest type of the SFCL.

Many studies have been devoted to the application of SFCLs in power system. The optimal design objectives considered in these works are as follows [117].

- Optimal location to install the SFCL.
- Optimal impedance of the SFCL.
- Coordination between SFCLs and the other protective devices.

Several studies have been conducted for optimal allocation of SFCL in power systems. In [115], the optimal impedance of an SFCL has been selected by analyzing the transient stability index based on the equal-area criterion. Comparison of the SFCL and the Dynamic Voltage Restoration (DVR) for enhancing the Low Voltage Ride-Through (LVRT) capability in a microgrid has been carried out in [32]. In the power networks with several generators, the authors in [37] have proposed an approach to select the optimal location of the SFCL based on sensitivity analysis of the angular separation of the rotors of synchronous machines. Application of a combined SFCL and STATCOM to improve the stability of the power system has been investigated in [66]. To select the optimal location of the SFCL, sensitivity analysis of variation in active power in the system with respect to the SFCL's resistive value during a fault has been conducted in [117]. To determine the optimal impedance value of the SFCL, an equal-area criterion analysis based on the power-angle curves has been utilized in [116]. An approach to finding the optimal location to install the SFCL in power systems has been proposed in [36] considering different types of faults.

2.10 Conclusion

In this chapter, the state-of-the-art fault management techniques in electric ship power systems have been reviewed. We first break down the overall fault management problem into several aspects, including fault detection and location, fault isolation, and post-fault reconfiguration. Then, an in-depth review of current fault management methods and techniques to mitigate the effect of faults on the system reliability and performance has been presented. Furthermore, some research background regarding the fault management in electric ships are discussed.

CHAPTER III

A NOVEL APPROACH FOR REAL-TIME IMPLEMENTATION OF MVDC SHIPBOARD POWER SYSTEM RECONFIGURATION

3.1 Introduction

Several papers in the literature have dealt with the reconfiguration problem in power systems [89, 120, 91, 74, 23, 132, 81, 94, 6, 92]. The reconfiguration objectives considered in these works include power loss reduction [89], preserving of the stability margins [120], minimization of the number of switch operations [91], and maximizing the number of the served loads [92]. However, in SPS, due to the underlying tightly-coupled distribution network, the active power loss is considered negligible compared to the other types of power systems, and it is not considered as a critical objective for SPS reconfiguration problem [74]. Another unique feature of SPS is that the priorities of the loads in different missions are different; thus, this fact also needs to be taken into account during the reconfiguration process. These features have motivated researchers to investigate reconfiguration methodologies exclusively for the SPS.

Currently-used techniques to solve the SPS reconfiguration problem include: meta-heuristic search techniques [120], graph theory [9], network flow approach [4], and expert system [101]. As a meta-heuristic optimization approach, Genetic Algorithm (GA) is widely adopted in literature, where the binary GA's variables are integrated into the problem formulation to search the optimal network configuration [41, 8]. In [107], authors have proposed a combined GA and graph theory algorithm to solve the reconfiguration problem for real-time analysis of the SPS. Particle Swarm Optimization (PSO) with Ant Colony Optimization (ACO) is used in [122] to find the optimal topology of the SPS's network while meeting the security constraints. However, as the number of feasible solutions increases during the reconfiguration process, the size of the optimization problem becomes critical, and convergence may be affected. Therefore, existing approaches may not be applicable for real-time operation of the SPS.

Real-time power system simulations can be done through Real Time Digital Simulator (RTDS) and its Graphical User Interface (GUI)-based design platform (RSCAD). A reconfiguration problem is essentially an optimization problem in which commercial simulation programs such as MATLAB and RTDS-MATLAB interface platforms are used to simulate and implement the problem [74, 107]. In [74], an intelligent reconfiguration strategy for a Medium Voltage AC (MVAC) is implemented in the RTDS, where the reconfiguration algorithm is executed on the Digital Signal Processor (DSP). A Real-Time Automation Controller (RTAC) is used in [107] to perform the reconfiguration. However, those approaches require intensive computation overhead and need extensive simulations due to the complexity of SPS models. Therefore, there would be an inconsistency between the time required for actual hardware operation and that for software computation [17, 96].

Another issue regarding the real-time implementation of the SPS reconfiguration problem is the communication delay between the RTDS and other optimization platforms. A communication delay is resulted from the synchronization and communication between the optimization tools such as MATLAB and the RTDS to exchange the information. This information include the power network's states from the RTDS and computed control outputs from the optimization tool. One approach to deal with this issue is to utilize the script environment inside the Runtime environment of RSCAD software in the RTDS to reduce the communication delays. With the proposed approach, the implementation of the optimization technique happens inside the RTDS, and it will remove the extra communication between RTDS and other computational platforms such as MATLAB. There have been no systematic approach to address the MVDC SPS reconfiguration problem, particularly with a full RTDS implementation. This study aims to implement an intelligent real-time reconfiguration algorithm in the RTDS platform through an optimization technique implemented inside the RTDS.

Generally, the use of the RTDS scripting environment is sometimes computationally infeasible due to the limited functionality of the RTDS scripting language. In this dissertation, Simulated Annealing (SA) optimization technique, which enjoys some advantages over other meta-heuristic methods, is employed to solve the reconfiguration problem in RTDS. The main advantage of SA optimization technique is its simplicity, even for complex problems. In addition, this algorithm is not a population-based algorithm, which makes the algorithm less computationally expensive.

The main contributions of this study are summarized as follows.

- With respect to the previous research works on the topic, such as [74, 107, 106], this study is presenting a novel approach to implement the real-time intelligent reconfiguration of the SPS. In this work, the detailed modeling of the MVDC SPS has been performed with RTDS, which is the closest representation of the real SPS. With the proposed approach, the extra communication between RTDS and other optimization platforms such as MATALB will be removed, and the RTDS scripting environment is utilized to solve the reconfiguration problem.

- The SA optimization technique has been employed to solve the reconfiguration optimization problem and find the local optimal set of switches after the fault occurrence in the RTDS. This method has some advantages compared to the other meta-heuristic methods, such as flexibility and its likelihood to approach the local optimality, that make it suitable for the real-time implementation of the MVDC SPS reconfiguration.

3.2 MVDC shipboard power system reconfiguration problem

A new system integration and multi-zonal power distribution architecture called Medium-Voltage DC (MVDC) has been developed for shipboard power distribution. The MVDC SPS microgrid has several advantages compared with traditional MVAC architecture including [134]: improved management of faults and disturbances utilizing the controlled power electronics devices and enhanced power transfer capability based on the DC level. The model that represents an MVDC architecture is shown in Figure 3.1. This architecture employs two 5kV main DC bus (Port bus and Starboard bus), which are fed by main and auxiliary generators. The MVDC SPS system is divided into a number of electric zones, and each zone has load centers that are connected to both the Port bus and Starboard bus [109]. Each zonal load can be fed from one of the main DC buses at a certain time. The zonal loads are categorized into three types according to their priority in each ship's mission operation modes: *Vital Loads* (VL), *Semi-Vital Loads* (SVL), and *Non-Vital loads* (NVL). Thus, during the reconfiguration process of the SPS, the loads' priority levels need to be taken into account. In the case of emergency, non-vital loads must be shed to keep power in the vital and semi-vital loads.

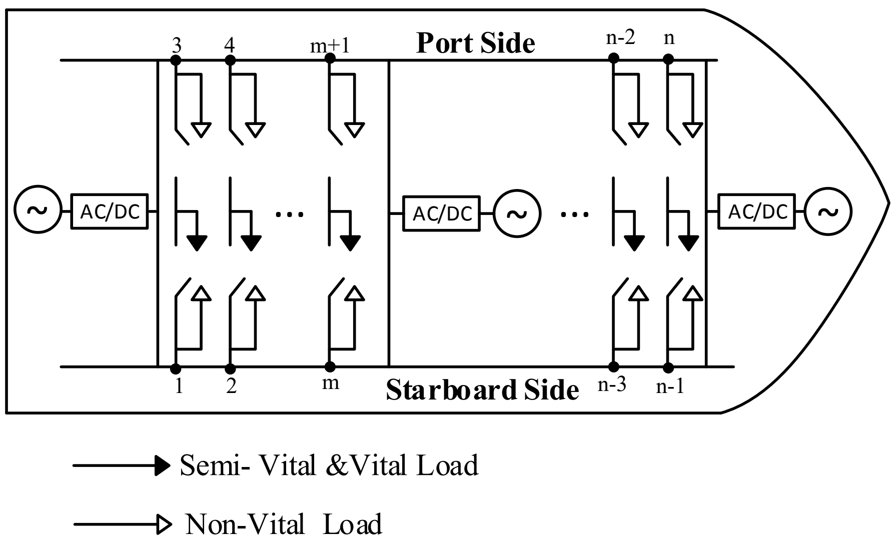

Figure 3.1: Zonal MVDC shipboard power system model

In the operation of the SPS, in order to ensure the maximum delivery power/service to the system's load following a fault, the shipboard network needs to be automatically reconfigured. In this dissertation, two objectives are considered in order to deal with the reconfiguration optimization problem for the MVDC SPS as follows.

- Maximizing the total served load based on the loads' magnitude.
- Maximizing the total served load based on the loads' priority.

Hence, the overall objective function of the reconfiguration problem is formulated as follows:

$$\max J = aJ_1 + bJ_2 \tag{3.1}$$

where:

$$J_1 = \sum_{i=1}^{N} X_i P_i \tag{3.2}$$

$$J_2 = \sum_{i=1}^{N} W_i X_i P_i \tag{3.3}$$

subject to

$$\sum_{i=1}^{M} X_{Gi} P_{gen} \geq \sum_{i=1}^{N} X_i P_i \tag{3.4}$$

In Equations (3.1)-(3.4), N and M are the number of the loads and generating units, respectively. W_i is the priority level associated with i^{th} load based on the operating ship's mission, P_i is the power consumption for i^{th} load; P_{gen} is the generated power for i^{th} generation unit; X_i is a breaker status corresponding to the i^{th} load; X_{Gi} is a breaker status corresponding to the i^{th} generator. The status of the breaker can take binary values: 0 and 1, representing the breaker `open` status and `closed` status, respectively. Parameters a, b are the weighting factors that are adjusted to reflect the relative importance of each objective function with respect to the other in the overall objective function defined in (3.1). In this study, the factor a will be set to 0, where the objective of the reconfiguration is to maximize the total loads' power consumptions based on the loads' priority levels, and b will set to 0, where the objective is to maximize the total power consumptions by each load regardless of the loads' priority. A key point regarding this objective function is that the amount of the generation must be optimized. It means that the difference between the total generations and load consumptions needs to be minimized. The inequality constraint in (3.4) implies that the total generation from the generation units must be greater than the available loads during the reconfiguration process. Power flow constraints for the power balancing requirements, voltage limits, and lines capacity are also considered in this problem. If a solution does not satisfy these constraints, it will be rejected, and the SA optimization will search for a new solution.

3.3 Simulated Annealing Algorithm

3.3.1 Framework of Simulated Annealing

Simulated Annealing (SA) is a probabilistic meta-heuristic method that is inspired by the physical gradual cooling procedure that produces crystals, which is successfully utilized in many optimization problems [53]. In this process, the temperature of a solid is increased to a high temperature, and this causes particles of the solid to move randomly and organize themselves in the liquid phase. After this phase, by slowly decreasing the temperature, the solid will reach thermal equilibrium. At each temperature T, the system reaches an equilibrium in such a way that the probability that the system is in some state with energy E is given by (3.5).

$$P(E=k) = \frac{e^{\frac{-(E-E_0)}{k_b T}}}{Z(T)} \tag{3.5}$$

where:

- $Z(T)$: Normalization function
- k_b: Boltzmann constant
- E: Current state of the system energy
- E_0: New state of the system energy
- T: Temperature

Unlike many other meta-heuristics that use a maximum number of iterations, SA has built-in stopping criteria checkpoint. SA allows the temperature to decrease until it reaches zero. Once the temperature is zero, SA has frozen the solution, and that signifies the stopping of the algorithm. While this approach may lead the algorithm to have a longer runtime, the cooling can be adjusted based on the needed accuracy. In this research work, the number of cooling steps for each case study is adjusted after observing the SA optimization behavior in finding the local optimal solutions. This setting has shown to result in average steady convergence.

A general SA optimization is implemented by the following steps [95].

- **Step I**: Starting with an initial temperature T_0, pick an initial set of parameter values with function value E.

- **Step II**: Select another point in the search space randomly within a neighborhood of the original point, and calculate the objective value.

- **Step III**: The difference between the objective value of the current solution, $\Delta = E_{new}$-E_{old} is computed. If $\Delta \geq 0$, the new solution is stored, otherwise, it will be stored with a probability of $p = exp(\Delta/T)$.

- **Step IV**: Whether the new solution is accepted or not, repeat steps I-III. At each stage, compare the function value of new points with the function value of the present point until the sequence of accepted points is judged, by some criterion, to have reached a state of equilibrium.

- **Step V**: For a given temperature, once an equilibrium state has been found, the temperature is decreased to a new temperature as described by the annealing schedule. Then, the process initiates again from step II, and the point after the last iteration of the algorithm will be taken as an initial state, and this procedure will continue until some stopping criterion is satisfied.

By making an analogy between the annealing process and the optimization problem, a great class of optimization problems can be solved following the same procedure of transition from an equilibrium state to another, reaching a minimum energy of the system. The solutions to an optimization problem are equivalent to the states of the physical system, and the cost of a solution is equivalent to the energy of a state. In applying the SA algorithm to solve an optimization problem, the main idea is to choose a feasible solution randomly and then find a neighbor to this solution. It is also important to have a proper rule to find a diversified neighborhood so that a large amount of solution space can be explored.

3.3.2 Application of SA technique for MVDC SPS reconfiguration

In this reconfiguration problem, the decision variables are a set of binary variables representing the status of the loads' breaker statuses. The reconfiguration objective is to find the local optimum set of the loads' breaker statuses according to the objective function defined in (3.1). The objective values are extracted from the (3.2) and (3.3) according to the desired objective function either maximizing the total served load base on the loads' magnitude or priority. Then, the constraint defined in (3.4) is integrated to the objective function as a penalty factor. The parameter temperature (T) is defined as an absolute value of the difference between the calculated objective function and the penalty factor. Consequently, the value of cooling step (annealing schedule) is calculated by (3.6).

$$\text{Cooling step for reconfiguration problem} = \frac{T}{\text{Maximum number of iteration}} \tag{3.6}$$

where,

$$T = |\text{calculated objective function from (3.2) and (3.3)} - \text{calculated penalty factor from (3.4)}| \tag{3.7}$$

The SA optimization uses binary chromosomes for the sake of initialization or finding new answers. A binary chromosome is the most commonplace chromosome that is used, especially in genetic programming. It refers to a set of ones and zeros, in which the underlying formations have special meaning to the problem they are solutions for. Here, each 1 stands for a switch being closed and 0 being open. For instance, in a system with 5 switches, the chromosome, $[1,0,0,1,0]$, implies that switches 1 and 4 are closed and switches 2,3, and 5 are open. In each step, the switches' states vectors are used to calculate the energy state based on the objective function defined in (3.1). This means that the energy state represents the calculated objective function in each step. The process of changing the current answers is done by a random change of cells. The cells filled with 0 will change to

1, and the cells filled with 1 will change to 0. The number of cells that will change is also controlled by the intensity factor. The behavioral parameter of SA, after empirical tuning process, is set for an intensity equal to 0.7.

3.4 Hardware implementation of MVDC SPS reconfiguration

3.4.1 Real-Time Digital Simulator (RTDS) overview

RTDS is a digital electromagnetic transient power system simulator that operates in real time and is capable of simulating power system networks at a pace of real-world clock time. The main difference between real-time simulators and non-real-time simulation platforms is the execution time of the simulation, i.e., the time it takes to solve the system equations and deliver back the output results. One of the advantages of RTDS is that the overall processing procedure is executed in parallel. The entire hardware unit is bundled into modular units called racks. Inside each rack, there are various digital signal processors, such as Giga Processor Card (GPC) and Triple Processor Card (TPC), that are used for solving the overall network solution and auxiliary components.

RSCAD is a Graphical User Interface (GUI) that is utilized by RTDS for the simulation operation. The RSCAD consists of different modules that are designed to allow the user to execute all the necessary steps to design and run the simulations, and it allows the user to analyze simulation output. It is mainly used for creating, simulating and evaluating power systems network models. The RSCAD's library gives access to the pre-defined power system components and control system models. The built model in the RSCAD draft must be compiled to assure that there is no error in the system's configuration and the processors are correctly assigned. The model needs to be compiled inside the Draft without any compilation errors, so the system can be run in the Runtime environment of the RCSCAD software. In the Runtime, the user will be able to control and interact with the simulation, and it mainly serves as the graphical user display for monitoring and control actions.

The Runtime module in RSCAD allows the user to check the system at run-time, change the values of inputs using sliders and add switches where there is a need for breakers in the power network. This also provides meters and plots to check the system's response. Moreover, it provides the simulation results and also contains the script file, which can be programmed to run continuous loops of the simulation in the case of relay testing and power system automation.

3.4.2 Conventional methods for real-time implementation of optimization in power systems

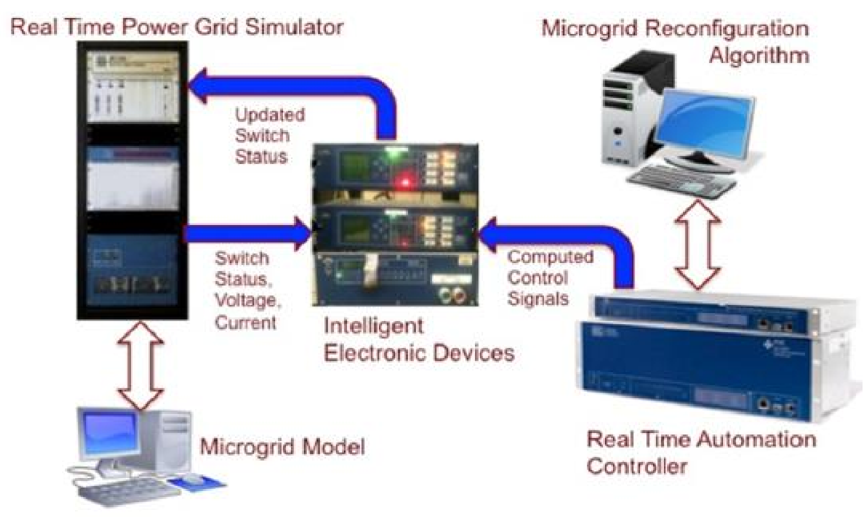

Figure 3.2: Example testbed for real-time microgrid reconfiguration from [107]

As discussed earlier, the RTDS is used for real-time operation and control of power networks. Many algorithms for power systems resiliency, reconfiguration, real-time control, and operation have been developed. For most of these studies, it is necessary to validate and analyze the system in the real-time application [45]. For example, Figure 3.2 depicts a conventional testbed for real-time modeling and simulation of microgrid reconfiguration. In this testbed, the reconfiguration algorithm is running in a controller-in-the-loop in the real-time. The system model is built in the RTDS, and Intelligent Electronic Devices (IEDs) are used to collect the input signals required for the optimization algorithm running in RTAC.

For most of the optimization-based studies in real-time, there are external devices to make a connection between the RTDS and optimization platforms as shown in Figure 3.3. Intrinsically, these approaches include communication platforms which can add more complexity to the implementation process.

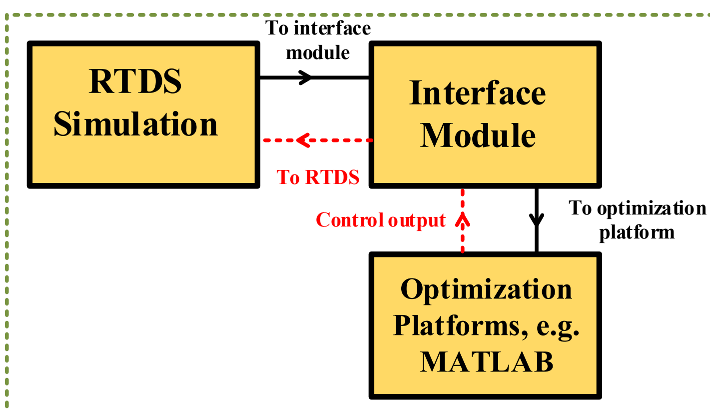

Figure 3.3: General schematic of the conventional RTDS interface with optimization platforms

3.4.3 Proposed approach for real-time implementation of optimization in power systems

The presented approach for real-time implementation of optimization-based power studies removes the extra communication between RTDS, and optimization platforms by implementing the optimization inside the RTDS. The proposed technique does not add any computational burden on the RTDS's processors as the optimization is executed on the RSCAD software. Figure 3.4. demonstrates the proposed scheme. In this approach, the interface module, which is the communication platform between the RTDS and the optimization platform is removed, and the optimization algorithm is implemented with the Unified Modeling Language (UML) in Runtime module in RSCAD software.

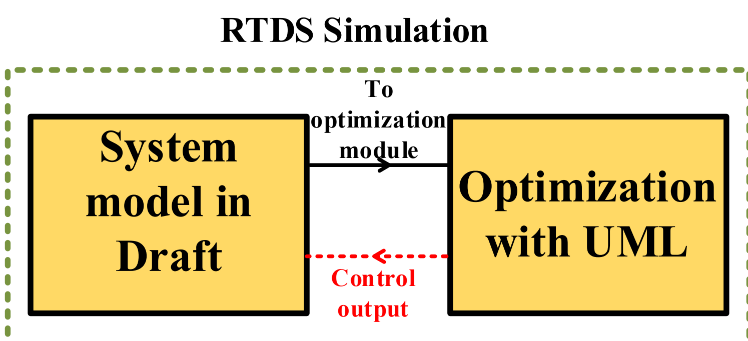

Figure 3.4: General schematic of the proposed RTDS interface with optimization platforms

UML in RSCAD Runtime module can be translated into a C program, and it is used to perform consecutive simulations. This feature can introduce additional functions or events to the system at runtime. Moreover, conditional/adaptive looping via `if-else`, `for` and `while` statements may also be added to the script file to increase the functionality of the simulation. The general configuration between the RTDS modules is depicted in

Figure 3.5. In this test setup, first, the detailed model of the MVDC SPS is built in the Draft module of the RSCAD. Then, the necessary switches indicating the loads' breakers and generators' breakers statuses are added in the Runtime module of the RSCAD. Inside the Runtime module, the UML is exploited to read the breakers' statuses and perform the necessary functions to implement the intelligent reconfiguration in case of a fault. The calculated optimal value of the breakers is returned to the Runtime module as the controller output.

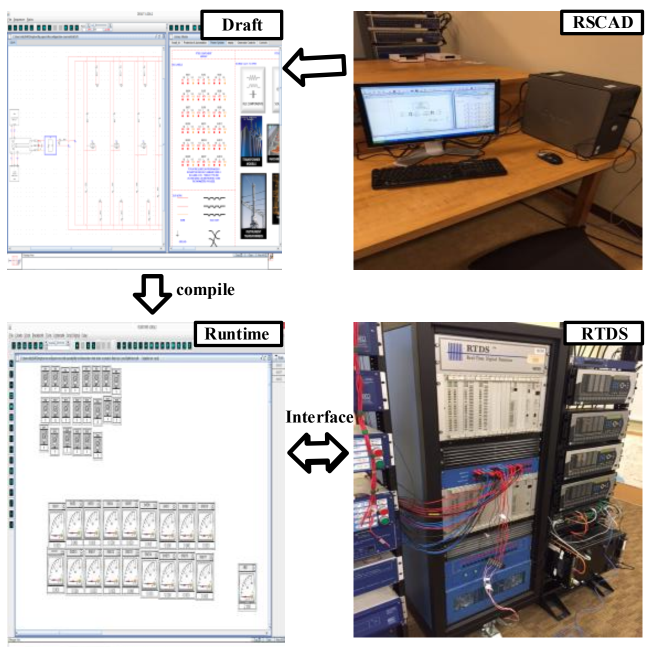

Figure 3.5: Real-time implementation setup using the RTDS

The following are the most important commands in the UML that are employed to perform the SA-based reconfiguration.

- `MetereCapture`: This command will return the current value of a meter. It is used to send the status of the generators' and loads' breakers to the script file.

- `SetSwitch`: This command will set a switch appearing on the Runtime page to a particular position, and the switches' statuses, calculated by the optimization, is sent back to the simulation through this command. If this command is set to 0 or 1, the switch will be set to the `off` or `on` position, respectively.

- `for`, `while`, and `if-else`: These commands are employed to build the main SA optimization and implement the reconfiguration algorithm.

Figure 3.6 shows the UML coding environment where the SA-based reconfiguration has been implemented. The system model including the generators and the zonal loads are modeled in RSCAD draft module. In the reconfiguration process, the loads' and switches' statuses will be read from the Runtime into the UML, and then the total generations and consumption are calculated according to the following equations.

$$\text{total available generation} = \sum_{i=1}^{M} X_{Gi} Pgen \tag{3.8}$$

$$\text{total available load} = \sum_{i=1}^{N} X_i Pi \tag{3.9}$$

If the total available generation is less than the total available loads' consumption following a fault in the system, the SA optimizer searches the local optimal switches statuses within the script according to the objective function defined in (3.1). The `SUSPEND` command is used in the script as a delay function. This command allows the reconfiguration algorithm inside the script environment to receive the system states from the Runtime. The overall procedure for implementing the SA algorithm inside the RTDS Runtime environment is shown in Figure 3.7.

```
Start
UpdatePlots
/* Apply the fault by disconnecting the generator */
SetSwitch  Subsystem #1 : CTLs : Inputs : SW1  =0 ;
SUSPEND 0.5;
captureMeterFunction ();
/* read the loads and generators status */
function captureMeterFunction
{
Xl [0] = MeterCapture ( SWD2 ) ;
                .
                .
                .
Return (0)
}
/* Calculate Pgen and Pload based on the system model in draft file */
If (Pgen<Pload)
{
/* Solve the SA-based reconfiguration optimization */
}
/* Set the optimized value to the switches */
SetSwitch  Subsystem #1 : CTLs : Inputs : SW2  =BDecision [1] ;
```

Figure 3.6: SA-based reconfiguration in RSCAD script environment

3.5 Results and discussion

To validate the performance of the proposed SA-based reconfiguration, two MVDC models with four and six zonal loads have been considered in this study as shown in Figure 3.8. The SA-based reconfiguration optimization is implemented in RSCAD software scripting environment. In this section, General Algebraic Modeling System (GAMS) software is used as a powerful optimization tool to verify the results from the RTDS-based reconfiguration.

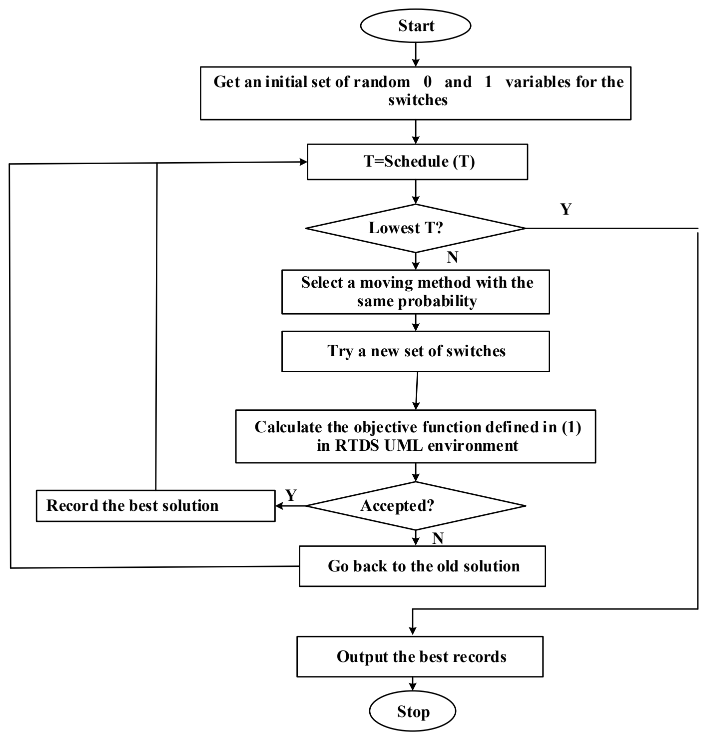

Figure 3.7: Overall procedure of optimization process via the RTDS

The reconfiguration optimization is applied to the MVDC SPS with four and six zonal loads to find the local optimal switching status vector after the occurrence of a contingency in the system. Three assumptions have been made in this study as follows.

- If a fault happens in the system, the protection system will immediately isolate the faulty sections from the rest of the system.

Table 3.1: Zonal Loads' consumption Characteristics a) four zone b) six zone

Load	**Consumption (MW)**	**Load**	**Consumption (MW)**
L_1	1.5	L_7	1.5
L_2	1	L_8	1.5
L_3	4	L_9	1
L_4	2.5	L_{10}	1.5
L_5	2	L_{11}	1
L_6	2.5	L_{12}	3

(a)

Load	**Consumption (MW)**	**Load**	**Consumption (MW)**
L_1	1.5	L_{10}	1
L_2	1	L_{11}	1
L_3	4	L_{12}	1
L_4	2.5	L_{13}	3
L_5	2	L_{14}	2
L_6	2.5	L_{15}	2.75
L_7	1	L_{16}	1
L_8	1.5	L_{17}	3.25
L_9	4	L_{18}	5.5

(b)

Table 3.2: Zonal Loads' generating units characteristics a) four zone b) six zone

	P_{max} (MW)	**P_{min} (MW)**	**Type**
Unit 1	20	0	Main
Unit 2	7	0	Auxiliary

(a)

	P_{max} (MW)	**P_{min} (MW)**	**Type**
Unit 1	28	0	Main
Unit 2	10	0	Auxiliary

(b)

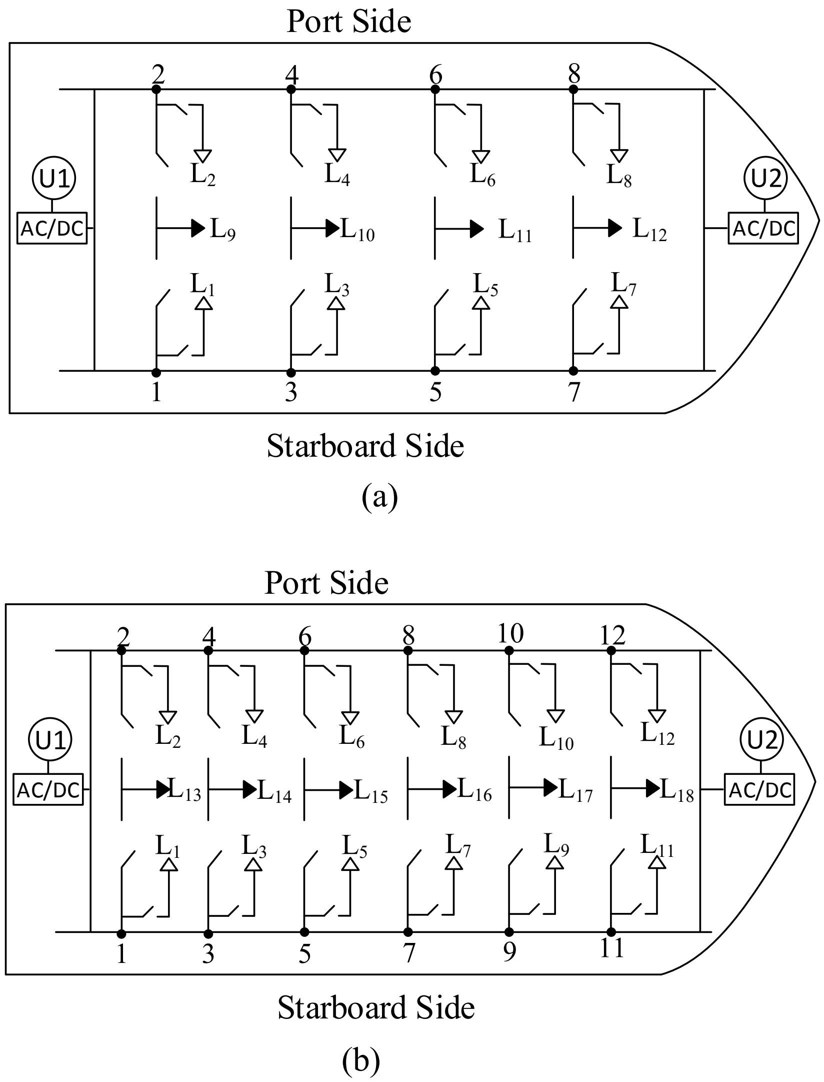

Figure 3.8: MVDC SPS model with a) four b) six zonal loads

- Partial load shedding is not possible for the loads. It means that the loads can only be in `on` or `off` positions.
- It is assumed that the summation of available generations is sufficient to feed all the power consumption units under normal operation.

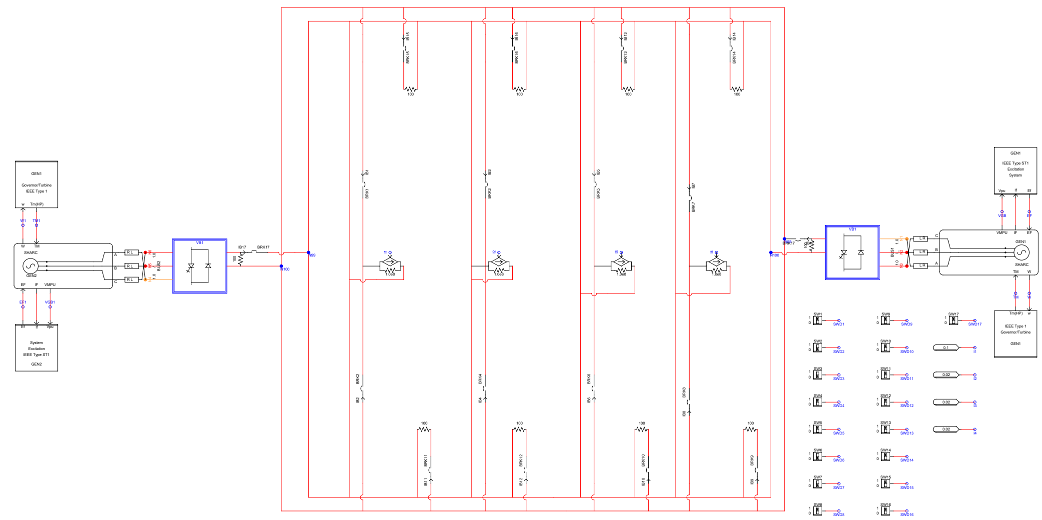

Figure 3.9: MVDC SPS four zonal load in RSCAD draft

3.5.1 RTDS-based case study

The MVDC SPS models are modeled in RSCAD Draft environment as shown in Figure 3.9. Tables 3.1-3.2 show the power consumptions by each individual load in the zonal loads, the generation units' output power for each model, respectively. Loads' priority levels, with respect to the ship's mission, are tabulated in Table 3.3. According to these tables, onboard loads tend to change priorities according to the current operating conditions or the mission requirements. In this study, we try to use the values of loads, generation units, and loads' priorities as close as to the real MVDC SPS. The loads' priorities have a direct relation to the parameters that assigned to each load in any mission. For example, the priorities of loads L_1 and L_{10} are 1 and 3 in the cruise mode of ship operation, respectively. This shows the lower importance of L_1 compared with L_{10} in this mode of operation.

Table 3.3: Zonal Load's priority in different ship missions a) four zone b) six zone

	L_1	L_2	L_3	L_4	L_5	L_6	L_7	L_8	L_9	L_{10}	L_{11}	L_{12}
Cruise	1	1	1	1	1	1	1	1	3	3	6	6
Battle	1	1	5	5	1	1	1	1	1	1	3	3
Anchor	1	1	1	1	1	1	1	1	2	2	2	2

(a)

	L_1	L_2	L_3	L_4	L_5	L_6	L_7	L_8	L_9	L_{10}	L_{11}	L_{12}	L_{13}	L_{14}	L_{15}	L_{16}	L_{17}	L_{18}
Cruise	1	1	1	1	1	1	1	1	1	1	1	1	3	3	3	6	6	6
Battle	1	1	1	5	5	5	1	1	1	1	1	1	1	1	1	2	2	2
Anchor	1	1	1	1	1	1	1	1	1	1	1	1	2	2	2	2	2	2

(b)

Different fault scenarios have been considered in this dissertation to validate the performance of the proposed reconfiguration strategy as follows.

- Case 1: loss of auxiliary generator
- Case 2: loss of main generator
- Case 3: islanding scenario
- Case 4: islanding scenario; effect of pulse load

Tables 3.4-3.5 show the simulation results of the intelligent reconfiguration for two MVDC SPS models depicted in Figure 3.8 in different fault scenarios. The feasible solutions for each problem may be calculated by 2^n, n being the number of switches on each problem. For example, Case 1 in Table 4 has 2^{12}, meaning there are 4,096 possible settings for the switches. An exhaustive simulation in RTDS for this number of possibilities is very time-consuming. The method proposed in this research work will only run the simulation for, at most, 75 times which is significantly smaller. To show the significance of the method presented, the last column in Tables 3.4, 3.5 and 3.7 show the estimated exhaustive search time for each case. This column has been calculated by the number of simulations that need to be run multiplied by the average simulation runtime of each case. This shows the merits of the proposed SA-based reconfiguration to find the local optimal set of switches following a fault in the system. It is worth mentioning that for each case, the SA-based optimization was run 50 times, and the results shown in the tables are the average values of all the runs.

3.5.1.1 Case 1: loss of auxiliary generator

In this scenario, the auxiliary generator is tripped off-line due to an internal fault, and the main generator cannot provide sufficient power for the connected loads. In this case, load shedding is performed by the proposed reconfiguration algorithm. Suppose that the ship with four zonal loads is in the cruise mode, and the auxiliary generator is disconnected from the rest of the system by the protection system. In this case, the total available generation and total available load are 20 and 23 MW, respectively. This needs to shed at least 3 MW loads consumption. With respect to the loads' priorities shown in Table 3.3 in the cruise mode, loads L_9-L_{12} have the highest priorities and they must be in service in this scenario. According to Table 3.4, the intelligent reconfiguration suggests shedding L_2,L_5 and L_1,L_8 for the cases, where loads' magnitudes and loads' priorities are of our interest, respectively. All the loads suggested for load shedding action have the least priority levels in this case.

Now suppose that the SPS with six zonal loads is in the battle mode, and the auxiliary generator is out of service. In this case, loads L_4-L_6 are vital, and L_{16}-L_{18} are in the semi-vital category. Thus the reconfiguration optimization suggests to shedding the non-vital loads including L_1,L_3,L_9, and L_{13} for the case, where load's priorities have a greater impact on the objective function.

3.5.1.2 Case 2: loss of main generator

In Case 2, it is assumed the main generator is not providing any power to the system. To compare the influence of the weighting factors a and b on the reconfiguration optimization results, it is assumed that the SPS with four zonal loads is operating in the cruise mode and needs to change the operating mode to the anchor mode. In this case, as it can be seen from Table 3.4, loads L_9-L_{12} have the highest priority level. The simulation results in this table show that the reconfiguration algorithm suggests to serving loads L_2, L_7, L_8, L_{12}, where the loads' magnitude has a greater importance in the objective function. Here, the total magnitude of the served loads is 7 MW. If the objective is to serve the loads based on their priorities, reconfiguration algorithm suggests to serve loads L_9-L_{12}, where total load consumption would be 6.5 MW.

The same decisions have resulted for the SPS with six zonal loads. For example, loads L_{13}-L_{18} in the cruise operation have the highest priority among the loads. So, the reconfiguration solution proposes to keep these loads connected and shed the rest of the loads to keep the vital and semi-vital loads in service. In this case, according to the objective weighting factors a and b, the total available loads are 10 MW and 9.75 MW, respectively.

Table 3.4: Simulation results for SPS with four zonal loads

Case Study	Load shedding suggestion	Load served (MW)	Total generation (MW)	Execution time(s)	Exhaustive search (s)
Case 1					
Cruise					
a=1,b=0	L_2,L_5	20	G1=20	7.2	983.04
a=0,b=1	L_1,L_8	20	G1=20	7.1	969.38
a=0.5,b=0.5	L_1,L_8	20	G1=20	7.1	969.38
Battle					
a=1,b=0	L_2,L_5	20	G1=20	7.2	983.04
a=0,b=1	L_1,L_7	20	G1=20	7.1	969.38
a=0.5,b=0.5	L_1,L_7	20	G1=20	7.1	969.38
Anchor					
a=1,b=0	L_2,L_5	20	G1=20	7.2	983.04
a=0,b=1	L_1,L_8	20	G1=20	7.3	996.69
a=0.5,b=0.5	L_1,L_8	20	G1=20	7.3	996.69
Case 2					
Cruise					
a=1,b=0	L_1,L_3-L_6,L_9-L_{11}	7	G2=7	10.5	1075.2
a=0,b=1	L_1-L_8	6.5	G2=7	10.2	1044.48
a=0.5,b=0.5	L_1-L_8	6.5	G2=7	10.2	1044.48
Battle					
a=1,b=0	L_1,L_3-L_6,L_9-L_{11}	7	G2=7	10.5	1075.2
a=0,b=1	L_1,L_2,L_5-L_{12}	6.5	G2=7	10.8	1105.92
a=0.5,b=0.5	L_1,L_2,L_5-L_{12}	6.5	G2=7	10.8	1105.92
Anchor					
a=1,b=0	L_1,L_3-L_6,L_9-L_{11}	7	G2=7	10.4	1064.96
a=0,b=1	L_1-L_8	6.5	G2=7	10.2	1044.48
a=0.5,b=0.5	L_1-L_8	6.5	G2=7	10.2	1044.48
Case 3					
Cruise					
a=1,b=0	L_5,L_8,L_{11}	18.5	G1=11.5 , G2=7	14.9	1220.608
a=0,b=1	L_5,L_6	18.5	G1=11.5 , G2=7	14.2	1163.26
a=0.5,b=0.5	L_5,L_6	18.5	G1=11.5 , G2=7	14.2	1163.26
Battle					
a=1,b=0	L_5,L_8,L_{11}	18.5	G1=11.5 , G2=7	14.8	1212.416
a=0,b=1	L_5,L_6	18.5	G1=11.5 , G2=7	14.2	1163.26
a=0.5,b=0.5	L_5,L_6	18.5	G1=11.5 , G2=7	14.2	1163.26
Anchor					
a=1,b=0	L_5,L_8,L_{11}	18.5	G1=11.5 , G2=7	14.8	1212.416
a=0,b=1	L_5,L_6	18.5	G1=11.5 , G2=7	14.2	1163.26
a=0.5,b=0.5	L_5,L_6	18.5	G1=11.5 , G2=7	14.2	1163.26

Table 3.5: Simulation results for SPS with six zonal loads

Case Study	**Load shedding suggestion**	**Load served (MW)**	**Total generation (MW)**	**Execution time(s)**	**Exhaustive search (s)**
Case 1					
Cruise					
a=1,b=0	L_2-L_5,L_7,L_{10},L_{11}	28	G1=28	11.2	58720.256
a=0,b=1	L_1,L_4,L_7-L_9,L_{11},L_{12}	28	G1=28	11.4	59768.832
a=0.5,b=0.5	L_1,L_4,L_7-L_9,L_{11},L_{12}	28	G1=28	11.4	59768.832
Battle					
a=1,b=0	L_2-L_5,L_7,L_{10},L_{11}	28	G1=28	11.4	59768.832
a=0,b=1	L_1,L_3,L_9,L_{13}	28	G1=28	11.7	61341.696
a=0.5,b=0.5	L_1,L_3,L_9,L_{13}	28	G1=28	11.7	61341.696
Anchor					
a=1,b=0	L_2-L_5,L_7,L_{10},L_{11}	28	G1=28	11.4	59768.832
a=0,b=1	L_1,L_4,L_7-L_9,L_{11},L_{12}	28	G1=28	11.4	59768.832
a=0.5,b=0.5	L_1,L_4,L_7-L_9,L_{11},L_{12}	28	G1=28	11.4	59768.832
Case 2					
Cruise					
a=1,b=0	L_1-L_7,L_9,L_{13}-L_{17}	10	G2=10	13.5	64521.32
a=0,b=1	L_1-L_{15}	9.75	G2=10	13.9	65893.85
a=0.5,b=0.5	L_1-L_{15}	9.75	G2=10	13.9	65893.85
Battle					
a=1,b=0	L_1-L_7,L_9,L_{13}-L_{17}	10	G2=10	13.5	64521.32
a=0,b=1	L_1-L_3,L_7-L_9,L_{11},L_{13}-L_{15},L_{17},L_{18}	10	G2=10	13.1	62446.98
a=0.5,b=0.5	L_1-L_3,L_7-L_9,L_{11},L_{13}-L_{15},L_{17},L_{18}	10	G2=10	13.1	62446.98
Anchor					
a=1,b=0	L_1-L_7,L_9,L_{13}-L_{17}	10	G2=10	13.5	64521.32
a=0,b=1	L_1-L_{11},L_{13},L_{18}	10	G2=10	13.1	62446.98
a=0.5,b=0.5	L_1-L_{11},L_{13},L_{18}	10	G2=10	13.1	62446.98
Case 3					
Cruise					
a=1,b=0	L_9,L_{11},L_{16},L_{17}	31.25	G1=21.25 , G2=10	15.4	68621.74
a=0,b=1	L_7-L_{12}	31	G1=21.25, G2=9.75	15.8	69661.33
a=0.5,b=0.5	L_7-L_{12}	31	G1=21.25,G2=9.75	15.8	69661.33
Battle					
a=1,b=0	L_9,L_{11},L_{16},L_{17}	31.25	G1=21.25 , G2=10	15.5	69201.55
a=0,b=1	L_7-L_{12}	31	G1=21.25, G2=9.75	15.8	69661.33
a=0.5,b=0.5	L_7-L_{12}	31	G1=21.25, G2=9.75	15.8	69661.33
Anchor					
a=1,b=0	L_9,L_{11},L_{16},L_{17}	31.25	G1=21.25, G2=10	15.5	69201.55
a=0,b=1	L_7-L_{11},L_{16}	31	G1=21.25, G2=9.75	15.8	69661.33
a=0.5,b=0.5	L_7-L_{11},L_{16}	31	G1=21.25, G2=9.75	15.8	69661.33

3.5.1.3 Case 3: islanding scenario

Another fault scenario is considered where two faults between the nodes 4-6 and 3-5 occur simultaneously. This situation creates an islanding scenario, and the reconfiguration algorithm needs to decide the loads' breaker statuses based on the weighting factors in the objective function. In the SPS with four zonal loads, in all the ship mission modes, the reconfiguration output results demonstrate that the loads L_5,L_8,L_{11} are suggested to be shed in the case where the loads' magnitude weighting factor is greater in the objective function. In the case that the load's priority factor is greater than the other factor, reconfiguration optimization will shed L_5 and L_6.

In the six zonal loads SPS, suppose that the ship is in the battle operation mode, and suddenly, simultaneous faults occur between the nodes 6-8 and 5-7 as a result of a battle damage. Consequently, these branches are isolated by protective devices from the rest of the system. Automated reconfiguration controller that performs the SPS reconfiguration for the system restoration can help maintain the mission by shedding the non-vital loads and keep the power for the vital loads. In this case, the reconfiguration algorithm is proposing to shed the L_9,L_{11},L_{16}, and L_{17}, where the load's magnitude has a greater importance and shed loads L_7-L_{12} in the case that the load's priority has a more weight in the objective function. It can be seen that the total served loads are 31.25 MW and 31 MW respectively.

In all the above cases, the results where the load's priority and magnitude have an equal weighting factor are similar to the results in the case where the load's priority has a greater influence on the reconfiguration objective function. This is due to the small scale of the

SPS and the high weight of load priority function in the reconfiguration objective function [106].

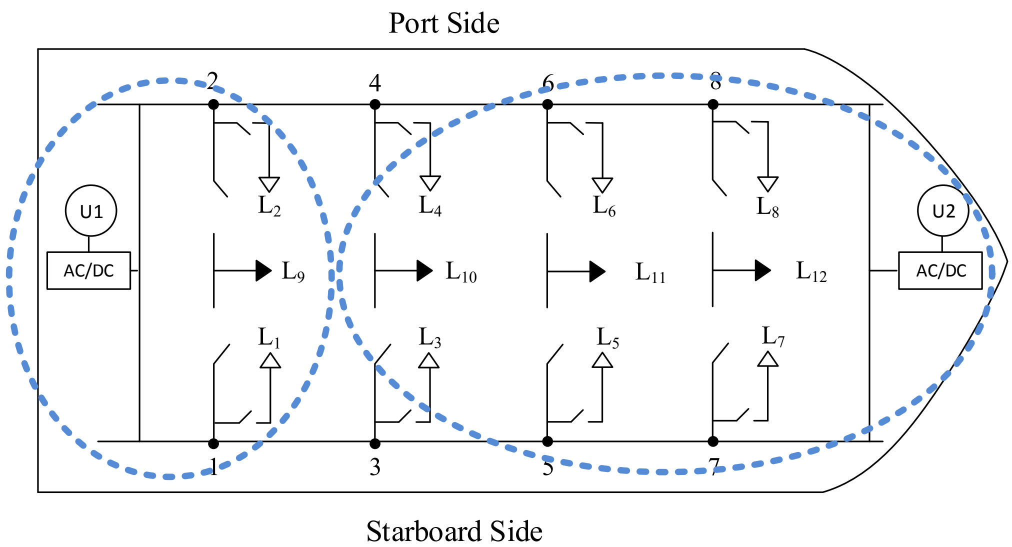

Figure 3.10: Islanding scenario for Case 4

(b)

3.5.1.4 Case 4: islanding scenario; effect of pulse load

Electric ships may include pulse loads that draw a very high, short duration current in an intermittent pattern. When the pulse load is in operation mode, it offers a very small resistance, and it acts like a short circuit to the SPS. Therefore, this load is one of the sources of the transients in electric ship power systems. The pulse loads consume different power according to the ship's mission. In this dissertation, to investigate the effect of the pulse load on the reconfiguration problem, load L_7 is considered as a pulse load, which consumes 1.5 MW in previous case studies. The SPS with four zonal loads is considered in this case study. Suppose that the ship is working in the cruise mode, and, following a battle condition, the pulse load profile changed from 1.5 MW to 4 MW. Another islanding scenario including simultaneous fault scenario on branches between the nodes 2-4 and 1-3 is considered for this case. In this situation, the pulse load priority factor is altered from 1 to 8, which implies that the pulse load's priority has been changed from non-vital to vital load. Other loads' weighting factors are shown in Table 3.6. The total available load and generation in the left side of the ship (as shown in Figure 3.10) are 3.5 MW and 20 MW, respectively, and total available load and generation on the right side of the ship are 19.5 MW and 7 MW, respectively. The simulation result for this case is shown in Table 3.7. In this fault scenario, the reconfiguration algorithm requires to shed at least 12.5 MW load from the right side of the system, which are L_3, L_4, L_7, L_8, L_{12} and L_3, L_4, L_5, L_6, L_8, L_{12} in the case with respect to the loads' magnitude and loads' priority, respectively. From the reconfiguration outputs, it is concluded that the proposed method can successfully recommend the possible solutions for the reconfiguration problem following the fault events in MVDC SPS.

Table 3.6: Loads' priority factors in Case 4

	L_1	L_2	L_3	L_4	L_5	L_6	L_7	L_8	L_9	L_{10}	L_{11}	L_{12}
Cruise	1	1	1	1	1	1	1	1	3	3	6	6
Battle	1	1	1	1	1	1	8	1	1	4	4	1

Table 3.7: Simulation results for Case 4

Case Study	Load shedding suggestion	Total load served(MW)	Total generation (MW)	Execution time(s)	Exhaustive search(s)
a=1,b=0	L_3,L_4,L_7 L_8,L_{12}	10.5	G1=3.5 , G2=7	14.7	1187.3
a=0,b=1	L_3,L_4,L_5,L_6 L_8,L_{12}	10	G1=3.5 , G2=6.5	14.2	1163.26
a=0.5,b=0.5	L_3,L_4,L_5,L_6 L_8,L_{12}	10	G1=3.5 , G2=6.5	14.2	1163.26

3.5.2 GAMS-based case study

For general optimization problems, one of the favorite choices is the GAMS which is a high-level modeling system for mathematical optimization problems, and it is specifically designed for large and complex problems. This software allows creating and maintaining models for a wide variety of applications and disciplines. This optimization platform has the ability to develop different models including linear, nonlinear, mixed-integer linear programming (MILP), mixed-integer nonlinear programming (MINLP) and dynamic nonlinear programming (DNLP) [97]. The performance of the proposed reconfiguration controller was first tested in RTDS simulation using the laboratory setup shown in Figure 3.5. Then, the MVDC SPS mathematical model and reconfiguration problem was developed in the GAMS software.

In this section, the result of Case 2 and Case 3 for SPS with four zonal loads are only reported. The simulation results are shown in Table 3.8. The mathematical model simulation shows an excellent response and very close to the RTDS-based case studies even though several approximations were applied to that model. The RTDS results and the simulated results in the GAMS have confirmed the effectiveness and the accuracy of such proposed approach.

The simulation time for the reconfiguration problem in GAMS is reported as well. To clarify the difference between the execution time in RTDS-based and GAMS-based case studies, Figure 3.11 shows the time frame for real-time implementation of reconfiguration problem. In the RTDS-based intelligent reconfiguration, the execution time is the summation of running the system, SA optimization and returning the optimal set of switches to the RSCAD Runtime. However, in GAMS-based case studies, the execution time is solely the time needed for the execution of the optimization with the mathematical model of the system.

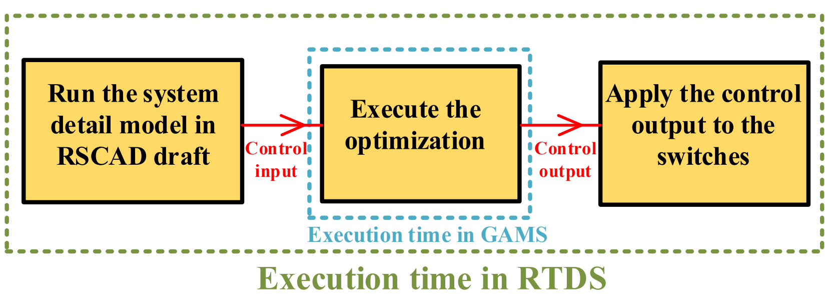

Figure 3.11: Time-frame for real-time reconfiguration executation in RTDS

Table 3.8: Simulation results for GAMS-based reconfiguration

Case Study	Load shedding suggestion	Load served (MW)	Total generation (MW)	Execution time(s)
Case 2				
Cruise				
a=1,b=0	L_3-L_7,L_9-L_{11}	20	G2=7	0.03
a=0,b=1	L_1-L_8	20	G2=7	0.02
a=0.5,b=0.5	L_1-L_8	20	G2=7	0.02
Battle				
a=1,b=0	L_3-L_7,L_9-L_{11}	20	G2=7	0.02
a=0,b=1	L_1,L_2,L_5,L_{12}	20	G2=7	0.02
a=0.5,b=0.5	L_1,L_2,L_5,L_{12}	20	G2=7	0.02
Anchor				
a=1,b=0	L_3-L_7,L_9-L_{11}	20	G2=7	0.02
a=0,b=1	L_1-L_8	20	G2=7	0.02
a=0.5,b=0.5	L_1-L_8	20	G2=7	0.02
Case 3				
Cruise				
a=1,b=0	L_5,L_8,L_{11}	18.5	G1=11.5 , G2=7	0.02
a=0,b=1	L_5,L_6	18.5	G1=11.5 , G2=7	0.02
a=0.5,b=0.5	L_5,L_6	18.5	G1=11.5 , G2=7	0.02
Battle				
a=1,b=0	L_5,L_8,L_{11}	18.5	G1=11.5 , G2=7	0.02
a=0,b=1	L_5,L_6	18.5	G1=11.5 , G2=7	0.02
a=0.5,b=0.5	L_5,L_6	18.5	G1=11.5 , G2=7	0.02
Anchor				
a=1,b=0	L_5,L_8,L_{11}	18.5	G1=11.5 , G2=7	0.02
a=0,b=1	L_5,L_6	18.5	G1=11.5 , G2=7	0.02
a=0.5,b=0.5	L_5,L_6	18.5	G1=11.5 , G2=7	0.02

As it has been reported, the simulation times in Tables 3.4, 3.5, and 3.7 compared with the simulation times for the case studies solved with GAMS software. The execution time is longer and this is one of the disadvantages of the proposed approach. We are dealing with real-time, with a high fidelity model of the system. The performed simulations help to identify the corresponding domain of analysis. In a pure research setting, when much of the efforts are given to reaching better accuracies of solutions, GAMS or MATLAB should be selected, whereas actual real-time implementations could take advantage of the meta-heuristic approach presented in this research work. The main disadvantage of using optimization software such as GAMS is their deficiency in implementing the detailed model of the system to perform the real-time power networks optimizations.

3.6 Conclusion

This chapter introduced a simulated annealing-based real-time reconfiguration algorithm which is fully implemented in the RTDS platform. The reconfiguration problem is formulated as a multi-objective optimization which aims to maximize the total power supply to the system loads following a fault. The SA optimization method is used to find the local optimal solutions which are the set of loads' breaker statuses. The performance of the proposed technique has been investigated through two MVDC SPS models including four and six zonal loads. The mathematical model of the reconfiguration problem is solved in the GAMS optimization software which verified the results from the RTDS-based reconfiguration problem. Simulation results show the satisfactory performance of the proposed approach to deal with different fault scenarios. The proposed method in this dissertation can be used in other real-time optimization-based power system studies such as FACTS devices design problem, distributed generations placement, and planning problems.

CHAPTER IV

APPLICATION OF COMBINED STATCOM-SFCL FOR STABILITY IMPROVEMENT OF THE MVDC MICROGRID DURING UNSYMETRICAL FAULTS

4.1 Introduction

One of the critical issues regarding fault management in SPS is responding to transient faults. These types of fault can affect the system for a short period of time. When a transient fault occurs in the SPS, a voltage dip will appear on the AC load of the system, where certain vital loads such as propulsion loads are connected to. Therefore, riding through the short-term disturbances, especially under unbalanced system AC faults, and maintaining the voltage stability during different types of faults in SPS is one of the most challenging issues.

One possible approach to deal with transient overvoltages issue is to employ STATCOM to help the system by controlling the injected reactive power to keep the AC bus voltage at the desired value in post-fault situations [14, 15, 48, 125, 110]. STATCOM is a Voltage Source Converter (VSC)-based regulating device which has the capability of absorbing and generating reactive power in AC transmission and distribution systems [77]. STATCOM is a member of the Flexible Alternating Current Transmission System (FACTS) devices family, which operates in shunt with the power system and it is used to regulate the voltage, damp the oscillation of power line, and improve the system stability under various transients, voltage flicker, and sag-swell. STATCOM is also used to control the active and reactive power in power systems [104, 133]. The performance of the STATCOM under unbalanced conditions is highly dependent on its controller parameters. Traditional methods of tuning, based on trial and error, do not guarantee an acceptable performance that is expected from the STATCOM. In order to improve the performance of the STATCOM, the controller parameters need to be optimally designed. The controller parameters design can be viewed as an optimization problem that aims to improve the transient response of the system following a contingency in the system.

Several papers have dealt with the FACTS devices controller design problem. The conventional methods of controller design using linear controller techniques such as Linear Quadratic Regulator (LQR) are well-suited when a linear model of the system is available. The performance of these controllers degrades by changing the operating conditions [78]. On the other hand, heuristic methods are applicable for a wider range of the system model including detailed dynamic models of the system. Heuristic optimization techniques have been widely-utilized for FACTS device design problem to find controller gains to meet the desired objective function. Genetic Algorithm (GA) and Particle Swarm Optimization (PSO) are among the most popular approaches that are extensively used in this regard [73, 42, 84, 88, 67, 72, 56]. GA is employed in [42] to design STATCOM parameters in a multi-machine power system to mitigate the power system oscillation during the faults. In [84], GA and PSO are utilized to tune the parameters of Thyristor-Controlled Series Compensation's (TCSC) controller, and their performances are compared under different disturbances. An adaptive control strategy using PSO, integrated with Artificial Immune

System (AIS) optimization technique is applied in [73] to an SPS to mitigate the effect of pulsed loads. The desired objective function in [73] is keeping the bus voltage close to its reference value. In [1], the optimal setting of the STATCOM's controller is determined with the Imperialist Competitive Algorithm (ICA) algorithm, and the objective is to attenuate oscillation in a multi-machine power system in case of faults. In [2], the STATCOM's controller design problem is formulated as a multi-objective problem, and the Cuckoo Search (CS) algorithm is employed to find the optimal parameters of the controller.

The drawbacks of existing optimization approaches applied to FACTS devices design problems are that they cannot offer a fast convergence for a large search space, and they may converge to local optima instead of the global optimum. To overcome these issues, this research work investigates the application of a novel optimization algorithm to solve the STATCOM design problem. FGA is a novel heuristic optimization algorithm that takes inspiration from genetic algorithm [54]. This algorithm is a GA with some fundamental differences. The pivotal idea of FGA is that chromosomes and individuals (answers) are not the same entities. In this technique, the crossover operation has been changed and the need for mutation is eliminated. Furthermore, diversity rate and generation blueprint are other features of the proposed fluidity in FGA, making it more adjustable for different optimization problems. In this section, FGA is utilized to find optimal STATCOM's controller parameters in an MVDC SPS to minimize the effects of the unsymmetrical transient faults.

Super Conducting Fault Current Limiters (SFCL) provide a viable solution to mitigate the short circuit currents during a fault. The presence of the SFCL in a power system increases the stability of the system by minimizing the the fault current. Resistive-type

SFCL (R-SFCL) is the simplest type of the SFCL. The operation principle of the R-SFCLs is based on the transition to the resistive state in order to insert impedance into the fault current path during a fault. Several papers have dealt with the SFCL allocation problem in the power systems [76, 32, 37, 116, 86]. The objectives include optimal placement of the SFCL, optimal size of the SFCL, coordination problem with other protective devices such as circuit breakers, and reduction of the number of SFCL used in the power system. In this dissertation, SFCL is utilized to maintain the vital AC load's performance close to normal conditions. Therefore, the optimal placement of the SFCL is not considered as an objective for SFCL allocation problem. Previous research in optimal sizing of the SFCL only consider three-phase short circuit faults. There is no research that considers different types of possible fault, including single line to ground fault and double line to ground fault, in order to design the SFCL. This study aims to find the optimal size of the SFCL unit with respect to the cost of the SFCL installation in the system by considering different faults in the system.

In this study, a combined STATCOM-SFCL scheme has been proposed to enhance the stability of MVDC SPS during unsymmetrical faults. The advantages of using SFCLs to reduce the fault current level include their simple structure, low costs, and higher reliability. However, SFCLs do not have reactive power compensation capability during faults in the system. Utilizing additional compensation devices such as STATCOM can help the system by controlling the injected reactive power to help the system during unsymmetrical faults. STATCOM can assist the SFCL to keep the vital load's terminal voltage close to the normal state in an economic sense. The economic advantage of the proposed scheme is due to the fact that the STATCOM can be permanently used in the system and support the system by improving the power quality and harmonics mitigation in the absence of faults in a power network [59].

4.2 STATCOM model and control

4.2.1 STATCOM controller structure

The equivalent circuit of STATCOM or D-STATCOM (Distribution Static Synchronous Compensator) is shown in Figure 4.1. STATCOM consists of a three phase Gate Turn Off (GTO)-based VSC, a transformer, a filter and a DC capacitor [73]. The input to the VSC is a DC capacitor and the three phase output is connected to the Point of Common Coupling (PCC). In order to adjust the bus voltage, the STATCOM controls the reactive power injected into the system and absorbed from the system [104]. The relation between active and reactive power is expressed by the following equation.

$$S = P + jQ = 3\frac{V_{pcc}V_c}{x_l}\sin\alpha + j3(\frac{V_{pcc}V_c}{x_l}\cos\alpha - \frac{V_{pcc}^2}{x_l}) \tag{4.1}$$

where:

- S: Apparent power flow
- P: Active power
- Q: Reactive power
- V_{pcc}: Three phase voltage at PCC
- V_c: Inverter output three phase voltage
- x_l: Reactance along with STATCOM and PCC
- α: Angle of difference between V_{pcc} and V_c

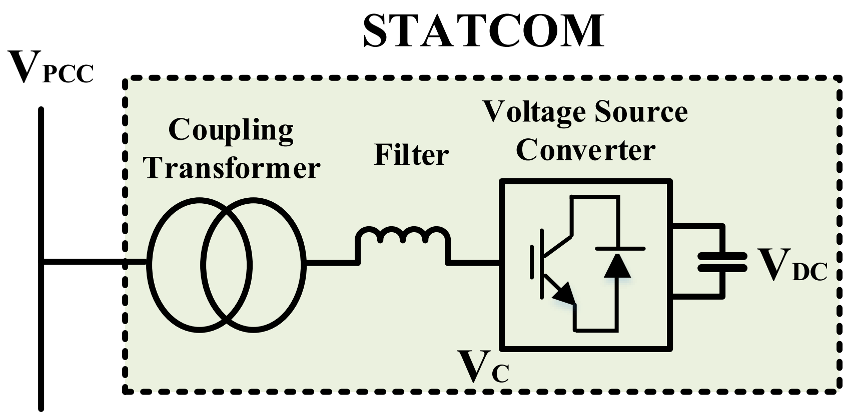

Figure 4.1: STATCOM schematic diagram

In the normal operation, α is close to zero; however in the case of an abnormal situation, the voltage deviates from its pre-defined value, and STATCOM will control the injected reactive power into the PCC to regulate the bus voltage [72].

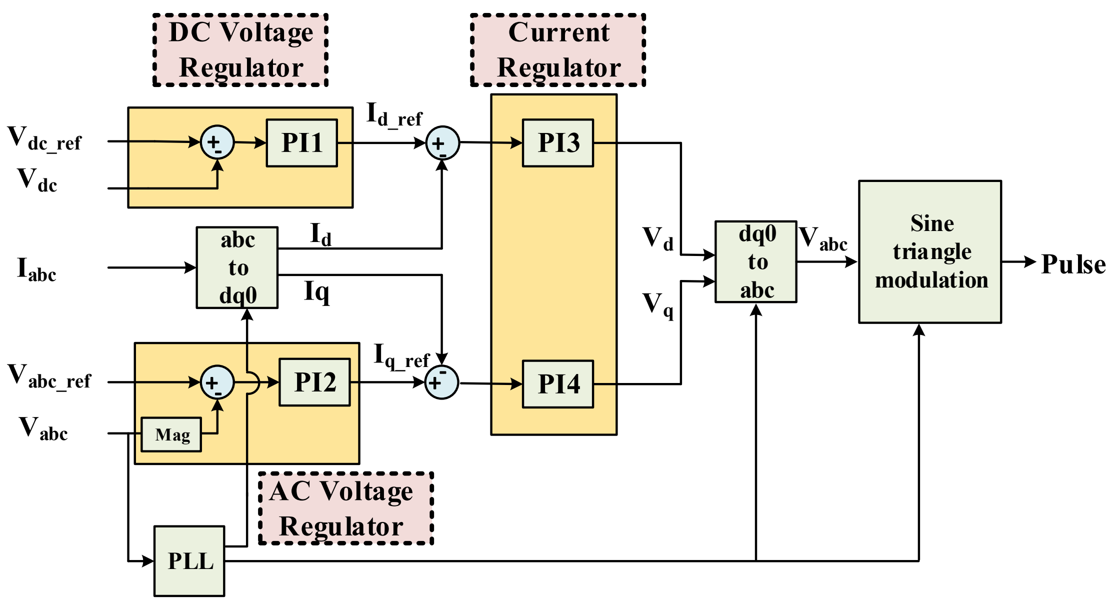

Figure 4.2: STATCOM control structure

The control circuit of STATCOM which is considered in this work is known as a decoupled control system as shown in Figure 4.2 [59, 58]. The PI1, and PI2 are the outer loop control that aims to generate the set point for the inner control system loop of PI3 and PI4, which are I_{dref} and I_{qref}, respectively. The DC link capacitor, V_{DC}, is controlled by D-axis control system, and the Q-axis control system is used to regulate the AC bus voltage. The I_{qref} comes from the voltage regulation controller, and the I_{dref} is generated from the DC-link voltage regulator. The V_d and V_q voltages are the outputs of the inner control loops, and they are transformed to the *abc* framework and feed the PWM generator to produce the desired pulses. The Phased-Locked Loop (PLL) is used to calculate a reference angle to transform the *dq* component to the *abc* component of the STATCOM current and voltage.

4.2.2 STATCOM controller design

4.2.2.1 Objective function

In this study, the STATCOM parameters tuning process is formulated as a multi-objective optimization problem. There are two objectives that need optimization as follow:

1. Minimize the AC bus voltage deviation from its pre-defined value (J_1).
2. Set the DC bus voltage of the STATCOM to the reference value (J_2).

Hence, the two objectives J_1 and J_2 are specified as in (4.2) and (4.3) [15].

$$J_1 = \sum_{t=1}^{n} (V_{bus}(t) - V_{bus.ref})^2 \tag{4.2}$$

$$J_2 = \sum_{t=1}^{n} (V_{dc.bus}(t) - V_{dc.bus.ref})^2 \tag{4.3}$$

The multi-objective optimization problem is derived by incorporating the weighting factors to J_1 and J_2 functions to build the overall objective function J as represented in (4.4).

$$J = w_1.J_1 + w_2.J_2 \tag{4.4}$$

In (4.4), w_1 and w_2 are the weighting factors that are adjusted to reflect the relative importance of each objective function with respect to the other. To attain greater performance for the AC bus voltage regulation, a set of weighting factors is also incorporated to the cost function J_1 as follows.

$$J_1 = a.J_{11} + b.J_{12} \tag{4.5}$$

$$J_{11} = \sum_{t=1}^{n} (V_{bus}(t) - V_{bus.ref})^2 \tag{4.6}$$

$$J_{12} = \sum_{t=1}^{n-1} (V_{bus}(t+1) - V_{bus}(t))^2 \tag{4.7}$$

J_{11} is the cost function to minimize the difference between AC bus voltage average value and its nominal value, and J_{12} aims to minimize the voltage fluctuation. a and b are the parameters associated with each objective functions J_{11} and J_{12}, respectively.

To find the optimum solution for the defined objective function, the six parameters of the PI controllers in the STATCOM control structure that consist of $K_p - I$, $K_i - I$ (current regulators controller parameters), $K_p - vdc$, $K_i - vdc$ (DC bus regulators controller parameters), $K_p - vac$, $K_i - vac$ (AC bus regulators controller parameters) are need to be optimally found to meet the specified objective function.

4.2.2.2 Constraints

The STATCOM controller design problem is expressed as an optimization problem with a goal to minimize the objective function defined in (4.4) in order to enhance the system response to the abnormal conditions regarding the responses settling time and overshoot as follows.

$$
\begin{aligned}
\text{minimize} \quad & J \\
\text{subject to :} \quad & K_{pmin} - I \le K_p - I \le K_{pmax} - I \\
& K_{imin} - I \le K_i - I \le K_{imax} - I \\
& K_{pmin} - vdc \le K_p - vdc \le K_{pmax} - vdc \\
& K_{imin} - vdc \le K_i - vdc \le K_{imax} - vdc \\
& K_{pmin} - vac \le K_p - vac \le K_{pmax} - vac \\
& K_{imin} - vac \le K_i - vac \le K_{imax} - vac
\end{aligned}
$$

4.2.3 Fluid Genetic Algorithm (FGA) Optimization Technique

Fluid Genetic Algorithm (FGA) is a GA with some conceptual distinctions that make it more suitable for this optimization problem [54]. The main differences between GA and FGA techniques are highlighted in Table 4.1. The cornerstone of these difference is that chromosomes and individuals (answers) are not the same entities in FGA optimization technique. In GA, there is a one-to-one relationship between each chromosome and each individual. So, only one unique answer may be produced from each chromosome and vice versa. FGA is putting forward a new way to free the algorithm from having to deal with local optima and mutation procedure. FGA proposes that each time a chromosome produces an individual, it might create a different one. One individual will be randomly associated with the chromosome. FGA's chromosomes are the predisposition of an individual before an answer is produced. A function named *born-an-individual* is a random procedure that produces an answer to the problem according to the chromosome (predisposition).

	GA	FGA
Chromosome	√	Changed
Individual (answer)	√	Changed
Fitness value	√	√
Decoding function	√	√
Crossover	√	Changed
Mutuation	√	×
Selection function	√	√
Stopping criteria	√	√
Individual learning rate	×	√
Global learning rate	×	√
Diversity rate	×	√
Born an individual	×	√
Generation blue print	×	√

Table 4.1: Highlighted differences between GA and FGA

Figure 4.3 can be a chromosome of a binary individual in FGA. The born-an-individual function works by producing one and zero for each cell of the individuals based on the value in the respecting cell in the chromosome. For instance, the first cell in the chromosome is 0.41; therefore, there is a 41 percent chance for the first cell individual to be one and 59 percent chance to be zero. In the case of the chromosome in Figure 4.4, every (2^7 =

128) 7 binary combination has a chance to be the associated individual only with different probabilities.

0.41	0.26	0.99	0.21	0.63	0.39	0.85

Figure 4.3: FGA's Crossover

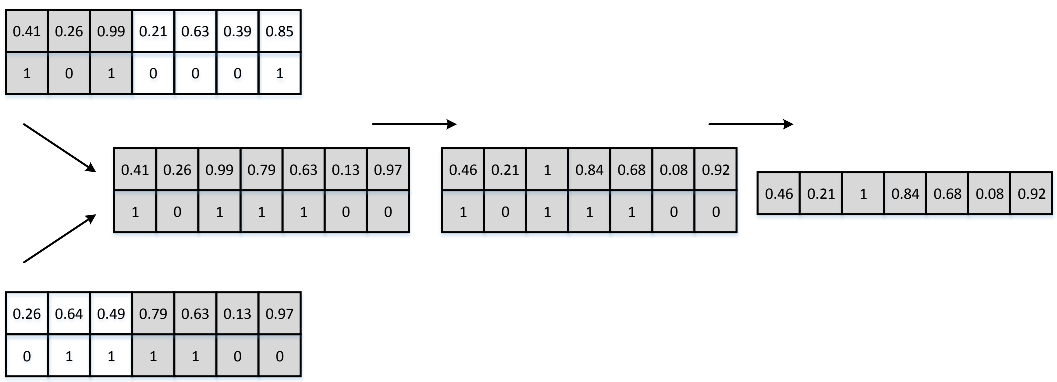

Figure 4.4: FGA's sample chromosome

Due to all these possibilities, there is no need for the mutation operation. The new structure leads to less chance for the algorithm to entrap in a local optima. Indeed, the mutation procedure in GA is performed intrinsically. For instance, in the case of the chromosome in Figure 4.3, there is a chance for the born child to have one or zero in each and every cells. Because of all these possibilities, the mutation will be done by these possibilities. That is the reason FGA does not need mutation.

Crossover in FGA also uses a new concept - *Individual Learning Rate* (ILR). As a start, the same procedures for GA's binary chromosomes is applied for FGA's chromosomes. Figure 4.4 depicts the procedure and clarifies the involvement of learning rate (LR = 0.05). It should be noted that chromosomes and individuals both enter the crossover function, but the operator will only output one chromosome. The two entering chromosomes will mingle randomly. The result will go through some changes based on the learning rate value. The following procedure will be done for each and every cell of the chromosome at this stage of crossover procedure. If the individual's cell is one, the value of the related chromosome will be added by learning rate, and if the individual's cell is zero, it will be deducted by the same value.

There are three other new concepts tied with born-a-child function: *generation blue print*, *global learning rate*, and *diversity rate*. The generation blue print is a chromosome with cells filled with the average value of all the chromosomes in every iteration (generation). The blue print for the first generation always starts with 0.5 for all of the cells' values. The function will always get two inputs: one is the blue print and the other is the chromosome. The probability that the value of one or zero will be produced is calculated using (4.8). Here, η_g, PVC_i, PVB_i, η_{DR}, and EPV_i are global learning rate, probability value from chromosome for the cell i, probability value from blue print for the cell i, diversity rate, and effective probability value i, respectively. As seen in (4.8), the two conditions try to keep the probability of EPV bellow 1 and above 0. This is to protect the FGA from getting stuck in local optima.

$$
\begin{cases}
\eta_g \times PVB_i + (1-\eta_g) \times PVC_i < \eta_{DR} \implies EPV_i = \eta_{DR} \\
\eta_g \times PVB_i + (1-\eta_g) \times PVC_i > \eta_{DR} \implies EPV_i = 1-\eta_{DR} \\
\text{Otherwise} \implies EPV_i = \eta_g \times PVB_i + (1-\eta_g) \times PVC_i
\end{cases}
\tag{4.8}
$$

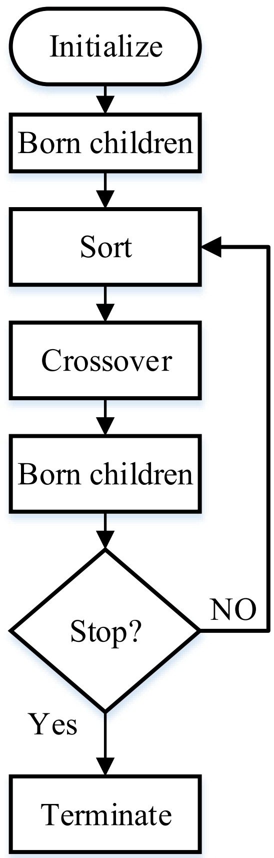

Figure 4.5: FGA optimization flowchart

Figure 4.5 shows FGA's optimization technique implementation flowchart. There are two born children steps. In the first one, right after initialization, every randomly produced chromosomes will go through born-a-child function and will have an individual (answer) associated with them. Moreover, after every crossover procedure, born-a-child function creates an individual for newly produced chromosomes. In addition, as presented in this figure, the FGA does not need mutation for escaping local optima. The behavioral parameters of FGA have been selected after experimented tuning process.

4.3 Resistive SFCL model and working principle

4.3.1 Resistive-type SFCL model

In this study, the Resistive-type SFCL (R-SCFCL) has been considered due to its simple operation principle and smaller size compared to the other types of SFCL. The topology of the R-SFCL unit is shown in Figure 4.6 [117, 115]. This unit consists of a stabilizer resistance of the n^{th} unit; $R_{nc}(t)$, the superconductor resistance of the n^{th} unit; $R_{ns}(t)$, which is in parallel with the superconductor resistance, and the coil inductance of the n^{th} unit L_n. The subscript n denotes the number of connected units. The basic operation of the resistive-type SFCL is the transition from superconducting mode to the normal state. This procedure is called quenching process. Under the normal operation, the impedance of the superconducting element and the other resistance are zero. As the current through the superconducting element exceeds a certain value, the impedance of this element will be increased to limit the fault current level. The value of L_n is dependent on the wound coils. The inductance causes AC loss in the system in the normal operation. Therefore, the value of this inductance must be selected as small as possible. The following equation represents the quenching characteristics of the variable resistance,

$$R_{SFCL}(t) = R_m(1 - exp^{(-t/T)}) \tag{4.9}$$

where R_m is the maximum impedance value of the superconducting element, T is the time constant of transition from the superconducting state to the normal state.

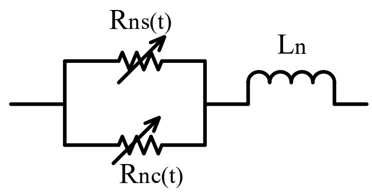

Figure 4.6: The structure of a resistive SFCL

4.3.2 Optimal sizing of the SFCL

In this study, the objective of the optimal sizing of the SFCL includes three incongruent objectives to find an appropriate value for the SFCL's impedance. The three conflicting objectives are the minimization of resistance (due to the costs), the minimization of voltage, and active power variation. Less resistance is more economic, and less voltage and active power variation mean the SFCL can provide better power quality in the system. Therefore, the desired objective functions are defined as follows.

4.3.2.1 Improvement of voltage quality

To improve the voltage quality, the integral absolute value of the AC loads terminal voltage deviation must be minimized as follow.

$$f_1 = \int_{t_0}^{t_f} |\Delta V_{bus}| dt \tag{4.10}$$

where ΔV_{bus} is the difference of the load bus voltage from the nominal bus voltage, t_0 and t_f are the simulation times.

4.3.2.2 Alleviation of output active power fluctuation

To minimize the active power variation, the minimization of the load's bus active power fluctuation is computed as follows.

$$f_2 = \int_{t_0}^{t_f} |\Delta P_{bus}| dt \tag{4.11}$$

where ΔP_{bus} is the deviation of the load bus actual power from the reference power.

4.3.2.3 Minimization of SFCL's impedance

In order to select an optimal impedance value of SFCL with minimum cost, the following objective is considered.

$$f_3 = Z_{SFCL} \tag{4.12}$$

4.3.2.4 Formulation of optimization problem

The following optimization problem presents the formulation, a weighted single function multi-objective optimization problem, by combining (4.10)-(4.12). Since the values of f_1, f_2 and f_3 are not in the same range before applying the weights, these values are transformed to fall between -1 and 1 based on all the possible solutions in the solution set. The general objective function for optimal sizing of the SFCL is expressed by the following equation.

$$\min f = w_1.f_1 + w_2.f_2 + w_3.f_3 \tag{4.13}$$

where w_1, w_2, and w_3 are the parameters associated with the importance of each objective functions in the overall objective function. In such decision-making cases, there is no one optimal solution as the improvement of one objective may lead to the disimprovement of the other. In what follows, the multi-objective optimization process will be elaborated to solve the SFCL sizing problem.

4.3.3 Multi-objective optimization process

A Multi-Objective Problem (MOP) requires the effort to simultaneously satisfy of two or more conflicting objective functions. As such, MOP normally does not have a single best solution but a set of solutions. These set of solutions are called Pareto optimal set where there is no other solution that dominates them. The Pareto optimality theory is used to find this set of optimal solutions. In mathematical terms, the Pareto optimization can be formulated as follows [74].

$$\begin{aligned} \text{minimize} \quad & f_i(x) \quad i = 1,2,...,M_{obj} \\ \text{subject to} \quad & g_j(x) \leq 0 \quad j = 1,2,...,N_{ineq} \\ & h_k(x) = 0 \quad k = 1,2,...,K_{eq} \end{aligned} \tag{4.14}$$

where $f_i(x)$ is ith objective function, x is the decision vector that represent a solution, and M_{obj} is the number of objective functions. N_{ineq} and K_{eq} are the inequality and equality constrains of the optimization problem, respectively. There are two possibilities for the solutions for a multi-objective optimization problem. One solution dominates the other solution, or neither dominates the other solution. In a minimization problem, a solution x_1 dominates x_2 if the following conditions are met:

$$\forall i \in \{1,2,...,M_{obj}\} : f_i(x_1) \leq f_i(x_2) \tag{4.15}$$

$$\exists j \in \{1,2,...,M_{obj}\} : f_j(x_1) \leq f_j(x_2) \tag{4.16}$$

Violation in any of the statements in (4.15)-(4.16) means x_1 does not dominate x_2. If the solution x_1 dominates x_2, x_1 is considered as the non-dominated solution. The all non-dominated solutions in the search space is called the Pareto optimal set.

There are several approaches to find the non-dominated solutions in a multi-objective optimization problem. One of these methods is to integrate the weighting factors to the objectives to form the weighted sum of the objectives as follows.

$$f(x) = w_1.f_1 + ... + w_i.f_i \tag{4.17}$$

where:

$$w_1 + .. + w_i = 1 \tag{4.18}$$

Now, the multi-objectives are converted to a single objective optimization problem.

In this study, in order to select the optimal impedance value of the SFCL, different fault scenarios including Single Line to Ground Fault (SLG), Double Line to Ground Fault

(DLG), Line to Line fault (LL), Three Phase fault (LLL), and Three Phase to Ground fault (LLLG) have been considered. For each fault scenario, the two objectives f_1 and f_2 are calculated. The values of these two objective function for each scenario are given in Table 4.2. The highlighted values are the minimum value of each objective function for each fault scenarios.

Table 4.2: Simulation results for different case studies

No.	Impedance	SLG Fault		DLG Fault		LL Fault		LLL Fault		LLLG Fault	
		ΔV	ΔP	ΔV	ΔP	ΔV	ΔP	ΔV	ΔP	ΔV	ΔP
1	0.25	1.77E+02	4.20E+03	6.56E+02	4.57E+03	6.81E+02	5.85E+03	1.10E+03	6.02E+03	1.10E+03	6.02E+03
2	0.5	1.32E+02	4.26E+03	5.73E+02	3.51E+03	5.81E+02	4.56E+03	9.59E+02	4.48E+03	9.59E+02	4.48E+03
3	0.75	94.9037	4.19E+03	4.81E+02	2.74E+03	4.99E+02	3.60E+03	8.22E+02	3.33E+03	8.22E+02	3.33E+03
4	1	59.2194	4.10E+03	3.91E+02	3.26E+03	4.16E+02	2.91E+03	6.96E+02	3.08E+03	6.96E+02	3.08E+03
5	1.25	40.437	3.89E+03	3.18E+02	3.79E+03	3.40E+02	2.84E+03	5.78E+02	4.08E+03	5.78E+02	4.08E+03
6	1.5	32.383	3.51E+03	2.51E+02	4.18E+03	2.66E+02	3.33E+03	4.71E+02	4.88E+03	4.71E+02	4.88E+03
7	1.75	30.8401	3.13E+03	1.92E+02	4.41E+03	2.06E+02	3.61E+03	3.74E+02	5.51E+03	3.74E+02	5.51E+03
8	2	31.9031	2.76E+03	1.43E+02	4.50E+03	1.60E+02	3.71E+03	2.86E+02	5.98E+03	2.86E+02	5.98E+03
9	2.25	31.52	2.65E+03	1.01E+02	4.50E+03	1.19E+02	3.73E+03	2.08E+02	6.30E+03	2.08E+02	6.30E+03
10	2.5	32.5111	2.72E+03	71.503511	4.31E+03	88.307135	3.61E+03	1.39E+02	6.49E+03	1.39E+02	6.49E+03
11	2.75	31.562	2.94E+03	47.490571	4.09E+03	61.85061	3.40E+03	81.65706	6.59E+03	81.485278	6.59E+03
12	3	32.3969	3.16E+03	39.508296	3.70E+03	41.572606	3.17E+03	55.78232	6.32E+03	72.508266	6.32E+03
13	3.25	32.6228	3.39E+03	35.116436	3.31E+03	33.992647	2.91E+03	49.40271	5.65E+03	60.142211	5.65E+03
14	3.5	33.5813	3.60E+03	32.24642	2.93E+03	34.022104	2.61E+03	42.74494	5.03E+03	45.759962	5.01E+03
15	3.75	34.4734	3.79E+03	32.585916	2.61E+03	32.469223	2.67E+03	39.31405	4.46E+03	39.31485	4.46E+03
16	4	35.9391	3.96E+03	31.310589	2.58E+03	32.186859	2.93E+03	38.20948	3.95E+03	37.422225	3.85E+03
17	4.25	34.7949	4.11E+03	33.266157	2.85E+03	32.879527	3.20E+03	35.93447	3.48E+03	36.29707	3.63E+03
18	4.5	35.6967	4.27E+03	33.005725	3.11E+03	32.260919	3.45E+03	34.78127	3.08E+03	34.794157	2.93E+03
19	4.75	36.8447	4.41E+03	32.384718	3.34E+03	31.611222	3.65E+03	33.20021	2.70E+03	33.62504	2.70E+03
20	5	37.8855	4.55E+03	34.169233	3.57E+03	32.338485	3.86E+03	32.61895	2.42E+03	32.422182	2.42E+03
21	5.25	39.0334	4.68E+03	33.263654	3.76E+03	35.76093	4.07E+03	32.25152	2.65E+03	31.953445	2.65E+03
22	5.5	38.7077	4.79E+03	33.649249	3.96E+03	35.76013	4.24E+03	31.84575	2.91E+03	31.825736	2.91E+03
23	5.75	39.2744	4.90E+03	34.822747	4.13E+03	34.953631	4.39E+03	31.62165	3.15E+03	32.261613	3.16E+03
24	6	38.713	5.01E+03	35.913401	4.29E+03	35.352215	4.54E+03	33.43767	3.39E+03	31.957457	3.37E+03
25	6.25	40.6437	5.11E+03	35.872134	4.44E+03	38.230995	4.69E+03	32.54314	3.59E+03	32.002614	3.58E+03
26	6.5	40.1407	5.20E+03	34.835456	4.57E+03	36.760161	4.81E+03	33.06844	3.78E+03	32.937491	3.78E+03
27	6.75	42.3038	5.30E+03	35.799978	4.70E+03	34.696067	4.91E+03	32.54725	3.96E+03	32.114874	3.96E+03
28	7	41.3808	5.36E+03	35.869735	4.82E+03	36.442584	5.04E+03	33.20824	4.12E+03	33.292783	4.13E+03
29	7.25	42.6811	5.43E+03	36.667222	4.89E+03	37.307332	5.11E+03	34.5093	4.26E+03	34.699788	4.26E+03
30	7.5	43.5971	5.53E+03	37.021545	5.05E+03	35.816849	5.23E+03	34.69351	4.43E+03	33.032502	4.42E+03
31	7.75	43.046	5.60E+03	36.712151	5.16E+03	38.524798	5.34E+03	34.22283	4.56E+03	35.674193	4.57E+03
32	8	42.7152	5.66E+03	37.74947	5.26E+03	41.154606	5.45E+03	36.06739	4.70E+03	33.46509	4.68E+03
33	8.25	46.3095	5.74E+03	37.148731	5.34E+03	41.872377	5.53E+03	35.18654	4.81E+03	33.888999	4.80E+03
34	8.5	46.4409	5.81E+03	36.988199	5.43E+03	42.756249	5.62E+03	36.83357	4.93E+03	34.429854	4.92E+03
35	8.75	44.4551	5.85E+03	38.139264	5.51E+03	43.787995	5.69E+03	34.76638	5.03E+03	37.423639	5.04E+03
36	9	46.4409	5.92E+03	36.988199	5.60E+03	42.756249	5.76E+03	36.83357	5.14E+03	34.429854	5.14E+03
37	9.25	46.8292	5.98E+03	41.616207	5.67E+03	42.355759	5.81E+03	38.85619	5.23E+03	38.370333	5.23E+03
38	9.5	47.984	6.04E+03	42.9567	5.75E+03	42.074972	5.89E+03	37.84939	5.32E+03	38.067179	5.33E+03
39	9.75	45.5872	6.07E+03	42.491199	5.82E+03	44.405429	5.96E+03	39.39112	5.42E+03	39.367975	5.42E+03
40	10	45.7564	6.12E+03	41.587543	5.87E+03	43.621282	6.02E+03	37.77195	5.49E+03	38.084223	5.49E+03

To better understand the conflicting effect of the impedance value of the SFCL on the bus voltage deviation (objective f_1) and bus active power deviation (objective f_2), Figure 4.7 shows the variation of these objectives with respect to the SFCL's impedance value for a SLG fault. As it is shown, the minimum voltage deviation and active power deviation for this fault scenario are corresponding to the resistance values of 1.75 Ω and 2.25 Ω, respectively. This situation is repeated for each fault scenario in the system. In this case, there is no single solution that optimizes each objective simultaneously. Therefore, the objective functions are conflicting, and there is a (possibly infinite) number of Pareto optimal solutions.

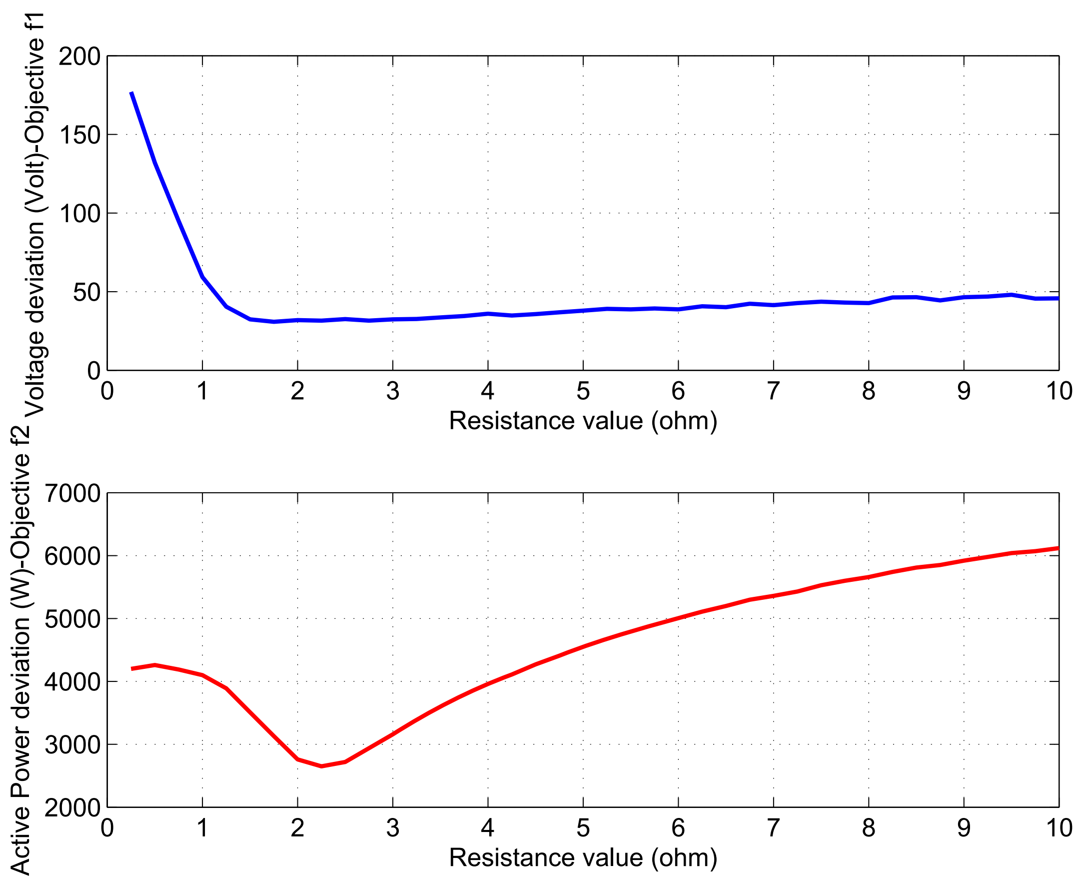

Figure 4.7: Variation of objectives f_1 and f_2 with respect to resistance value for SLG fault

Different types of faults may have a different probability of occurrences and different level of consequences for different cases. These factors are considered by PO_i and C_i. It is important to take into account these factors in the simulation-based decision-making framework. SLG fault is the most common fault, and on the other hand, the less severe fault in the power system [103]. Hence the following expressions are introduced to consider the probability of occurrences of the faults occurrence and their consequences.

$$\Delta V_f = \sum_{i=1}^{5} SV_i \times PO_i \times C_i \tag{4.19}$$

$$\Delta P_f = \sum_{i=1}^{5} SP_i \times PO_i \times C_i \tag{4.20}$$

where i, SV_i, SP_i, PO_i, and C_i are the faults index, simulation value of objective f_1, simulation value of objective f_2, probability of occurrences weight of fault i, and consequence weight of fault i, respectively. The factors PO_i and C_i considered in this study are reported in Table 4.3.

Table 4.3: Probability of occurrences and consequences factors of the faults

Fault type	**Probability of occurrence factor**	**Consequence factor**
SLG	0.45	0.2
DLG	0.2	0.2
LL	0.15	0.2
LLL	0.1	0.2
LLLG	0.1	0.2

The general decision-making framework to find the optimal SFCL's impedance value is summarized as follows.

- **Step I**: Different fault scenarios including SLG, DLG, LL, LLL, and LLLG are applied to the power network.
- **Step II**: For each fault scenario, the objectives (4.10)-(4.12) are calculated.
- **Step III**: According to the calculated parameters in step II, the two factors ΔV_f and ΔP_f are evaluated based on the faults probability of occurrences and consequences factors (Equations (4.19),(4.20).
- **Step IV**: Pareto optimal set is recognized.
- **Step V**: Output the optimal impedance of the SFCL.

The multi-objective optimization problem discussed is applied to the MVDC SPS to find the optimal impedance value of the SFCL. The tuning of SFCL is handled as a multi-objective optimization problem where there are three conflicting objectives: impedance value, voltage deviation, and active power deviation. In these decision-making environments, simultaneous optimization of all the objectives is impossible and the concept of Pareto optimal front is used to find a set of answers that are better than all the other answers among all the solutions but not necessary better than one another. The Pareto optimal set in two-dimensional and three-dimensional objective function for SFCL sizing problem is represented in Figure 4.8. However, to find one solution that considers the relative importance of all objectives, a weighted single objective function has been developed. In this approach, first, the value of all the objectives are transformed to fall between zero and one. Then, three weights are assigned to the all objectives. The solution that leads to the best weighted total will be selected.

Several tests have been carried out to examine the result of the SFCL sizing problem. Different weighting factors for the objectives f_1, f_2, and f_3 have been considered according to (4.13) as shown in Table 4.4.

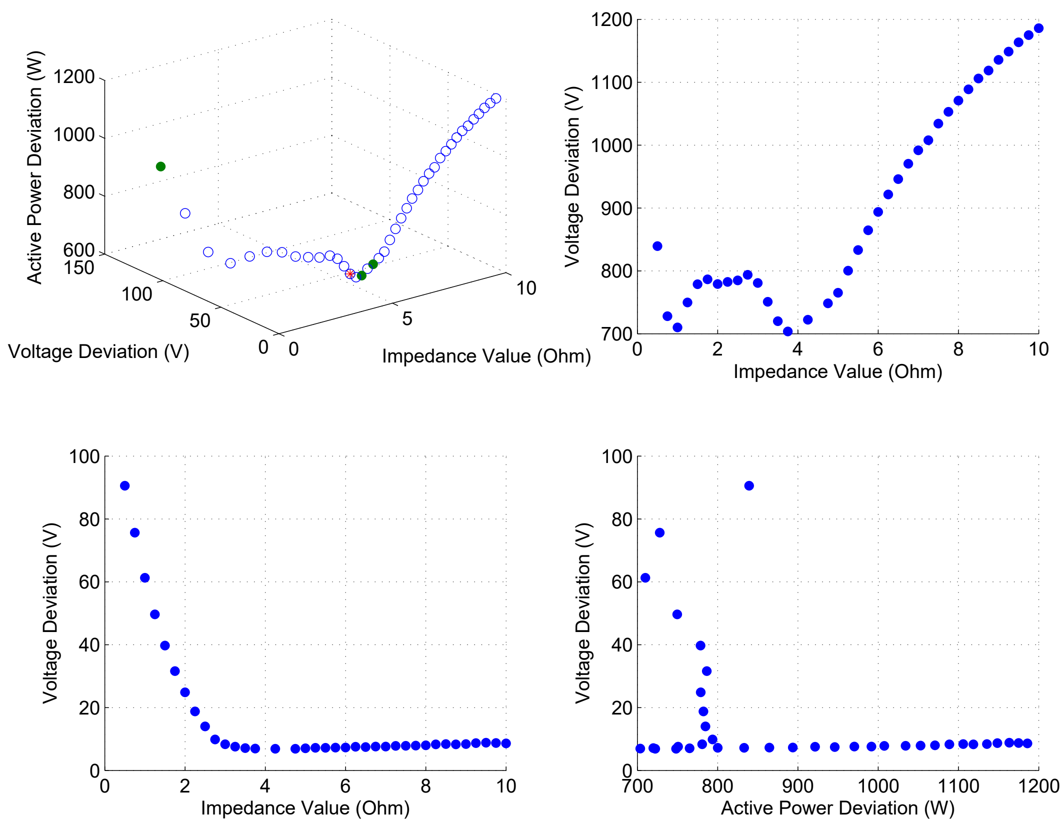

Figure 4.8: The Pareto optimal set in two-dimensional and three-dimensional objective function for SFCL

Table 4.4: Weighting factors for different case scenarios

	W_1	W_2	W_3
Case 1	1	1	1
Case 2	2	1	1
Case 3	5	1	1
Case 4	10	1	1
Case 5	1	5	1
Case 6	1	20	1
Case 7	1	1	20

4.4 Results and discussion

To verify the performance of the proposed approach for MVDC SPS application, a simplified SPS is considered as a case study as shown in Figure 4.9. The combined STATCOM-SFCL is connected to the AC bus of the network in order to provide support for the propulsion load which is considered as vital load in the load area and the rest of the system. In this study, the model of the MVDC SPS, STATCOM-SFCL, and controller are simulated in MATLAB/Simulink platform. For simplicity, the generators are modeled by a three-phase voltage source with an internal R-L impedance and the propulsion load is represented with a three-phase balanced load as a parallel combination of RL elements. The active and reactive power absorbed by the load are 5 MW and 1 MVar, respectively.

In the multi-objective decision making for SFCL sizing problem, there is no best single solution and any solution in the Pareto optimal set might be the best for different situations. The weighted single objective function is introduced to lead to one single solution based on different level of importance of these objectives. The simulation results for SFCL tuning process with respect to the weighting factor in Table 4.4 are shown in Table 4.5. Different case studies including different weighting factors are simulated. As it is shown in this table, higher impedance value is not necessarily resulted in less voltage fluctuation and active power deviation. For example the SFCL's impedance value (f_3) in case 4 is less than in impedance value in case 3, but the active power (f_2) in case 4 is more than active power in case 3 and voltage deviation (f_1) in case 4 is less than voltage deviation in case 3.

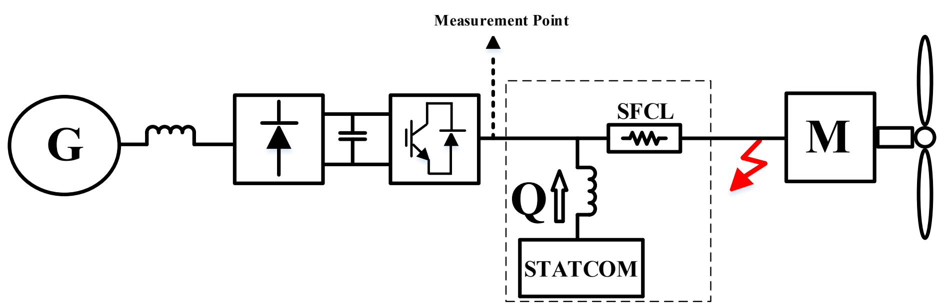

Figure 4.9: Single line diagram of the MVDC incorporated STATCOM-SFCL

In this power system network, a STATCOM is employed to regulate voltage by injecting or absorbing the reactive power. In this regard, when the voltage at a bus is greater than the output AC voltage of the voltage source PWM inverter, the STATCOM draws reactive power from the network, and vice versa. In this study, maintaining the AC bus voltage close to its desired value has more importance than the STATCOM's DC bus voltage regulation. So, the value of the factors w_1 and w_2 are set to 0 and 1, respectively. To compare the influence of the weighting factors a and b in (4.5) on the AC bus voltage magnitude with the use of STATCOM alone, the peak values of the voltage at the load bus with different parameters a and b are shown in Table 4.6. It is inferred that by increasing the factor a, which corresponds to the average voltage value in all the cases, the peak magnitude of the voltage will be decreased. Figure 4.10 shows the convergence of the fitness function versus the number of iterations for FGA optimization method. Within the first 30 iterations, the amount of fitness improvement for FGA is high. The FGA optimization keeps improving even after iteration 50. The optimal values of the controller parameters found by FGA optimization technique optimizer with the parameters $a = 0.5$ and $b = 0.5$ are also tabulated in Table 4.7.

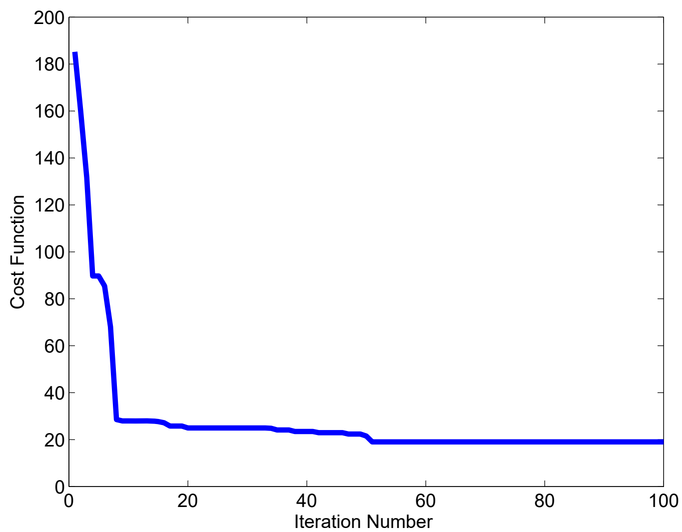

Figure 4.10: Convergence fitness for FGA optimization technique

Three scenarios have been tested to analyze the performance of the proposed method as follows.

- Case I: single phase to ground short circuit fault
- Case II: double phase to ground short circuit fault
- Case III: three phase short circuit fault

Table 4.5: Simulation results for different case studies

	f_1	f_2	f_3
Case 1	7.1029	719.92	3.5
Case 2	8.3090	780.7546	3
Case 3	13.9948	784.862	2.5
Case 4	39.7233	778.6894	1.5
Case 5	6.9527	703.6638	3.75
Case 6	6.89	722.2773	4.25
Case 7	6.9625	703.5488	4

Table 4.6: Voltage at load bus peak magnitude in different scenarios

Weighting factors / **Scenario**	**a=0 , b=1**		**a=0.5 , b=0.5**		**a=1 , b=0**	
Case I	1.045	1.085	1.043	1.083	1.042	1.083
Case II	1.046	1.089	1.046	1.086	1.044	1.085
Case III	1.045	1.083	1.043	1.083	1.043	1.083

Table 4.7: Optimal STATCOM controller parameters found by different approaches

Controller Parameter	**Value**
Kp-i	0.717
Ki-i	1.252e+02
Kp-Vdc	0.002
Ki-Vdc	0.258
Kp-Vac	1.201
Ki-Vac	1.953

For each fault, nine conditions are simulated and compared in Figure 4.11 to Figure 4.13. For each fault scenario, AC bus voltage, active power passes through the AC side of the system are reported. Each scenario in these figures is correspondent with the cases tabulated in Table 4.5. Fault resistance is also set as 0.1 Ω in this study.

4.4.1 Case I: single phase to ground short circuit fault

In this scenario, a 500 ms single phase to ground short circuit fault is applied to the AC load bus at t=0.2 s. Figure 4.11 shows the simulation results of this case study. As observed in this figure, the three phase rms voltage falls to about 0.83 pu during the fault without any compensation. Applying STATCOM restores the voltage to about 0.89 pu. It is also concluded from this figure that although applying STATCOM with FGA-based controller design improves the system performance, it can not fully support the system in terms of power quality improvement. The integration of SFCL to the STATCOM enhances the performance of the proposed scheme. In STATCOM-SFCL cases, the voltage restores to about 0.98 pu which is a notable improvement in the performance of the system in case of the fault. The variations of the active power is also shown in this figure. If a fault occurs, the active power will rise to about 6.5 MW, when there is no compensation in the system. However, this value can be reduced to 4.7 MW in case of utilizing STATCOM-SFCL scheme. This result shows that using the proposed scheme will enhance the stability of the SPS during such a fault which is relatively close to the nominal 5 MW level under healthy operation. Among the cases reported in the Table 4.4, the case 3 and case 6 has the best and worst performance, respectively.

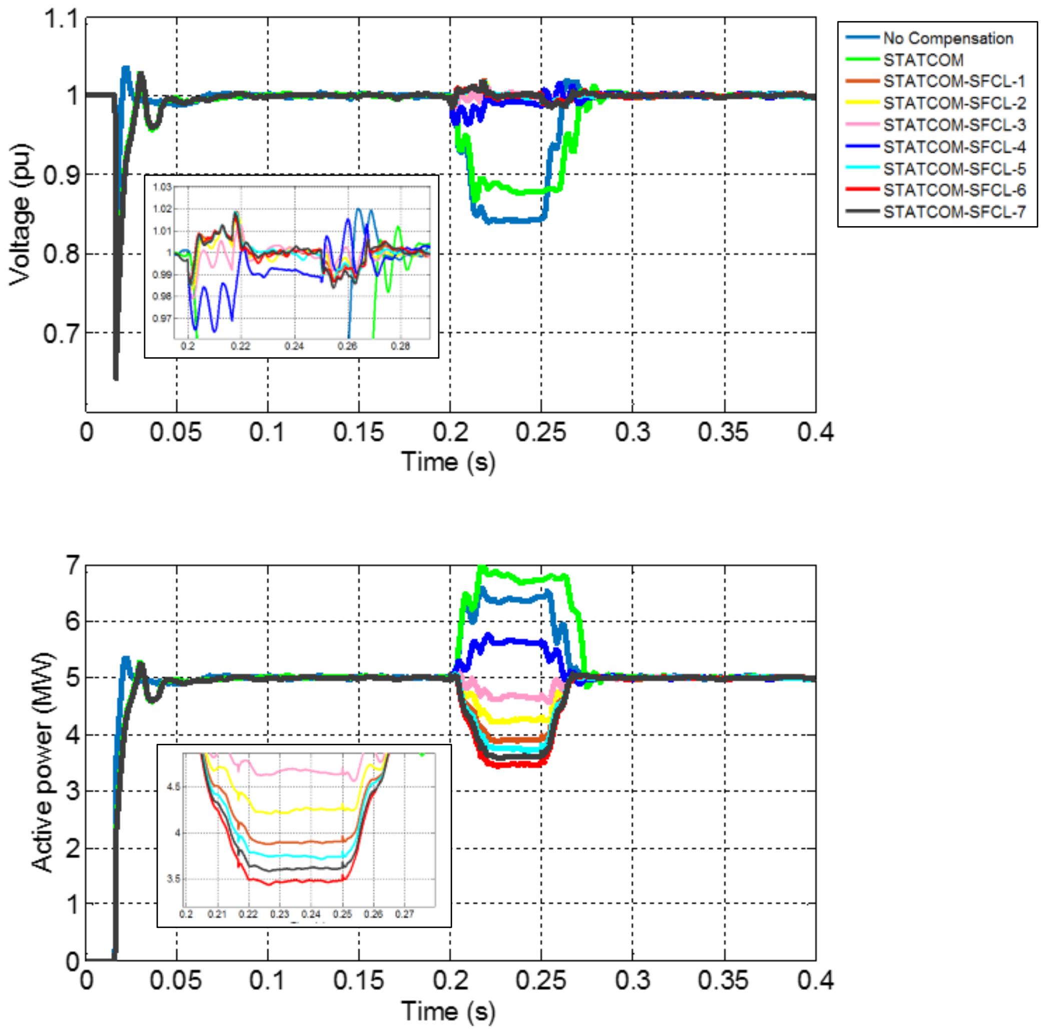

Figure 4.11: System response for single line to ground fault

4.4.2 Case II: double phase to ground short circuit fault

In this scenario, a double phase to ground short circuit fault is applied to the load bus at t=0.2 s and the fault cleared at t=0.25 s. The simulation results for this fault scenario has been shown in Figure 4.12. It is observed that applying STATCOM-SFCL scheme enhances the stability of the system by returning the voltage from 0.44 pu to 0.99 pu. It can also help the system to maintain the nominal active power passes through the load. In this fault scenario, the case 5 and case 4 has the best and worst performance, respectively.

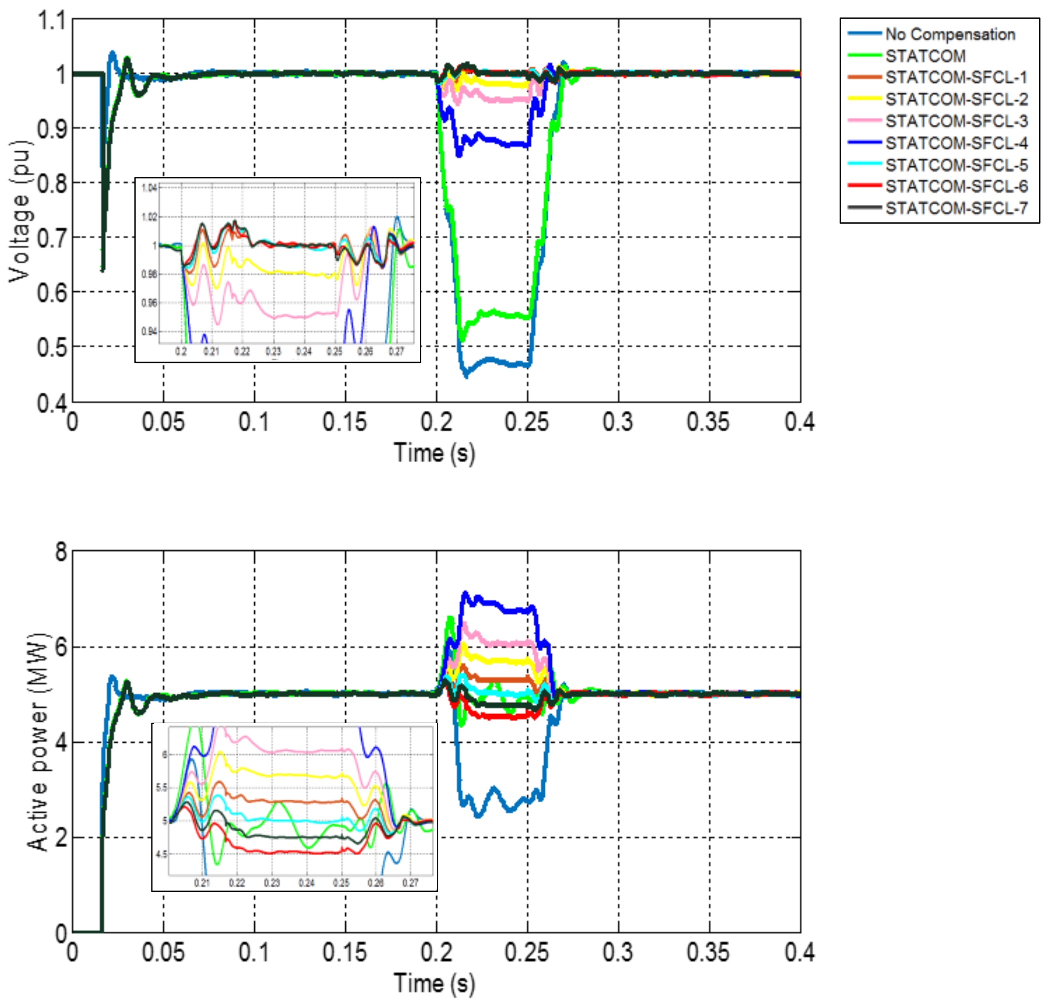

Figure 4.12: System response for double line to ground fault

By comparison of Figure 4.11 and 4.12, it can be seen that the active power will be increased during the fault in the case of system without any compensation in SLG fault scenario. The Figure 4.13 shows the three phase voltage magnitude in SLG and DLG fault cases. This is due to the magnitude of the phase a in SLG case which is more than the phase a in DLG fault scenario.

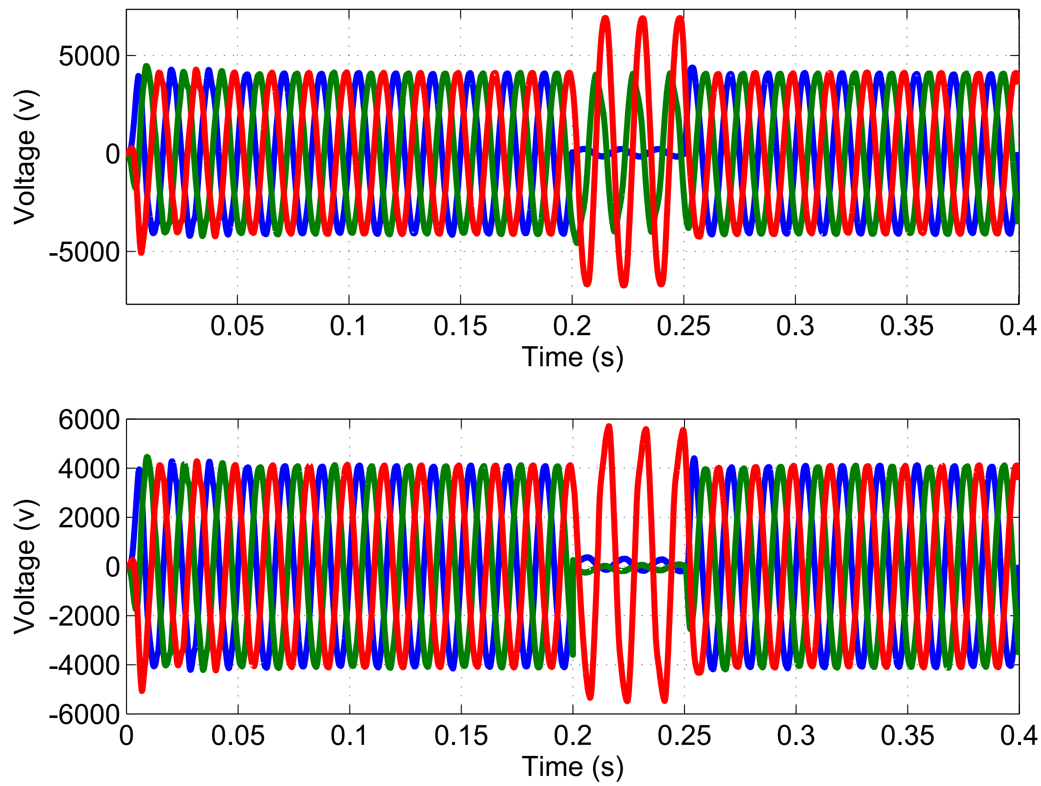

Figure 4.13: Comparison of three phase voltage magnitude for SLG and DLG in the system without compensation

4.4.3 Case III: three phase short circuit fault

In this fault scenario, the STATCOM is integrated into the SFCL to support the excessive reactive power during a fault. Time domain simulation performed, as shown in Figure 4.14. In this scenario, a three phase short circuit fault is applied to the load bus at t=0.2 s and the fault cleared at t=0.25 s. The STATCOM alone cannot improve the system performance. However, applying STATCOM-SFCL improves the stability of the system significantly by returning the voltage from 0.3 pu to 0.97 pu. It can also help the system to maintain the nominal active power passes through the load. In this case the SFCL with an impedance value of 4.75 Ω shows the best performance in case of three phase fault scenario.

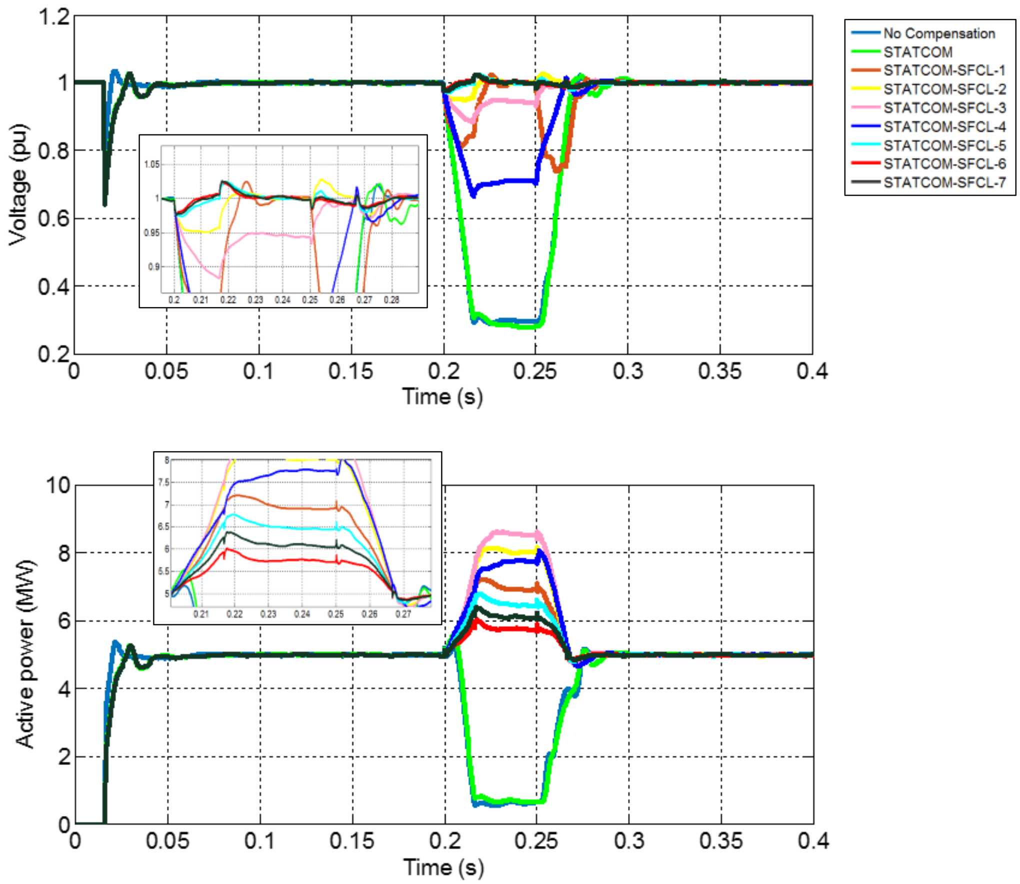

Figure 4.14: System response for three phase fault

4.4.4 Concluding remarks on the selection of optimal SFCL impedance value

It is important to conclude that integration of the shunt compensator (STATCOM) with SFCL with optimized parameters helps to enhance the stability of the system. In summary, the results of the comparisons between different fault scenarios confirm that there is no single solution for the optimal value of the SFCL's impedance value. In our opinion, the selection process of the optimal impedance value for SFCL has to take into account all types of faults. As discussed, different fault types have a different probability of occurrence and consequences; therefore, depending on these factors, the selecting criteria may be different. For example, we obtain the optimal impedance value for SFCL 2.5 Ω for the SLG fault, where these values are 3.75 Ω and 4.75 Ω for DLG fault and LLL fault, respectively. In the MVDC SPS network, we can note that the SLG fault is the most recurrent fault if we based our analysis on the real ship data (approximatively 50 of all faults). Consequently, we could select SFCL with an impedance of 2.5 Ω as the optimal value of the SFCL.

4.5 Conclusion

In this study, an FGA optimization algorithm for optimal designing of a STATCOM's controller is proposed. The STATCOM's controller parameters design is formulated as an optimization problem, and a typical control strategy of a STATCOM is considered in this study. The optimal parameters of six PI controllers are calculated by using the FGA optimization technique. Moreover, in order to enhance the performance of the system in case of fault, a novel multi-objective optimization problem has been formulated to select the size of the SFCL. The simulation results confirmed the performance of proposed scheme for power quality improvement in an MVDC SPS.

CHAPTER V

CONCLUSION AND FUTURE WORK

5.1 Conclusion

This dissertation presents two categories of research work towards the design of a post-fault recovery system for MVDC SPS as follows.

This research work introduced a simulated annealing-based real-time reconfiguration algorithm which is fully implemented in the RTDS platform. The reconfiguration problem is formulated as a multi-objective optimization problem which aims to maximize the total power supply to the system loads following a fault. The SA optimization method is utilized to find the local optimal solutions which are the set of loads' breaker statuses. The performance of the proposed technique has been investigated through two MVDC SPS models including four and six zonal loads. The mathematical model of the reconfiguration problem is solved in the GAMS optimization software which verified the results from the RTDS-based reconfiguration problem. The simulation results show the satisfactory performance of the proposed approach to deal with different fault scenarios. The proposed method in this paper can be used in other real-time optimization-based power system studies such as FACTS devices design problem, distributed generations placement, and planning problems.

Moreover, in this dissertation, an FGA optimization algorithm for optimal designing of a STATCOM's controller parameters is proposed. The simulation results confirmed the performance of the STATCOM for power quality improvement in terms of voltage profile in a hybrid AC/DC system. The STATCOM's parameters design is formulated as a multi-objective optimization problem, and a typical control strategy of a STATCOM is considered in this study. The optimal parameters of six PI controllers are calculated by using the FGA optimization technique. The simulation results show that the FGA method has given an acceptable performance under all the fault and tested. Therefore, FGA can be considered as an efficient alternative for solving FACTS devices controller design problems. Moreover, an optimal design of SFCL has been formulated as a multi-objective optimization problem. Different possible unsymmetrical faults have been used to select the optimal impedance value of the SFCL. It is also shown that the proposed method can be used to find the optimal impedance of the SFCL based on the probability of occurrence and the consequences of different faults. The simulation results confirm the application of the proposed approach to design an SFCL to improve the stability of the power network during transient faults in the power systems.

5.2 Future work direction

The research contributions presented in this dissertation can be further extended as follow.

More case studies can be added to further assess the performance of the proposed technique for shipboard reconfiguration problem. These case studies are including different fault scenarios on the propulsion loads and zonal loads. Moreover, in this dissertation, several assumptions have been made for the sake of simplicity for the reconfiguration problem. As a further study, the protection systems can be modeled in details to evaluate the effect of their delay in reconfiguration performance in responding to the faults in SPS.

In order to solve the reconfiguration problem in this study, the loads' profile has been considered constant. A new method for SPS reconfiguration problem where the uncertainties regarding the loads are taken into account can be further studied. Such an approach require the system operator to solve a stochastic optimization problem. In order to solve the problem of the stochastic based reconfiguration problem, a novel method based on chance-constraints modeling can be introduced; thus, the stochastic optimization problem is converted to its equivalent deterministic optimization formula.

Other optimization-based studies in power systems can be tested through the real-time optimization approach proposed in Chapter 3. As an example, the FACTS devices tuning optimization presented in Chapter 4 can be used to evaluate the presented approach in this dissertation.

5.3 List of publications

- **Journal Papers**
  1. M. Babaei, J. Shi, S. Abdelwahed. "A Survey on Fault Detection, Isolation, and Reconfiguration Methods in Electric Ship Power Systems." IEEE Access journal (Accepted).

2. M. Babaei, R. Jafari-Marandi, S. Abdelwahed., J. Kluss "A novel approach for real-time implementation of MVDC shipboard power system reconfiguration", International Journal of Electrical Power and Energy Systems. (Accepted).
3. M. Babaei, R. Jafari-Marandi, S. Abdelwahed. J. Kluss "Application of Combined STATCOM-SFCL for Stability Improvement of the MVDC Microgrid During Unsymmetrical Faults", 2017. International Journal of Electrical Power and Energy Systems. (Under review).

- **Conference Papers**

1. M. Babaei, R. Jafari-Marandi, Sherif Abdelwahed "Real-time Implementation of MVDC Shipboard Power system Reconfiguration" IEEE Electric Ship Technologies Symposium,2017
2. M. Babaei, R. Jafari-Marandi, S. Abdelwahed, Brian Smith."Application of STATCOM for MVDC Shipboard Power System" IEEE Electric Ship Technologies Symposium 2017
3. M. Babaei,, R. Jafari-Marand, S. Abdelwahed, and B. Smith "Simulated Annealing-Based Optimal Design of STATCOM Under Unbalanced Conditions and Faults" IEEE Power and Energy Conference at Illinois (PECI), 2017.
4. M. Babaei, T. Qunais, S. Abdelwahed."A Linear Quadratic Tracking Based Voltage Controller for VSI; MVDC Shipboard Power System Application." IEEE Power and Energy Society General Meeting, 2017
5. N. Zohrabi, J. Shi, M. Babaei, S. Abdelwahed "Steady-State Specications and Design Requirements for Medium-Voltage DC Shipboard Power System" American Society of Naval Engineers (ASNE), 2016
6. M. Babaei, J. Shi, N. Zohrabi, S. Abdelwahed. "Development of a Hybrid Model For Shipboard Power Systems." In Electric Ship Technologies Symposium (ESTS), 2015 IEEE, pp.145-149. IEEE, 2015.
7. M. Babaei, R. Jafari-Marandi, Sherif Abdelwahed, J. Kluss "A Novel Approach For Optimal Design of Superconducting Fault Current Limiter" IEEE-Texas Power and Energy Conference (TPEC). 2018

REFERENCES

[1] S. Abd-Elazim and E. Ali, "Imperialist competitive algorithm for optimal STATCOM design in a multimachine power system," *International Journal of Electrical Power & Energy Systems*, vol. 76, 2016, pp. 136–146.

[2] S. Abd-Elazim and E. Ali, "Optimal location of STATCOM in multimachine power system for increasing loadability by Cuckoo Search algorithm," *International Journal of Electrical Power & Energy Systems*, vol. 80, 2016, pp. 240–251.

[3] M. Al-Kuwaiti, N. Kyriakopoulos, and S. Hussein, "A comparative analysis of network dependability, fault-tolerance, reliability, security, and survivability," *IEEE Communications Surveys & Tutorials*, vol. 11, no. 2, 2009.

[4] M. Aman, G. Jasmon, A. Bakar, and H. Mokhlis, "Optimum network reconfiguration based on maximization of system loadability using continuation power flow theorem," *International journal of electrical power & energy systems*, vol. 54, 2014, pp. 123–133.

[5] B. Amanulla, S. Chakrabarti, and S. Singh, "Reconfiguration of power distribution systems considering reliability and power loss," *IEEE Transactions on Power Delivery*, vol. 27, no. 2, 2012, pp. 918–926.

[6] B. Amanulla, S. Chakrabarti, and S. Singh, "Reconfiguration of power distribution systems considering reliability and power loss," *IEEE Transactions on Power Delivery*, vol. 27, no. 2, 2012, pp. 918–926.

[7] T. Amba, K. L. Butler-Purry, and M. Falahi, "Genetic algorithm based damage control for shipboard power systems," *Electric Ship Technologies Symposium, 2009. ESTS 2009. IEEE*. IEEE, 2009, pp. 242–252.

[8] T. Amba, K. L. Butler-Purry, and M. Falahi, "Genetic algorithm based damage control for shipboard power systems," *Electric Ship Technologies Symposium, 2009. ESTS 2009. IEEE*. IEEE, 2009, pp. 242–252.

[9] M.-R. Andervazh, J. Olamaei, and M.-R. Haghifam, "Adaptive multi-objective distribution network reconfiguration using multi-objective discrete particles swarm optimisation algorithm and graph theory," *IET Generation, Transmission & Distribution*, vol. 7, no. 12, 2013, pp. 1367–1382.

[10] V. Arcidiacono, A. Monti, and G. Sulligoi, "Generation control system for improving design and stability of medium-voltage DC power systems on ships," *IET Electrical Systems in Transportation*, vol. 2, no. 3, 2012, pp. 158–167.

[11] M. Aurangzeb, P. Crossley, and P. Gale, "Fault location using the high frequency travelling waves measured at a single location on a transmission line," 2001.

[12] M. Babaei, R. Jafari-Marandi, and S. Abdelwahed, "Real-time implementation of MVDC shipboard power system reconfiguration," *Electric Ship Technologies Symposium (ESTS), 2017 IEEE*. IEEE, 2017, pp. 514–519.

[13] M. Babaei, R. Jafari-Marandi, and S. Abdelwahed, "Real-time implementation of MVDC shipboard power system reconfiguration," *Electric Ship Technologies Symposium (ESTS), 2017 IEEE*. IEEE, 2017, pp. 514–519.

[14] M. Babaei, R. Jafari-Marandi, S. Abdelwahed, and B. Smith, "Application of STATCOM for MVDC shipboard power system," *Electric Ship Technologies Symposium (ESTS), 2017 IEEE*. IEEE, 2017, pp. 142–147.

[15] M. Babaei, R. Jafari-Marandi, S. Abdelwahed, and B. Smith, "A simulated Annealing-based optimal design of STATCOM under unbalanced conditions and faults," *Power and Energy Conference at Illinois (PECI), 2017 IEEE*. IEEE, 2017, pp. 1–5.

[16] O. Badran, S. Mekhilef, H. Mokhlis, and W. Dahalan, "Optimal reconfiguration of distribution system connected with distributed generations: A review of different methodologies," *Renewable and Sustainable Energy Reviews*, vol. 73, 2017, pp. 854–867.

[17] S.-M. Baek and J.-W. Park, "Nonlinear parameter optimization of FACTS controller via real-time digital simulator," *IEEE Transactions on Industry Applications*, vol. 49, no. 5, 2013, pp. 2271–2278.

[18] M. E. Baran and N. R. Mahajan, "Overcurrent protection on voltage-source-converter-based multiterminal DC distribution systems," *IEEE transactions on power delivery*, vol. 22, no. 1, 2007, pp. 406–412.

[19] S. Bose, *Cyber-physical Modeling, Analysis, and Optimization: A Shipboard Smart-grid Reconfiguration Case Study*, doctoral dissertation, Kansas State University, 2012.

[20] S. Bose, B. Natarajan, C. Scoglio, S. Das, and N. N. Schulz, "Analysis of robustness for shipboard power system with non-radial power flow," *Electric Ship Technologies Symposium (ESTS), 2011 IEEE*. IEEE, 2011, pp. 181–186.

[21] S. Bose, B. Natarajan, C. M. Scoglio, N. N. Schulz, D. M. Gruenbacher, and S. Das, “Shipboard power systems reconfigurationA cyber-physical framework for response time analysis,” *IEEE Transactions on Industrial Informatics*, vol. 10, no. 1, 2014, pp. 439–449.

[22] S. Bose, S. Pal, B. Natarajan, C. M. Scoglio, S. Das, and N. N. Schulz, “Analysis of optimal reconfiguration of shipboard power systems,” *IEEE Transactions on Power Systems*, vol. 27, no. 1, 2012, pp. 189–197.

[23] S. Bose, S. Pal, B. Natarajan, C. M. Scoglio, S. Das, and N. N. Schulz, “Analysis of optimal reconfiguration of shipboard power systems,” *IEEE Transactions on Power Systems*, vol. 27, no. 1, 2012, pp. 189–197.

[24] G. Buja, A. da Rin, R. Menis, and G. Sulligoi, “Dependable design assessment of integrated power systems for all electric ships,” *Electrical Systems for Aircraft, Railway and Ship Propulsion (ESARS), 2010*. IEEE, 2010, pp. 1–8.

[25] K. Butler and N. Sarma, “General reconfiguration methodology for AC radial shipboard power systems,” *Power Engineering Society Winter Meeting, 2000. IEEE*. IEEE, 2000, vol. 2, pp. 1226–1230.

[26] K. L. Butler, N. Sarma, and V. R. Prasad, “A new method of network reconfiguration for service restoration in shipboard power systems,” *Transmission and Distribution Conference, 1999 IEEE*. IEEE, 1999, vol. 2, pp. 658–662.

[27] P. Cairoli, I. Kondratiev, and R. A. Dougal, “Coordinated control of the bus tie switches and power supply converters for fault protection in DC microgrids,” *IEEE Transactions on Power Electronics*, vol. 28, no. 4, 2013, pp. 2037–2047.

[28] N. K. Chanda and Y. Fu, “ANN-based fault classification and location in MVDC shipboard power systems,” *North American Power Symposium (NAPS), 2011*. IEEE, 2011, pp. 1–7.

[29] A. H. Chang, B. R. Sennett, A.-T. Avestruz, S. B. Leeb, and J. L. Kirtley, “Analysis and design of DC system protection using Z-source circuit breaker,” *IEEE Transactions on Power Electronics*, vol. 31, no. 2, 2016, pp. 1036–1049.

[30] C. Chang, S. Kumar, B. Liu, and A. Khambadkone, “Real-time detection using wavelet transform and neural network of short-circuit faults within a train in DC transit systems,” *IEE Proceedings-Electric Power Applications*, vol. 148, no. 3, 2001, pp. 251–256.

[31] C. Chang, Z. Xu, and A. Khambadkone, “Enhancement and laboratory implementation of neural network detection of short circuit faults in DC transit system,” *IEE Proceedings-Electric Power Applications*, vol. 150, no. 3, 2003, pp. 344–350.

[32] L. Chen, H. Chen, J. Yang, L. Zhu, Y. Tang, L. H. Koh, Y. Xu, C. Zhang, Y. Liao, and L. Ren, "Comparison of Superconducting Fault Current Limiter and Dynamic Voltage Restorer for LVRT Improvement of High Penetration Microgrid," *IEEE Transactions on Applied Superconductivity*, vol. 27, no. 4, 2017, pp. 1–7.

[33] E. Chow and A. Willsky, "Analytical redundancy and the design of robust failure detection systems," *IEEE Transactions on automatic control*, vol. 29, no. 7, 1984, pp. 603–614.

[34] E. Christopher, M. Sumner, D. W. Thomas, X. Wang, and F. de Wildt, "Fault location in a zonal DC marine power system using active impedance estimation," *IEEE Transactions on Industry Applications*, vol. 49, no. 2, 2013, pp. 860–865.

[35] K. A. Corzine and R. W. Ashton, "Structure and analysis of the Z-source MVDC breaker," *Electric Ship Technologies Symposium (ESTS), 2011 IEEE*. IEEE, 2011, pp. 334–338.

[36] G. Didier and J. Lévêque, "Influence of fault type on the optimal location of superconducting fault current limiter in electrical power grid," *International Journal of Electrical Power & Energy Systems*, vol. 56, 2014, pp. 279–285.

[37] G. Didier, J. Leveque, and A. Rezzoug, "A novel approach to determine the optimal location of SFCL in electric power grid to improve power system stability," *IEEE Transactions on Power Systems*, vol. 28, no. 2, 2013, pp. 978–984.

[38] N. Doerry, "Next generation integrated power systems (NGIPS) for the future fleet," *IEEE Electric Ship Technologies Symposium*, 2009.

[39] D. Dong, Y. Pan, R. Lai, X. Wu, and K. Weeber, "Active fault-current foldback control in thyristor rectifier for DC shipboard electrical system," *IEEE Journal of Emerging and Selected Topics in Power Electronics*, vol. 5, no. 1, 2017, pp. 203–212.

[40] T. Dragičević, X. Lu, J. C. Vasquez, and J. M. Guerrero, "DC microgridsPart II: A review of power architectures, applications, and standardization issues," *IEEE transactions on power electronics*, vol. 31, no. 5, 2016, pp. 3528–3549.

[41] D.-L. Duan, X.-D. Ling, X.-Y. Wu, and B. Zhong, "Reconfiguration of distribution network for loss reduction and reliability improvement based on an enhanced genetic algorithm," *International Journal of Electrical Power & Energy Systems*, vol. 64, 2015, pp. 88–95.

[42] S. S. S. Farahani, M. Nikzad, M. B. Tabar, M. G. Naraghi, and A. Javadian, "Genetic Algorithms for Tuning Supplementary STATCOM Stabilizer in a Multi Machine Electric Power System," *Research Journal of Applied Sciences, Engineering and Technology*, vol. 3, no. 8, 2011, pp. 843–851.

[43] A. Geraci, F. Katki, L. McMonegal, B. Meyer, J. Lane, P. Wilson, J. Radatz, M. Yee, H. Porteous, and F. Springsteel, *IEEE standard computer dictionary: Compilation of IEEE standard computer glossaries*, IEEE Press, 1991.

[44] Y. Gong, Y. Huang, and N. Schulz, "Integrated protection system design for shipboard power system," *Electric Ship Technologies Symposium, 2005 IEEE*. IEEE, 2005, pp. 237–243.

[45] X. Guillaud, M. O. Faruque, A. Teninge, A. H. Hariri, L. Vanfretti, M. Paolone, V. Dinavahi, P. Mitra, G. Lauss, C. Dufour, et al., "Applications of real-time simulation technologies in power and energy systems," *IEEE Power and Energy Technology Systems Journal*, vol. 2, no. 3, 2015, pp. 103–115.

[46] M. A. Guimaraes, J. F. Lorenzeti, and C. A. Castro, "Reconfiguration of distribution systems for stability margin enhancement using tabu search," *Power System Technology, 2004. PowerCon 2004. 2004 International Conference on*. IEEE, 2004, vol. 2, pp. 1556–1561.

[47] Y. Hashemi and K. Valipour, "FDM based multi-objective optimal sitting and design of TC-FLSFCL for study of distribution system reliability," *International Journal of Electrical Power & Energy Systems*, vol. 61, 2014, pp. 463–473.

[48] H. Heydari-doostabad, M. R. Khalghani, and M. H. Khooban, "A novel control system design to improve LVRT capability of fixed speed wind turbines using STATCOM in presence of voltage fault," *International Journal of Electrical Power & Energy Systems*, vol. 77, 2016, pp. 280–286.

[49] K. Huang, D. A. Cartes, and S. K. Srivastava, "A multiagent-based algorithm for ring-structured shipboard power system reconfiguration," *IEEE Transactions on Systems, Man, and Cybernetics, Part C (Applications and Reviews)*, vol. 37, no. 5, 2007, pp. 1016–1021.

[50] K. Huang, D. A. Cartes, and S. K. Srivastava, "A multiagent-based algorithm for ring-structured shipboard power system reconfiguration," *IEEE Transactions on Systems, Man, and Cybernetics, Part C (Applications and Reviews)*, vol. 37, no. 5, 2007, pp. 1016–1021.

[51] K. Huang, S. Srivastava, and D. Cartes, "Decentralized reconfiguration for power systems using multi agent system," *Systems Conference, 2007 1st Annual IEEE*. IEEE, 2007, pp. 1–6.

[52] Q. Huang, K. Borisov, and H. Ginn, "PEBB-based shunt active power filter for shipboard power systems," *Electric Ship Technologies Symposium, 2005 IEEE*. IEEE, 2005, pp. 393–399.

[53] R. A. Jabr, R. Singh, and B. C. Pal, "Minimum loss network reconfiguration using mixed-integer convex programming," *IEEE Transactions on Power systems*, vol. 27, no. 2, 2012, pp. 1106–1115.

[54] R. Jafari-Marandi and B. K. Smith, "Fluid Genetic Algorithm (FGA)," *Journal of Computational Design and Engineering*, vol. 4, no. 2, 2017, pp. 158–167.

[55] R. Jayabalan and B. Fahimi, "Fault diagnostics in naval shipboard power system for contingency management and survivability," *Electric Ship Technologies Symposium, 2005 IEEE*. IEEE, 2005, pp. 108–111.

[56] A. R. Jordehi, J. Jasni, N. I. A. Wahab, and M. Z. A. A. Kadir, "Particle swarm optimisation applications in FACTS optimisation problem," *Power Engineering and Optimization Conference (PEOCO), 2013 IEEE 7th International*. IEEE, 2013, pp. 193–198.

[57] S. N. K. Butler-Purry, "Self healing reconfiguration for restoration of naval shipboard power systems," *IEEE Transactions on Power Systems*, vol. 19, no. 2, 2004, pp. 754 – 762.

[58] S. Kannan, S. Jayaram, and M. Salama, "Design of a de-coupled Controller for a shunt converter: Control design and performance," *proc. 32nd North American Power symp., Waterloo, ON, Canada*, 2000.

[59] S. Kannan, S. Jayaram, and M. Salama, "Real and reactive power coordination for a unified power flow controller," *IEEE Transactions on Power Systems*, vol. 19, no. 3, 2004, pp. 1454–1461.

[60] M. Kempkes, I. Roth, and M. Gaudreau, "Solid-state circuit breakers for medium voltage DC power," *Electric Ship Technologies Symposium (ESTS), 2011 IEEE*. IEEE, 2011, pp. 254–257.

[61] N. V. Kovački, P. M. Vidović, and A. T. Sarić, "Scalable algorithm for the dynamic reconfiguration of the distribution network using the Lagrange relaxation approach," *International Journal of Electrical Power & Energy Systems*, vol. 94, 2018, pp. 188–202.

[62] H. Li, W. Li, M. Luo, A. Monti, and F. Ponci, "Design of smart MVDC power grid protection," *IEEE Transactions on Instrumentation and Measurement*, vol. 60, no. 9, 2011, pp. 3035–3046.

[63] W. Li, M. Luo, A. Monti, and F. Ponci, "Wavelet based method for fault detection in medium voltage DC shipboard power systems," *Instrumentation and Measurement Technology Conference (I2MTC), 2012 IEEE International*. IEEE, 2012, pp. 2155–2160.

[64] W. Li, A. Monti, and F. Ponci, "Fault detection and classification in medium voltage DC shipboard power systems with wavelets and artificial neural networks," *IEEE Transactions on Instrumentation and Measurement*, vol. 63, no. 11, 2014, pp. 2651–2665.

[65] L. Liu, K. P. Logan, D. A. Cartes, and S. K. Srivastava, "Fault detection, diagnostics, and prognostics: software agent solutions," *IEEE Transactions on Vehicular Technology*, vol. 56, no. 4, 2007, pp. 1613–1622.

[66] B. Mahdad and K. Srairi, "Application of a combined superconducting fault current limiter and STATCOM to enhancement of power system transient stability," *Physica C: Superconductivity*, vol. 495, 2013, pp. 160–168.

[67] M. Mandour and S. Abd-Elazeem, "Robust design of STATCOM controller for improving power system damping performance via GA," *Ain Shams Journal of Electrical Engineering*, vol. 43, no. 2, 2008, pp. 237–248.

[68] A. Maqsood, Corzine, and A. Keith, "The Z-source breaker for ship power system protection," *Electric Ship Technologies Symposium (ESTS), 2015 IEEE*. IEEE, 2015, pp. 293–298.

[69] A. Maqsood and K. A. Corzine, "Integration of Z-Source Breakers Into Zonal DC Ship Power System Microgrids," *IEEE Journal of Emerging and Selected Topics in Power Electronics*, vol. 5, no. 1, 2017, pp. 269–277.

[70] F. Maturana, R. Staron, F. Discenzo, D. Scheidt, M. Pekala, J. Bracy, and M. Zink, "An interoperable agent-based control system for survivable shipboard automation," *ASNE Reconfiguration and Survivability Symposium*, 2005.

[71] H. Mirzaee, B. Parkhideh, and S. Bhattacharya, "Design and control of series dc active filter (sdaf) for shipboard medium-voltage dc power system," *Electric Ship Technologies Symposium (ESTS), 2011 IEEE*. IEEE, 2011, pp. 452–458.

[72] P. Mitra and G. K. Venayagamoorthy, "A DSTATCOM controller tuned by particle swarm optimization for an electric ship power system," *Power and Energy Society General Meeting-Conversion and Delivery of Electrical Energy in the 21st Century, 2008 IEEE*. IEEE, 2008, pp. 1–6.

[73] P. Mitra and G. K. Venayagamoorthy, "An adaptive control strategy for DSTATCOM applications in an electric ship power system," *IEEE Transactions on Power Electronics*, vol. 25, no. 1, 2010, pp. 95–104.

[74] P. Mitra and G. K. Venayagamoorthy, "Implementation of an intelligent reconfiguration algorithm for an electric ship's power system," *IEEE Transactions on Industry Applications*, vol. 47, no. 5, 2011, pp. 2292–2300.

[75] P. Mitra and G. K. Venayagamoorthy, "Implementation of an intelligent reconfiguration algorithm for an electric ship's power system," *IEEE Transactions on Industry Applications*, vol. 47, no. 5, 2011, pp. 2292–2300.

[76] A. Moghadasi, A. Sarwat, and J. M. Guerrero, "Multiobjective optimization in combinatorial wind farms system integration and resistive SFCL using analytical hierarchy process," *Renewable Energy*, vol. 94, 2016, pp. 366–382.

[77] M. Moghbel, M. A. Masoum, A. Fereidouni, and S. Deilami, "Optimal Sizing, Siting and Operation of Custom Power Devices with STATCOM and APLC Functions for Real-Time Reactive Power and Network Voltage Quality Control of Smart Grid," *IEEE Transactions on Smart Grid*, 2017.

[78] S. Mohagheghi, Y. del Valle, G. K. Venayagamoorthy, and R. G. Harley, "A proportional-integrator type adaptive critic design-based neurocontroller for a static compensator in a multimachine power system," *IEEE Transactions on Industrial Electronics*, vol. 54, no. 1, 2007, pp. 86–96.

[79] M. H. Moradi, S. Razini, and S. M. Hosseinian, "State of art of multiagent systems in power engineering: A review," *Renewable and Sustainable Energy Reviews*, vol. 58, 2016, pp. 814–824.

[80] T. Nagata and H. Sasaki, "A multi-agent approach to power system restoration," *IEEE transactions on power systems*, vol. 17, no. 2, 2002, pp. 457–462.

[81] M. R. Narimani, A. A. Vahed, R. Azizipanah-Abarghooee, and M. Javidsharifi, "Enhanced gravitational search algorithm for multi-objective distribution feeder reconfiguration considering reliability, loss and operational cost," *IET Generation, Transmission & Distribution*, vol. 8, no. 1, 2014, pp. 55–69.

[82] K. R. Padamati, N. N. Schulz, and A. K. Srivastava, "Application of genetic algorithm for reconfiguration of shipboard power system," *Power Symposium, 2007. NAPS'07. 39th North American*. IEEE, 2007, pp. 159–163.

[83] Y. Pan, P. Silveira, M. Steurer, T. Baldwin, and P. Ribeiro, "A fault location approach for high-impedance grounded DC shipboard power distribution systems," *Power and Energy Society General Meeting-Conversion and Delivery of Electrical Energy in the 21st Century, 2008 IEEE*. IEEE, 2008, pp. 1–6.

[84] S. Panda and N. P. Padhy, "Comparison of particle swarm optimization and genetic algorithm for FACTS-based controller design," *Applied soft computing*, vol. 8, no. 4, 2008, pp. 1418–1427.

[85] J.-D. Park, J. Candelaria, L. Ma, and K. Dunn, "DC ring-bus microgrid fault protection and identification of fault location," *IEEE Transactions on Power Delivery*, vol. 28, no. 4, 2013, pp. 2574–2584.

[86] W.-J. Park, B. C. Sung, and J.-W. Park, "The effect of SFCL on electric power grid with wind-turbine generation system," *IEEE Transactions on Applied Superconductivity*, vol. 20, no. 3, 2010, pp. 1177–1181.

[87] L. L. Qi, A. Antoniazzi, L. Raciti, and D. Leoni, "Design of Solid-State Circuit Breaker-Based Protection for DC Shipboard Power Systems," *IEEE Journal of Emerging and Selected Topics in Power Electronics*, vol. 5, no. 1, 2017, pp. 260–268.

[88] D. Radu and Y. Besanger, "A multi-objective genetic algorithm approach to optimal allocation of multi-type FACTS devices for power systems security," *2006 IEEE Power Engineering Society General Meeting*. IEEE, 2006, pp. 8–pp.

[89] R. Rajaram, K. S. Kumar, and N. Rajasekar, "Power system reconfiguration in a radial distribution network for reducing losses and to improve voltage profile using modified plant growth simulation algorithm with Distributed Generation (DG)," *Energy Reports*, vol. 1, 2015, pp. 116–122.

[90] R. Rajaram, K. S. Kumar, and N. Rajasekar, "Power system reconfiguration in a radial distribution network for reducing losses and to improve voltage profile using modified plant growth simulation algorithm with Distributed Generation (DG)," *Energy Reports*, vol. 1, 2015, pp. 116–122.

[91] P. C. Ramaswamy, J. Tant, J. R. Pillai, and G. Deconinck, "Novel methodology for optimal reconfiguration of distribution networks with distributed energy resources," *Electric Power Systems Research*, vol. 127, 2015, pp. 165–176.

[92] P. C. Ramaswamy, J. Tant, J. R. Pillai, and G. Deconinck, "Novel methodology for optimal reconfiguration of distribution networks with distributed energy resources," *Electric Power Systems Research*, vol. 127, 2015, pp. 165–176.

[93] R. S. Rao, K. Ravindra, K. Satish, and S. Narasimham, "Power los minimization in distribution system using network reconfiguration in the presence of distributed generation," *IEEE transactions on power systems*, vol. 28, no. 1, 2013, pp. 317–325.

[94] R. S. Rao, K. Ravindra, K. Satish, and S. Narasimham, "Power loss minimization in distribution system using network reconfiguration in the presence of distributed generation," *IEEE transactions on power systems*, vol. 28, no. 1, 2013, pp. 317–325.

[95] E. Rashidi, M. Parsafard, H. Medal, and X. Li, "Optimal traffic calming: A mixed-integer bi-level programming model for locating sidewalks and crosswalks in a multimodal transportation network to maximize pedestrians safety and network usability," *Transportation research part E: logistics and transportation review*, vol. 91, 2016, pp. 33–50.

[96] S. Ray and G. K. Venayagamoorthy, “Real-time implementation of a measurement-based adaptive wide-area control system considering communication delays,” *IET generation, transmission & distribution*, vol. 2, no. 1, 2008, pp. 62–70.

[97] E. Rosenthal, “GAMS-A users guide,” *GAMS Development Corporation*. Citeseer, 2008.

[98] M. Saeedifard, M. Graovac, R. Dias, and R. Iravani, “DC power systems: Challenges and opportunities,” *Power and Energy Society General Meeting, 2010 IEEE*. IEEE, 2010, pp. 1–7.

[99] N. Sahoo, B. Panigrahi, P. Dash, and G. Panda, “Multivariable nonlinear control of STATCOM for synchronous generator stabilization,” *International journal of electrical power & energy systems*, vol. 26, no. 1, 2004, pp. 37–48.

[100] T. Sakaguchi and K. Matsumoto, “Development of a knowledge based system for power system restoration,” *IEEE Transactions on Power Apparatus and Systems*, , no. 2, 1983, pp. 320–329.

[101] T. Sakaguchi and K. Matsumoto, “Development of a knowledge based system for power system restoration,” *IEEE Transactions on Power Apparatus and Systems*, , no. 2, 1983, pp. 320–329.

[102] R. J. Sarfi, M. Salama, and A. Chikhani, “A survey of the state of the art in distribution system reconfiguration for system loss reduction,” *Electric Power Systems Research*, vol. 31, no. 1, 1994, pp. 61–70.

[103] M. C. Schmidt, *Electric power research trends*, Nova Publishers, 2007.

[104] F. Shahnia, S. Rajakaruna, and A. Ghosh, *Static compensators (STATCOMs) in power systems*, Springer, 2015.

[105] F. Shariatzadeh, N. Kumar, and A. K. Srivastava, “Optimal Control Algorithms for Reconfiguration of Shipboard Microgrid Distribution System Using Intelligent Techniques,” *IEEE Transactions on Industry Applications*, vol. 53, no. 1, 2017, pp. 474–482.

[106] F. Shariatzadeh, N. Kumar, and A. K. Srivastava, “Optimal Control Algorithms for Reconfiguration of Shipboard Microgrid Distribution System Using Intelligent Techniques,” *IEEE Transactions on Industry Applications*, vol. 53, no. 1, 2017, pp. 474–482.

[107] F. Shariatzadeh, C. B. Vellaithurai, S. S. Biswas, R. Zamora, and A. K. Srivastava, “Real-time implementation of intelligent reconfiguration algorithm for microgrid,” *IEEE Transactions on Sustainable Energy*, vol. 5, no. 2, 2014, pp. 598–607.

[108] F. Shariatzadeh, C. B. Vellaithurai, S. S. Biswas, R. Zamora, and A. K. Srivastava, "Real-time implementation of intelligent reconfiguration algorithm for microgrid," *IEEE Transactions on Sustainable Energy*, vol. 5, no. 2, 2014, pp. 598–607.

[109] J. Shi, R. Amgai, and S. Abdelwahed, "Modelling of shipboard medium-voltage direct current system for system level dynamic analysis," *IET Electrical Systems in Transportation*, vol. 5, no. 4, 2015, pp. 156–165.

[110] R. Sirjani and A. R. Jordehi, "Optimal placement and sizing of distribution static compensator (D-STATCOM) in electric distribution networks: A review," *Renewable and Sustainable Energy Reviews*, vol. 77, 2017, pp. 688–694.

[111] I. I. A. Society, "Recommended Practice for 1 kV to 35 kV Medium-Voltage DC Power Systems on Ship," *IEEE Std*. IEEE, 2010.

[112] J. M. Solanki and N. N. Schulz, "Using intelligent multi-agent systems for shipboard power systems reconfiguration," *Intelligent Systems Application to Power Systems, 2005. Proceedings of the 13th International Conference on*. IEEE, 2005, pp. 3–pp.

[113] A. Stankovic and M. Calovic, "Graph oriented algorithm for the steady-state security enhancement in distribution networks," *IEEE Transactions on Power Delivery*, vol. 4, no. 1, 1989, pp. 539–544.

[114] C.-L. Su, C.-K. Lan, T.-C. Chou, and C.-J. Chen, "Performance evaluation of multiagent systems for navy shipboard power system restoration," *IEEE Transactions on Industry Applications*, vol. 51, no. 4, 2015, pp. 2769–2779.

[115] B. C. Sung, D. K. Park, J.-W. Park, and T. K. Ko, "Study on a series resistive SFCL to improve power system transient stability: modeling, simulation, and experimental verification," *IEEE transactions on industrial electronics*, vol. 56, no. 7, 2009, pp. 2412–2419.

[116] B. C. Sung, D. K. Park, J.-W. Park, and T. K. Ko, "Study on a series resistive SFCL to improve power system transient stability: modeling, simulation, and experimental verification," *IEEE transactions on industrial electronics*, vol. 56, no. 7, 2009, pp. 2412–2419.

[117] B. C. Sung, D. K. Park, J.-W. Park, and T. K. Ko, "Study on optimal location of a resistive SFCL applied to an electric power grid," *IEEE Transactions on applied superconductivity*, vol. 19, no. 3, 2009, pp. 2048–2052.

[118] J. Tang and P. McLaren, "A wide area differential backup protection scheme for shipboard application," *IEEE Transactions on Power Delivery*, vol. 21, no. 3, 2006, pp. 1183–1190.

[119] P. Thomas, "Fault detection and diagnosis in engineering systems: Janos J. Gertler; Marcel Dekker Inc., New York, 1998, ISBN 0-8247-9427-3,", 2002.

[120] S. R. Tuladhar, J. G. Singh, and W. Ongsakul, "Multi-objective approach for distribution network reconfiguration with optimal DG power factor using NSPSO," *IET Generation, Transmission & Distribution*, vol. 10, no. 12, 2016, pp. 2842–2851.

[121] S. H. K. Vuppalapati and A. Srivastava, "Application of ant colony optimization for reconfiguration of shipboard power system," *International Journal of Engineering, Science and Technology*, vol. 2, no. 3, 2010, pp. 119–131.

[122] S. H. K. Vuppalapati and A. Srivastava, "Application of ant colony optimization for reconfiguration of shipboard power system," *International Journal of Engineering, Science and Technology*, vol. 2, no. 3, 2010, pp. 119–131.

[123] C. Wang, X. Wang, J. Xiao, J. Chen, and S. Zhang, "Fault reconfiguration of shipboard power system based on triple quantum differential evolution algorithm," *Journal of Shanghai Jiaotong University (Science)*, vol. 21, no. 4, 2016, pp. 433–442.

[124] K. Wang and M. L. Crow, "Power system voltage regulation via STATCOM internal nonlinear control," *IEEE transactions on Power systems*, vol. 26, no. 3, 2011, pp. 1252–1262.

[125] L. Wang, C.-H. Chang, B.-L. Kuan, and A. V. Prokhorov, "Stability improvement of a two-area power system connected with an integrated onshore and offshore wind farm using a STATCOM," *IEEE Transactions on Industry Applications*, 2016.

[126] L. Y. Wang, C. and Y. Zhao, "Application of dynamic neighborhood small population particle swarm optimization for reconfiguration of shipboard power system," *Engineering Applications of Artificial Intelligence*, vol. 26, no. 4, 2013, pp. 1255–1262.

[127] A. Wright and C. Christopoulos, *Electrical power system protection*, Springer Science & Business Media, 2012.

[128] P. Xiao, G. K. Venayagamoorthy, and K. A. Corzine, "Seven-level shunt active power filter for high-power drive systems," *IEEE Transactions on Power Electronics*, vol. 24, no. 1, 2009, pp. 6–13.

[129] Y. Xu and W. Liu, "Novel multiagent based load restoration algorithm for microgrids," *IEEE Transactions on Smart Grid*, vol. 2, no. 1, 2011, pp. 152–161.

[130] H.-T. Yang, W.-J. Tang, and P. Lubicki, "Placement of Fault Current Limiters in a Power System Through a Two-Stage Optimization Approach," *IEEE Transactions on Power Systems*, 2017.

[131] X. Yang and Y. Zhang, "Intelligent real-time fault restoration of the large shipboard power system based on genetic algorithm," *International Journal of Information Technology*, vol. 11, no. 12, 2005, p. 129135.

[132] C. Zhang, Z. Lin, F. Wen, G. Ledwich, and Y. Xue, "Two-stage power network reconfiguration strategy considering node importance and restored generation capacity," *IET Generation, Transmission & Distribution*, vol. 8, no. 1, 2014, pp. 91–103.

[133] X.-P. Zhang, C. Rehtanz, and B. Pal, *Flexible AC transmission systems: modelling and control*, Springer Science & Business Media, 2012.

[134] W. Zhu, J. Shi, and S. Abdelwahed, "End-to-end system level modeling and simulation for medium-voltage DC electric ship power systems," *International Journal of Naval Architecture and Ocean Engineering*, 2017.